

This is to certify that the

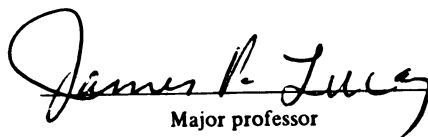
thesis entitled

Effects of Thermal Aging and Moisture Absorption on
Mechanical and Physical Properties of Cyanate Ester Polymers
presented by

Aparna Venkatramani

has been accepted towards fulfillment
of the requirements for

Master's degree in Materials Science
and Engineering


Major professor

Date 10/3/00

LIBRARY
Michigan State
University

PLACE IN RETURN BOX to remove this checkout from your record.
TO AVOID FINES return on or before date due.
MAY BE RECALLED with earlier due date if requested.

DATE DUE	DATE DUE	DATE DUE

**EFFECTS OF THERMAL AGING AND MOISTURE ABSORPTION ON
MECHANICAL AND PHYSICAL PROPERTIES OF CYANATE ESTER
POLYMERS**

By

Aparna Venkatramani

A THESIS

Submitted to
Michigan State University
in partial fulfillment of the requirements
for the degree of

MASTER OF SCIENCE

Department of Material Science and Mechanics

2000

ABSTRACT

**EFFECTS OF THERMAL AGING AND MOISTURE ABSORPTION ON
MECHANICAL AND PHYSICAL PROPERTIES OF CYANATE ESTER
POLYMERS**

By

Aparna Venkatramani

The aim of this research is to study the effects of thermal aging and hygrothermal effects on the mechanical and physical properties of cyanate ester (CE) and siloxane modified cyanate ester (SMCE) polymers. Thermal aging was conducted on these polymers in air at temperatures of 60⁰C, 80⁰C, 100⁰C in order to assess their susceptibility to thermo-oxidation processes, since thermo-oxidation can degrade the properties of some polymers. Also, the properties of polymers can be degraded by absorption of moisture, which can pose significant problems in CE and SMCE. Spectrographic techniques such as, fourier transform infrared spectroscopy (FTIR) and x-ray photoelectron spectroscopy (XPS) and thermal analysis techniques such as differential scanning calorimeter (DSC) were employed to evaluate and interpret changes observed in the physical properties. Environmentally induced changes in the mechanical properties of CE and SMCE were determined by conducting flexure and microhardness tests. Cyanate ester tended to gain weight when aged in air at elevated temperatures ranging from 60⁰C-100⁰C due to thermo-oxidation. In sharp contrast, siloxane modified cyanate ester showed essentially no weight gain in when aged at the same temperature range. Differential scanning

calorimeter tests showed that the glass transition temperature of CE remained unchanged even after aging in air. Thermomechanical analysis (TMA) showed a slight decrease in glass transition temperature on testing the same sample twice by the instrument. The flexural strength of cyanate ester was reduced by 20% after thermal aging in air for ~ 1000 hours. FTIR analysis revealed the formation of carbonyl groups as well as other significant spectral changes due to the thermo-oxidation process. XPS was utilized to study the elemental composition and binding energies. XPS spectroscopy showed an increase in surface concentration of oxygen with thermal aging for CE polymers. Microhardness results obtained by using a Vicker's indenter showed an increase in the hardness of CE but showed no change in the microhardness of SMCE polymers when aged in air. Moisture absorption studies revealed that SMCE absorbed substantially more water than CE resin regardless of how the samples were pre-conditioned. Absorbed moisture affected the T_g of both CE and SMCE. Microhardness tests showed the changes in the microhardness of CE and SMCE due to moisture absorption. An increase in the microhardness of CE was found due to moisture causing crosslinking of the polymer chains on the surface of the sample while the hardness in case of SMCE remained unchanged due to moisture absorption at all temperatures. The present investigation reconfirms that there are performance differences between CE and SMCE resins. The primary focus of this research is to discern the reasons for such observations.

Copyright by

Aparna Venkatramani

2000

To My Family and Friends

ACKNOWLEDGEMENT

I would like to thank the following people. Firstly, I would like to thank my master's thesis advisor, Dr. James P. Lucas, for his guidance, friendship, and suggestions throughout my graduate studies and research work. His support is greatly appreciated. It has been a great pleasure to work with him.

I would also like to thank Dr. K.N. Subramanian and Dr. Andre Lee for being on my graduate committee. Thanks are also extended to my colleagues Fu Guo and Rajbala Makar for their contributions, guidance and friendship.

I also acknowledge the Composite Materials and Structure Center for the use of much of the equipment necessary for conducting my research. Finally, I thank my parents, brother, and sister-in-law for their love, support and encouragement.

TABLE OF CONTENTS

LIST OF TABLES.....	x
LIST OF FIGURES.....	xi
LIST OF ABBREVIATIONS.....	xvi
CHAPTER 1	
INTRODUCTION.....	1
CHAPTER 2	
LITERATURE REVIEW.....	6
2.1 Cyanate Ester Based Polymer Materials.....	6
2.2 Thermo-Oxidation of Polymer Materials.....	13
2.2.1 Thermo-Oxidation Mechanisms.....	14
2.2.2 Thermo-Oxidative Kinetics in Polymer Materials.....	18
2.2.3 Chemical Change in Polymers Due to Thermo-Oxidation.....	20
2.2.4 Effects of Thermo-Oxidation on Chemical and Physical Properties.....	21
2.3 Hygrothermal Effect of Polymer Materials.....	22
2.3.1 Moisture Absorption Kinetics.....	23
2.3. 2 Effects of Moisture Absorption on Mechanical Properties.....	26
CHAPTER 3	
THERMO-OXIDATION OF CYANATE BASED POLYMER MATERIALS..	28
3.1 Experimental Procedure.....	28
3.1.1 Materials Description.....	28
3.1.2 Preparation of the Samples.....	33
3.1.3 Gravimetric Experiments.....	33
3.1.4 Glass Transition Temperature (T_g) Measurement Using DSC....	34
3.1.5 Glass Transition Temperature Measurement Using TMA.....	36

3.1.6 FTIR Testing.....	37
3.1.7 X-ray Photoelectron Spectroscopy (XPS) Testing	37
3.1.8 Three-point Bend Testing.....	38
3.1.9 Microhardness Testing.....	39
3.2 Results and Discussions.....	40
3.2.1 Assessment of Thermal Aging Effects of CE and SMCE	
Resins.....	40
3.2.1.1 Gravimetric Analysis.....	40
3.2.1.2 Glass Transition Temperature (T_g) Using DSC.....	55
3.2.1.3 Glass Transition Temperature (T_g) Using TMA.....	64
3.2.1.4 Thermo-oxidation Mechanism in CE Using FTIR.....	69
3.2.1.5 Thermo-oxidative Mechanism in CE Using XPS.....	74
3.2.1.6 Three-point Bend Test.....	84
3.2.1.7 Microhardness Testing.....	88
3.3 Summary and Conclusion.....	92

CHAPTER 4

HYGROTHERMAL EFFECT ON CYANATE BASED POLYMER MATERIALS

4.1 Experimental Procedure.....	94
4.1.1 Moisture Absorption Methods.....	94
4.1.2 Gravimetric Experiments.....	95
4.1.3 Glass Transition Temperature (T_g) Experiments.....	96
4.1.4 Microhardness Testing.....	96
4.2 Results and Discussion.....	97
4.2.1 Assessment of Hygrothermal Effects of CE and SMCE Resins...	97
4.2.1.1 Gravimetric Analysis.....	97
4.2.1.2 Glass Transition Temperature Using DSC	112
4.2.1.3 Microhardness Testing.....	125
4.3 Summary and Conclusion.....	127

CHAPTER 5

CONCLUSIONS AND RECOMMENDATIONS

5.1 Conclusions.....128

5.2 Recommendations.....130

BIBLIOGRAPHY.....131

LIST OF TABLES

- Table 3.1** The nominal physical properties of cyanate ester at room temperature. (p. 32)
- Table 3.2** The nominal physical properties of siloxane modified cyanate ester at room temperature. (p. 32)
- Table 3.3** Glass transition temperature of cyanate ester (CE) aged in ambient air for different aging time. (p. 58)
- Table 3.4** Glass transition temperature of siloxane modified cyanate ester (SMCE) aged in ambient air for different aging time. (p. 58)
- Table 3.5** X-ray photoelectron spectroscopy (XPS) results showing the % atomic concentration of elements in CE material. (p. 76)
- Table 3.6** X-ray photoelectron spectroscopy (XPS) results showing the % atomic concentration of elements in SMCE material. (p. 76)
- Table 4.1** Glass transition temperature for moisture absorbed SMCE polymer material. (p. 113)

LIST OF FIGURES

- Figure 2.1** Typical examples of commercial and developmental CE monomers. (p. 8)
- Figure 2.2** Cyclotrimerization process of cyanate ester. (p. 9)
- Figure 2.3** Schematic structures of polysiloxanes. (p. 12)
- Figure 3.1** Schematic structure of cyanate ester network. (p. 30)
- Figure 3.2** Schematic structure of siloxane modified cyanate ester (SMCE). (p. 31)
- Figure 3.3** Thermo-Oxidation curves of cyanate ester aged in ambient air for 1200 hours with square root of time. These curves compare the thermo-oxidation of CE at temperatures of 60⁰C, 80⁰C and 100⁰C respectively. (p. 43)
- Figure 3.4** Thermo-Oxidation curves for SMCE aged in ambient air for 1200 hours with square root of time. These curves compare the thermo-oxidation of SMCE at temperatures of 60⁰C, 80⁰C and 100⁰C respectively. (p. 44)
- Figure 3.5** Comparison of thermo-oxidation curves of CE and SMCE aged in ambient air at 100⁰C for 1200 hours. (p. 45)
- Figure 3.6** Comparison of thermo-oxidation curves of CE and SMCE aged in ambient air at 80⁰C for 1200 hours. (p. 46)
- Figure 3.7** Comparison of thermo-oxidation curves of CE and SMCE aged in ambient air at 60⁰C for 1200 hours. (p. 47)
- Figure 3.8** Linear graphs showing Thermo-Oxidation in CE materials aged in air for 1200 hours. These plots compare the thermal aging of CE polymers at temperatures 60⁰C, 80⁰C and 100⁰C respectively. (p. 52)
- Figure 3.9** Linear graphs showing thermo-oxidation in SMCE materials aged in air for 1200 hours. These plots compare the thermal aging of SMCE polymers at temperatures 60⁰C, 80⁰C and 100⁰C respectively. (p. 53)
- Figure 3.10** Linear graphs comparing the thermal aging in CE and SMCE polymers aged in air at 60⁰C, 80⁰C and 100⁰C for 1200 hours. (p. 54)
- Figure 3.11** Changes in glass transition temperature of CE with aging time. (p. 59)
- Figure 3.12** Changes in glass transition temperature of SMCE with aging time. (p. 60)

- Figure 3.13** DSC scan showing the T_g for CE aged in air at 100°C for a period of 0 hours, 200 hours, 500 hours and 900 hours respectively. (p. 61)
- Figure 3.14** DSC scan showing the T_g for SMCE aged in air at 100°C for a period of 0 hours, 200 hours, 500 hours and 900 hours respectively. (p. 62)
- Figure 3.15** TMA scans showing the glass transition temperature range and relaxation occurring in CE aged in air at 100°C for a period of 0 hours, 200 hours, 500 hours and 900 hours respectively. (p. 66)
- Figure 3.16** TMA showing the T_g for CE obtained by rerun of the same CE sample for the second time. The scan shows a decrease in T_g for CE in the second run of TMA. (p. 67)
- Figure 3.17** Comparison of T_g of CE aged in air at 100°C for a period of 0 hours, 200 hours, 500 hours and 900 hours respectively and obtained from DSC and TMA. (p. 68)
- Figure 3.18** FTIR spectra ($766\text{--}1036\text{ cm}^{-1}$) of CE aged in ambient air at 100°C . Change in spectra with aging time show the decrease in 911 cm^{-1} and 966 cm^{-1} peaks. (p. 71)
- Figure 3.19** FTIR spectra ($1661\text{--}2340\text{ cm}^{-1}$) of CE aged in ambient air at 100°C . Change in spectra with aging time show the increase in the 1726 cm^{-1} peaks. (p. 72)
- Figure 3.20** FTIR spectra ($1661\text{--}3977\text{ cm}^{-1}$) of SMCE aged in ambient air at 100°C . Change in spectra with aging time show the increase in the 1726 cm^{-1} peaks. (p. 73)
- Figure 3.21** XPS results showing the atomic concentration for CE and SMCE aged in air at 100°C for a period of 0, 500 and 900 hours respectively. (p. 77)
- Figure 3.22** XPS spectra showing the % atomic concentration and binding energies for CE aged in air for 0 hours. (p. 78)
- Figure 3.23** XPS spectra showing the % atomic concentration and binding energies for CE aged in air for 500 hours. (p. 79)
- Figure 3.24** XPS spectra showing the % atomic concentration and binding energies for CE aged in air for 900 hours. (p. 80)
- Figure 3.25** XPS spectra showing the % atomic concentration and binding energies for SMCE aged in air for 0 hours. (p. 81)
- Figure 3.26** XPS spectra showing the % atomic concentration and binding energies for

SMCE Aged in air for 500 hours. (p. 82)

Figure 3.27 XPS spectra showing the % atomic concentration and binding energies for SMCE Aged in air for 900 hours. (p. 83)

Figure 3.28 Degradation mechanism of thermally aged CE polymer by three-point bend test. (p. 85)

Figure 3.29 Illustration of the oxide layer formed due to the thermo-oxidation for a 3-point bend specimen. During 3-point bend testing, microcracks readily nucleate and grow in the oxide layer at low applied loads. Such microcracking at low loads leads to lower flexural strength in this material. (p 85).

Figure 3.30 Illustration showing the oxide layer which forms on the surface of CE. specimens during thermal aging in air. Microhardness was determined on such specimens. (p 89)

Figure 3.31 Microhardness results showing the changes in the microhardness for CE and SMCE aged in ambient air at 100⁰C for 0 hours, 200 hours 500 hours and 900 hours respectively. (p. 91)

Figure 4.1 Water absorption curves of CE at different environmental temperature with square root of time. The plots compare the moisture absorption for CE aged in air and at 100⁰C for 1000 hours and baked out in argon for 5 days. (p. 100)

Figure 4.2 Water absorption curves of SMCE at different environmental temperature with square root of time. At 100⁰C for 1000 hours and baked out in argon for 5 days. (p. 101)

Figure 4.3 Comparison of water absorption curves for comparing the weight change for CE and SMCE exposed to environmental chambers containing distilled water at 45⁰C with square root of time. (p. 102)

Figure 4.4 Comparison of water absorption curves for comparing the weight change for CE and SMCE exposed to environmental chambers containing distilled water at 60⁰C with square root of time. (p. 103)

Figure 4.5 Comparison of water absorption curves for comparing the weight change for CE and SMCE exposed to environmental chambers containing distilled water at 75⁰C with square root of time. (p. 104)

Figure 4.6 Comparison of water absorption curves for comparing the weight change for CE and SMCE exposed to environmental chambers containing distilled water at 90⁰C with square root of time. (p. 105)

- Figure 4.7** Comparison of diffusion rates in CE and SMCE polymer when exposed to moisture absorption at 45⁰C for 2000 hours with square root of time. (p. 108)
- Figure 4.8** Comparison of diffusion rates in CE and SMCE polymer when exposed to moisture absorption at 60⁰C for 2000 hours with square root of time. (p. 109)
- Figure 4.9** Comparison of diffusion rates in CE and SMCE polymer when exposed to moisture absorption at 75⁰C for 2000 hours with square root of time. (p. 110)
- Figure 4.10** Comparison of diffusion rates in CE and SMCE polymer when exposed to moisture absorption at 90⁰C for 2000 hours with square root of time. (p. 111)
- Figure 4.11** Comparison of glass transition temperature for SMCE samples aged in air at 100⁰C for 1000 hours and baked out in argon for 5 days and exposed to water maintained at 45⁰C, 60⁰C, 75⁰C and 90⁰C respectively. (p. 115)
- Figure 4.12** DSC scan showing the T_g for SMCE aged for 0 hours. (pg. 116)
- Figure 4.13** DSC scans showing the T_g for SMCE aged in air at 100⁰C and exposed to water at 45⁰C. (p. 117)
- Figure 4.14** DSC scans showing the T_g for SMCE aged in air at 100⁰C and exposed to water at 60⁰C. (p. 118)
- Figure 4.15** DSC scans showing the T_g for SMCE aged in air at 100⁰C and exposed to water at 75⁰C. (p. 119)
- Figure 4.16** DSC scans showing the T_g for SMCE aged in air at 100⁰C and exposed to water at 90⁰C. (p. 120)
- Figure 4.17** DSC scans showing the T_g for SMCE baked out in argon at 100⁰C for 5 days and exposed to water at 45⁰C. (p. 121)
- Figure 4.18** DSC scans showing the T_g for SMCE baked out in argon at 100⁰C for 5 days and exposed to water at 60⁰C. (p. 122)
- Figure 4.19** DSC scans showing the T_g for SMCE baked out in argon at 100⁰C for 5 days and exposed to water at 75⁰C. (p. 123)
- Figure 4.20** DSC scans showing the T_g for SMCE baked out in argon at 100⁰C for 5

days and exposed to water at 90⁰C. (p. 124)

Figure 4.21 The results determining the microhardness for CE and SMCE exposed to preaging conditions and submerged in water for 2000 hours at 45⁰C, 60⁰C, 70⁰C and 90⁰C respectively. (p. 126)

LIST OF ABBREVIATIONS

CE	Cyanate ester
SMCE	Siloxane modified cyanate ester
BMI	Bismaleimide
HSCT	High-speed civil transport
DSC	Differential scanning calorimeter
FTIR	Fourier transform infrared spectroscopy
PMS	N-phenylmaleimide styrene
T _g	Glass transition temperature
UP	Unsaturated polyester
M	Moisture content
M ₀	Initial moisture content
M _m	Equilibrium moisture content
UV	Ultra-violet
Δw%	Percentage by weight change
w ₀	Initial weight of samples
w _t	Measured and final weight of the samples
TMA	Thermomechanical analysis
FPA	Focal plane array
CHA	Concentric hemispherical analyzer
XPS	X-ray photoelectron spectroscopy

CHAPTER 1

INTRODUCTION

During the last few decades, polymeric materials have played an important role in replacing metals and metal composites in various applications. In the automobiles, aerospace, space and sporting goods industries, polymers and their composites are highly desirable, due to their lightweight, dimensional stability, good mechanical strength properties that are desirable in such applications [1]. In such applications, polymer composite materials are exposed to a wide range of temperatures, radiation, mechanical fatigue and extreme environmental conditions like oxygen and moisture [2,3]. Several authors [2-7] have reported the environmental degradation of mechanical and physical properties of polymer matrices.

Epoxy polymers have been widely used for many important applications such as adhesives, insulating materials, reinforced plastics and as matrix for advanced composite materials [7,8]. Unfortunately, epoxy resins have relatively high dielectric loss and a high propensity for water absorption. Therefore, cyanate ester polymer materials were developed. CE resins have low dielectric loss properties, low water absorption, excellent heat resistance and low volume shrinkage; properties that are useful in both the aerospace and electronic industries. These unique properties of CE materials make them attractive composite matrices and direct competitors for standard epoxy and BMI resins in high performance applications [1,9]. Other characteristics associated with cyanate esters functionality are easy processibility, miscibility, and reactivity with epoxy resins and

miscibility with many amorphous thermoplastics materials [10,11]. CE also offers an attractive selection of physical and mechanical properties. The high aromatic content in monomers and the cured network is responsible for the relatively high T_g , inherently low smoke generation and good flame retardancy, and relatively low crosslink density. The balanced dipoles in the cured state and absence of hydrogen-bonding functionality are responsible for the low dielectric properties of the polymer material. Such characteristics make CE resins prime candidates for use for a variety of applications from microelectronics to aerospace. They also find use in primary and secondary structures in military aircraft and have been evaluated for potential applications in the once proposed but now defunct US high-speed civil transport (HSCT).

Chemically, this family of thermosetting monomers and their prepolymers contain the reactive ring-forming cyanate ($-O-C\equiv N$) functional groups. Conversion of polyfunctional CE monomers to thermoset polymers occurs via cyclotrimerization to form three-dimensional networks of oxygen-linked triazine and bisphenyl units, correctly termed as polycyanurates or cyanate ester or triazine resins.

One of the major concerns of such polymeric based composite materials in industry and commercial applications is their environmental degradation, which occurs in a wide variety of service conditions such as moisture absorption, high temperature oxidation, and photo-radiation [2]. Degradation occurs as a result of severe environmental conditions, which involve chemical and physical attack, often caused by the combination of degradation agents, and may involve several physical, chemical and mechanical mechanisms. For example, many polymers are prone to degradation caused by

weathering in which photochemical reactions, involving solar ultraviolet photons and atmospheric oxygen, leading to possible chain scission [2,3,12,13].

Hygrothermal effects of polymer materials involves the absorption of water by the resin matrix, which often causes degradation, plasticization, swelling, blistering, and lowering of glass transition temperature (T_g) of the polymer matrix [3].

Most investigations [14-18] have shown that epoxy based composite materials absorb significant amount of water which induces the degradation and dimensional instability of polymer materials. Such changes tend to limit their application in high technology industry, which usually demands for high environmental stability standards of materials. Intensive research has been performed in an effort to provide thermosetting polymers with a reduced tendency to thermal oxidation and moisture absorption. Thermally stable and low moisture absorption materials were achieved by the development of cyanate ester resin based polymeric materials.

To examine the degradation mechanisms of the family of cyanate ester, model compounds like diphenyl cyanurate, triphenyl isocyanurate, cyanuric acid and triphenyl-s-triazine were studied at elevated temperatures both in air and in vacuo [1]. Triphenyl cyanurate was chosen as the model compound for the network structure as it contains the principal bonds present in the three-dimensional structure of the polymer. The mechanism of thermal degradation were studied using chromatographic and mass spectroscopic methods and showed that, as in the degradation of the dicyanate polymers, the principal decomposition products are carbon dioxide, carbon monoxide, phenol and cyanuric acid. From the model study it was concluded that triphenyl-s-triazine exhibited the highest thermal stability of the compounds investigated [8]. There have been many

studies [1] on the hygrothermal effect of cyanate ester based polymer materials. Results show that the water absorption decreases the glass transition temperature and mechanical strength of cyanate ester based polymer materials. Shimp and Ising [10] found that the class of cyanate ester resins homopolymers absorbs less than 3% of water over a period of 6 months as compared to the competing resins such as epoxies, BMI and condensation polyimides. The cyanurate linkage is very resistant to hydrolysis, withstanding ‘hundreds of hours’ of immersion in boiling water [1].

Kasehagen *et al.* [19] studied moisture absorption in cyanate ester resins. They found that hydrolysis of cyanate ester caused blistering of the network, which produced gaseous products such as carbon dioxide, alcohol, etc. and lowered the T_g and strength of the matrix. Cinquin *et al.* [20] also studied the water absorption in cyanate ester and found that moisture absorption in cyanate ester materials followed Langmuir’s law. They further determined that moisture absorption curves of these materials followed the Fick’s second law of diffusion. Lee *et al.* [6] also studied the water absorption in cyanate ester and showed that these materials absorbed small amounts of water when exposed to high humidity and the moisture profiles followed Fick’s law in the early stage of moisture absorption. As the material continued to undergo hydrolysis, it was observed that the water absorption behavior became Non-Fickian after prolonged exposure to high humidity.

This research focuses on the effects of thermal aging and effects of moisture absorption on cyanate ester (CE) and siloxane modified cyanate ester (SMCE) using gravimetric, analytical and spectroscopic techniques. The weight change of CE and SMCE when exposed to ambient air at different temperatures and when exposed to 100%

humidity (submersion in water bath) maintained at different temperatures were studied. FTIR was utilized to study the changes in the chemical structure of CE and SMCE during thermo-oxidation process. Glass transition temperatures changes with thermal aging time and with moisture absorption were determined to study the extent of degradation in CE and SMCE resins. Three- point bend test and microhardness tests were used to study the changes in flexural strength and microhardness of CE and SMCE with aging. XPS was used to study the elemental surface concentration for each element making up the chemical structure of the cyanate ester polymer materials following environmental exposure. This research is an extension of the thesis work by Z. Liu, (1999), at Michigan State University. This work clarifies and further explains the behavior of CE and SMCE polymer materials due to thermal aging in ambient air and moisture absorption.

CHAPTER 2

LITERATURE REVIEW

2.1 Cyanate Ester Based Polymer Materials

The families of materials that make up the cyanate esters have been developed primarily because of their high T_g and low dielectric properties [1,21]. These properties have made cyanate ester an attractive alternative to epoxies and BMI in the manufacture of printed circuit boards [9]. These materials are also potentially strong competitors to polyimides and epoxy materials in structural composites, particularly in the aerospace industry.

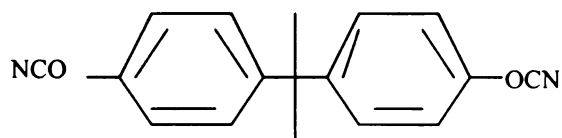
Cyanate ester has a unique chemistry that makes them of interest for the study of network formation. The primary polymerization reaction can be thought of as cyclotrimerization to form a triazine ring with one functionality unlike epoxy-amine system in which there are two or more distinct chemical functionalities with potentially different reactivities [22]. A cyanate ester crosslink structure, which may be of a thermoset or a thermoplastic nature, is derived from cyanate functional monomers and/or oligomers. Some cyanate monomers can be advanced to a prepolymer stage wherein up to about 50 percent of the functional groups react. Effectively, the product of such a reaction contains the triazine moiety and may or may not contain unreacted cyanate functional groups [22].

In particular, the cyanate functional monomers and/or oligomers consist essentially of cyanate ester of one or more compounds of the general formula,

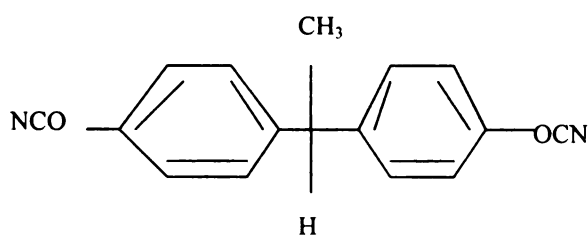


where, $m = 0$ to 5 , $q = 0$ to 5 , $x = 0$ up to 2 , Ar is a single or fused aromatic or substituted aromatic and combinations thereof linked in the ortho, meta and/or para position and Y is a linking unit selected from the group consisting of oxygen, carbonyl, sulphur, sulphur oxides, etc [22]. Commercial dicyanate monomers are divided into two categories: (1) monomers that are currently commercial products, and (2) developmental monomers that are previously, or currently, available as experimental products. The structures and commercial trade names of these categories of materials is listed in Figure 2.1. The cyclotrimerization process is explained by the chemical reactions as shown in Figure 2.2.

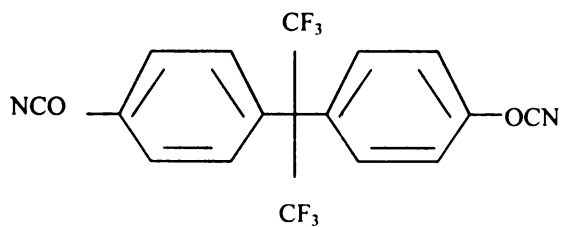
Commercial Cyanate Ester Monomers:



M.P = 79°C
AroCy B-10 (Ciba)

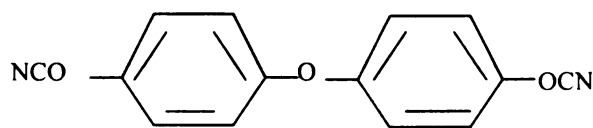


M.P=29°C
AroCy L-10 (Ciba)

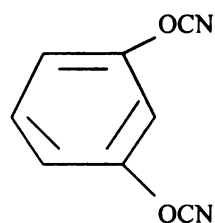


M.P=87°C
AroCy F-10 (Ciba)

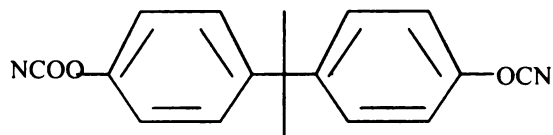
Developmental Cyanate Ester Monomers:



M.P= 87°C
ESR 288 (Ciba)



M.P = 78°C
REX 370 (Ciba)



Liquid
REX 370 (Ciba)

Figure 2.1 Typical examples of commercial and developmental cyanate ester monomers

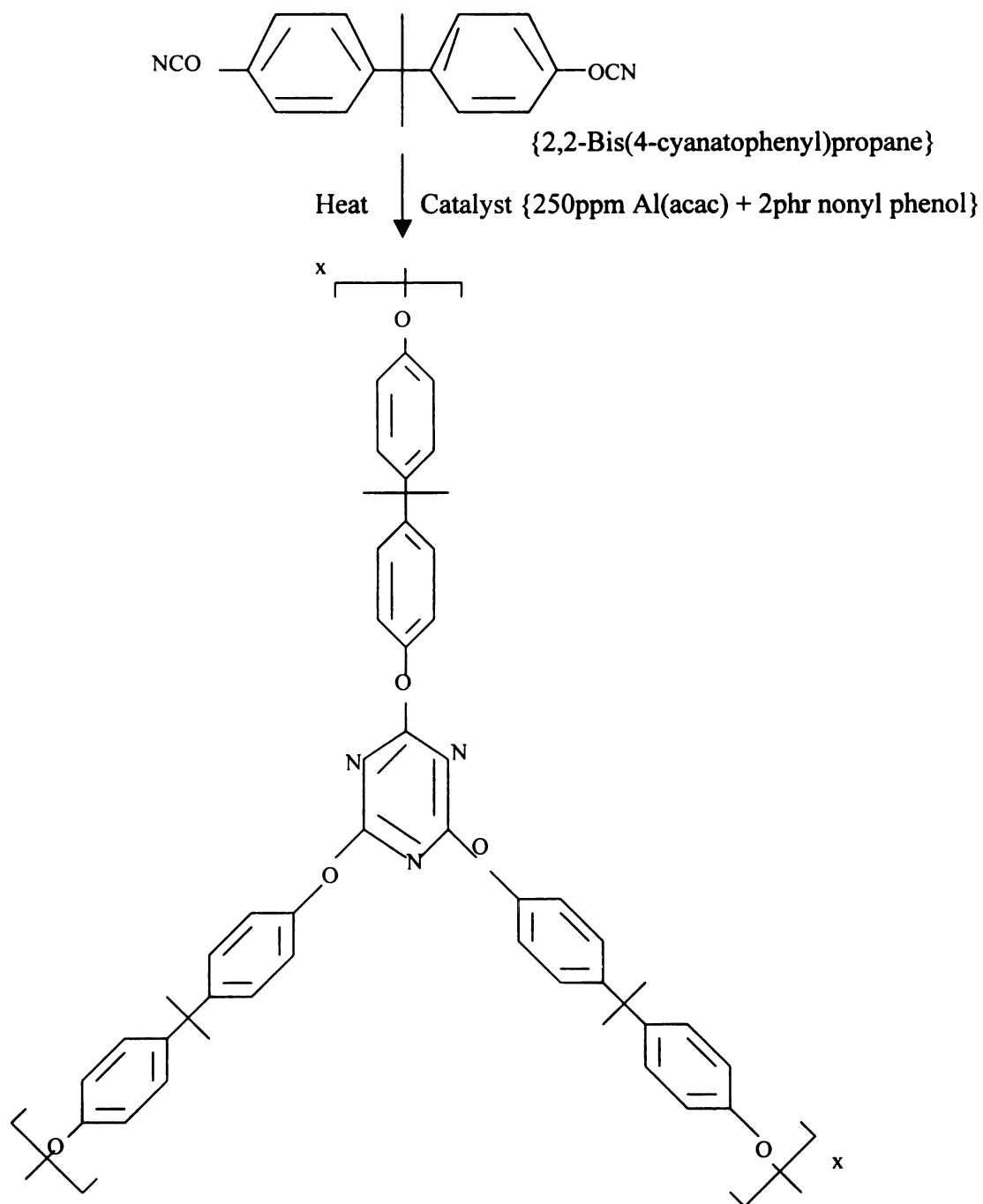


Figure 2.2 Cyclotrimerization Process of Cyanate Ester [4]

The formation of polycyanurates through polycyclotrimerization of cyanate ester is a typical step growth process. Starting from low molecular weight with at least two cyanate groups, the reacting system passes through a pregel state with a broad distribution of oligomers to reach the gelpoint at a certain value of the functional groups' conversion. The chemical and physical structure of the network is closely related to the underlying formation process. The $C\equiv N$ functional group in cyanate ester resin is of considerable importance since it is frequently used to quantify the conversion to prepolymer and fully cured polymer [1,21,22].

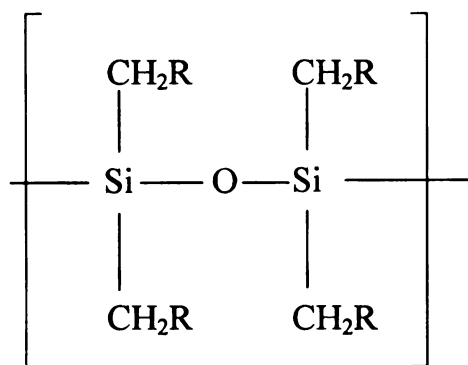
One major property of cyanate ester systems of concern is their inherent brittleness [9], which is a major drawback in such materials. Toughening thermoset matrices derived from the cyclotrimerization of aryl dicyanates, modified with minor amounts of thermoplastics resins is described, with emphasis on defining parameters contributing to increase fracture toughness. Rubber toughening has been applied successfully to CE. Rubbers, which have been used, include amine-terminated butadiene-acrylonitrile copolymers [1,9], amine terminated polybutylene ethers and a hydroxyl- terminated polydimethylsiloxane-polyester block copolymer in addition to thermoplastic modifiers like polysulphone, poly (ether sulphone), polyacrylates. Iijima *et al.* [24] found that N-phenylmaleimide-styrene copolymer was an effective modifier and an alternative to reactive rubber tougheners, for improving the brittleness of the resin, and from the viewpoint of maintenance of mechanical and thermal properties of the resin. Inclusion of 10 wt % N-phenylmaleimide-styrene (PMS) led to 160% increase in the fracture toughness for the modified resin with the slight loss of flexural strength and retention of

flexural modulus and the glass transition temperature, compared to the values of the unmodified resin [23].

Oligosiloxane elastomers are rubber tougheners, which have also been used to toughen CE with little reduction in T_g up to 10% addition of the elastomer.

Organosiloxane polymers are known for their excellent thermal and thermo-oxidative stabilities, very low glass transition temperature, high moisture resistance and good electrical properties [6]. Microcracking is decreased relative to the unmodified resin.

Polysiloxanes are inorganic polymers, that is, there are no carbon atoms in the backbone chains. The schematic structure of polysiloxane is shown in Figure 2.3. The backbone is a chain of alternating silicon and oxygen atoms. Polysiloxanes possesses an unusual combination of properties that are retained over a wide temperature range [24]. They have very good low temperature flexibility because of the low T_g value. Silicones are very stable to high temperature, oxidation, chemical and biological environments and weathering and possess good dielectric strength. Thus, silicones make good elastomers because the backbone chain is very flexible. The bonds between a silicon atom and the two oxygen atoms attached to it are very flexible. The angle formed by these bonds can open and close like a scissor without much trouble. This makes the whole backbone chain flexible.



R = H, n=10-1000

Figure 2.3 Schematic structure of Polysiloxane.

2.2 Thermo-Oxidation of Polymer Materials

Degradation of components made of polymeric materials occurs in a wide variety of environments and service conditions, and very often limits their service lifetime.

Degradation occurs as a result of environment-dependent chemical and physical attack, often caused by the combination of degradation agents, which may involve several chemical and mechanical mechanisms. For example, many polymers are prone to degradation caused by weathering in which photochemical reactions, involving solar ultraviolet photons and oxygen lead to chain scission, but degradation of polymers is much faster in the presence of oxygen at elevated temperatures [12,13]. In an aggressive oxygen environment polymer molecular chains may break (chain scission), cross-link, or suffer substitution reactions [2]. Substitution is the least common and causes the smallest property changes while, chain scission and cross-linking both occur under natural weathering conditions. The initiation of thermal aging proceeds by a radical chain process initiated by dissociation. Thermo-oxidation reaction of polymer materials usually causes the degradation of polymer properties, that is, it lowers tensile strength, lowers glass transition temperature, and lowers dimensional stability [3]. Chemical and physical properties of the polymers depend on the composition and structure of molecules that make up the polymer matrix. The thermal stability of the polymer resin matrix is greatly influenced by the strength of chemical bonds [1,12].

2.2.1 Thermo-Oxidation Mechanism

The oxidative degradation of polymers takes place by free radical chain reaction. An important difference from some other chain reactions is that besides the three steps, that is, initiation, propagation, and termination, two additional important steps must be considered here. The conversion of the formed hydrocarbon radicals to peroxy radicals, that is the main oxygen consuming reaction, and degenerate chain branching or rearrangement, that is the reaction responsible for the autoacceleration character of the process [25,26].

The most important steps in polymer oxidation are as follows [26].

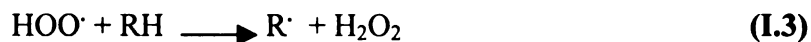
Initiation:



where RH is a polymer monomer,



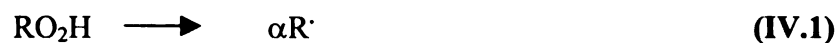
where R^\cdot is a free radical,



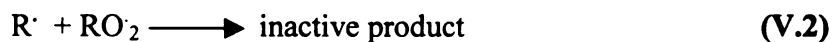
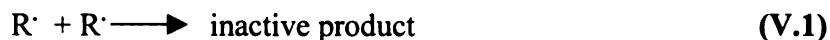
Radical conversion (stabilization):



ROO^\cdot is a peroxide radical,

Chain Propagation:**Degenerate chain branching:**

$\alpha\text{R}\cdot$ and $\beta\text{R}\cdot$ are degenerated radicals.

Termination:**(1) Initiation**

There are many factors that are responsible to initiate the free radicals, such as light (photo-oxidation), thermal energy and thermo-oxidation, and will react most readily with molecular oxygen. Initiation occurs by the direct reaction of oxygen molecules with the polymer material. This reaction is endothermic and very slow at low temperatures. The probability of this reaction occurring is higher when the polymer contains reactive

hydrogen [25,26], and consequently tertiary-hydrogen and secondary hydrogen adjunct electron-rich groups are very active.

Free radical are produced from non-radical intermediate by the process of chain branching, as shown by steps (I.1), (I.2) and (I.3) in the oxidation process. Audouin *et al.* [27-31] suggested that in the radical oxidation of hydrocarbon polymer, the initiation was only due to unimolecular or bimolecular hydroperoxide decomposition. Their results of analysis have been compared to the thermo-oxidative degradation of cross-linked polyethylene, polypropylene and linear poly (vinyl chloride) when aged in 110-170⁰C-temperature range. The results obtained in these investigations show that the initiation scheme is in good agreement with experimental results.

(2) Radical conversion

Radical conversion involves the important step wherein, conversion of the hydrocarbon radical to a peroxy radical takes place during oxidation, namely, it is the step in which majority of oxygen is absorbed by the polymer. This process is shown by step (II). As soon as the alkyl radical is generated in an initiation reaction, it reacts with oxygen. Here oxygen exists in a diradical state. This reaction is very rapid in nature as the alkyl radical reacts spontaneously with oxygen. This type of reaction is essentially a radical coupling reaction. The rate of this reaction depends on the concentration of oxygen inside the polymer, that is, on its pressure outside and its ease of diffusion [31]. Thus, the oxidation process may become diffusion controlled with low pressure and/or with high sample thickness.

(3) Chain propagation

Chain propagation in polymer oxidation consists of the hydrogen abstraction reaction of the peroxy radicals. With increasing rate constant of this reaction, the rate of oxidation increases and the kinetic chain length becomes greater. The chain propagation is shown by steps (III.1) and (III.2). This will produce more free radicals, with increase in rate of oxidation. The reactivity of hydrogen toward free radicals increase in the following order: primary < secondary < tertiary, in accordance with the decrease in bond dissociation energies. Because of the high reactivity of the tertiary hydrogen in polymers like polypropylene and polystyrene, intermolecular propagation takes place at a much faster rate in oxidation.

(4) Degenerate chain branching

The decomposition of hydroperoxides to radicals is the most important step in polymer oxidation. Hydroperoxides, commonly the major product of oxidative degradation, are potentially powerful initiators of further degradation. The thermal decomposition of hydroperoxides may proceed unimolecularly, bimolecularly, or with the participation of the R-H group. The presence of both carbonyl and carboxyl groups accelerate the decomposition; acid catalyzed decomposition, however, favors the formation of molecular products. Besides ketone and water, many other products can be formed in this step. The formation of most of the volatile products like, alcohols, acids and aldehydes is connected to the hydroperoxide decomposition reaction. This process is explained by steps (IV.1) and (IV.2).

(5) Termination

Most common type of termination reactions includes unimolecular or bimolecular termination of free radicals in polymer oxidation. This occurs by participation of peroxy radicals. Unimolecular termination takes place when solid polymers or polymer melts of high viscosity are oxidized. A bimolecular termination step is unlikely since it would depend upon two very small concentrations requiring polymer-polymer interaction in a medium of very high density. This process is very important at the low oxygen pressures and is shown in steps (V.1),(V.2) and (V.3).

2.2.2 Thermo-Oxidative Kinetics in Polymer Materials.

Many aging processes involve a reaction of polymer with small molecules like O_2 , H_2O and ozone typically found in the environment. On thermal aging the bonds between the atoms making up the polymer chains may break forming a variety of fragment radicals or small molecules, which may mutually combine or break. For an aging process involving the consumption of small molecules such as oxygen, there exists critical conditions of reaction rate and thickness above which the process becomes kinetically controlled by the diffusion of the small molecules in the polymer. In many cases the thickness of the degraded layer is of the order of magnitude D / k , where D is the diffusion coefficient and k is the pseudo-first-order rate constant for oxygen consumption [13]. Two processes explain thermal aging in polymers, (i) diffusion controlled and (ii) not diffusion controlled. Based on the mechanism of diffusion of oxygen into the polymer matrix there are two possible domains.

(1) Domain I: For low values of r and the sample thickness L , the kinetics is not diffusion controlled. The low molecular weight diffusing species is consumed homogeneously throughout the sample. Here, r is defined as the local reaction rate in a very thin superficial layer of the sample exposed to thermal aging.

(2) Domain II: For higher values of r and L , the kinetics is diffusion controlled. Most of the low molecular weight diffusing species is consumed in the superficial layers of the sample. The diffusing species are heterogeneously distributed within the sample thickness [13].

The thermo-oxidation of polymer materials is based on diffusion-controlled kinetics of oxygen into the resin matrix. Most authors [27-31] have explained this process of thermo-oxidation in polymers from Fick's second law:

$$\frac{\partial C}{\partial t} = D \frac{\partial^2 C}{\partial x^2} , \quad (2.1)$$

where, C = the concentration of diffusing species,

t = time, and

x = depth of penetration of reactive species.

When the reactant is consumed by the reaction at a rate r , the above reaction becomes,

$$\frac{\partial C}{\partial t} = D \frac{\partial^2 C}{\partial x^2} - r , \quad (2.2)$$

The local reaction rate r is a function of the local reaction concentration: $r \longrightarrow r(C)$.

Furthermore, it can be concluded that the system comes to a stationary state when $\partial C/\partial t = 0$ and then,

$$D \frac{\partial^2 C}{\partial x^2} - r(C) = 0, \quad (2.3)$$

It should be possible to determine the concentration profile $C(x)$ with this differential equation, provided that D and $r(C)$ are known.

The diffusion coefficient, D , depends on the conversion of the aging process, that is, of time and on the reactant concentration.

- (i) The diffusion coefficient depends on time, and in this case, the initially homogeneous sample becomes heterogeneous. Thermo-oxidation in the superficial layers leads to chain scission and a slight increase of the oxygen permeability whereas crosslinking in the core zone results in decrease of the oxygen permeability
- (ii) The diffusion coefficient also depends on the concentration of diffusing species. This anomalous behavior can be observed in the case where high concentrations of the diffusing species can induce noticeable matrix plasticization. In these cases, short-term physical aging processes are generally responsible for very important property changes.

2.2.3 Chemical Change in Polymers Due to Thermo-Oxidation

The chemical composition and structure of the molecules that make up the polymer resin matrix determine the dimensional and thermal stability of the polymer. The diffusion of oxygen into such polymer matrix causes morphological degradation of the polymer matrix. Vibrational analysis of polymers provides information on three important

structural features: chemical composition, configurational and conformational structure and interatomic forces associated either with valence bonding or intermolecular interactions [32]. Any physical or chemical treatment of a polymer induces structural change, the knowledge of which is essential for a better understanding of polymer properties. Chemical changes that occur during the thermo-oxidation process of hydrocarbon polymers can be determined using FTIR. It was established that carbonyl formation after the end of the induction period occurred only in a superficial region whose thickness was a decreasing function of temperature as predicted by the simple models of the diffusion controlled process [26]. Infrared spectroscopic studies showed that aldehydes (1735 cm^{-1}) and ketones (1720 cm^{-1}) are the main species present during the early stages of degradation, although carboxylic acids (1710 cm^{-1}) are the species dominating in the later stages. The presence of carboxylic and carbonyl group in the degraded polymer indicates that oxidation has taken place and also warns that the material is vulnerable to further deterioration [12].

2.2.4 Effects of Thermo-Oxidation on Chemical and Physical Properties of CE

The chemical composition and structure of the polymer material determines its thermal stability. A change in chemical, physical and mechanical properties during long-term exposure can be due to various processes such as physical aging (volume relaxation), crystallization, orientation or stress relaxation, crosslinking and chain scission [13]. It is found that rate of oxygen diffusion is much greater in amorphous materials than in crystalline domains, because the crystalline cores are inaccessible to molecular oxygen. The oxidation rate of polyethylene is inversely proportional to the degree of crystallinity

[27]. The mobility of radicals is greater in amorphous regions. This implies that the rate of diffusion of oxygen is much faster in amorphous polymers than in crystalline domains. It is also observed that the crystallinity increases with the degree of oxidation. This is attributed to the breaking of chains in amorphous regions, facilitating their crystallization. [33].

2.3 Hygrothermal Effect of Polymer Materials.

Hygrothermal effect on polymers is of great importance because water and temperature are the most common environmental factors causing performance reduction in polymers. The most prominent amongst the reasons is the fact that sorbed moisture promotes material degradation, plasticization, swelling and lowered T_g of the polymer matrix. Merdas *et al.* studied the consequences of water absorption on the physical properties of polyetherimide [34]. They found that water absorption affected important resin properties like glass transition temperature, tensile properties and viscoelastic behavior of the polymer resin. T_g decreased with exposure to moisture absorption, which indicates that water had a significant plasticizing effect on polyetherimide. Tensile properties of polyetherimide decreased with water absorption. Park *et al.* [35] studied the influence of water absorption on the glass transition and the low temperature relaxations of semiaromatic polyamides by means of the calorimeter and dynamic mechanical techniques. They found a depression in the glass transition temperature in diluted system due to the presence of free volume provided by the diluent, which allowed high segmental mobility at low temperatures. In addition to decrease in T_g , other useful properties of the material are also affected with diffusion of moisture into the polymer

resin. Smith *et al.* [36] also studied the effects of water on T_g . Their study involved the effects of water on T_g of poly methyl methacrylate polymers. They too found a depression in the glass transition temperature by about 20⁰K. Agarwal and Farris [38] investigated the diffusion of water into acrylic-based latex blend films. They found a significant change in the appearance and mechanical properties of the film. Many researchers [8] have studied the mechanism of moisture diffusion in epoxy resins. The absorption showed an increase in weight during the initial stages of moisture absorption followed by decrease at later times. This indicates that water diffusion is Fickian followed by the Non-Fickian model governing the final stages of the absorption process. They also found a decrease in T_g and moisture absorption induced swelling which increased with increase in moisture content.

2.3.1 Moisture Absorption Kinetics

Moisture induced property degradation tends to correlate well with the extent of absorbed moisture in the polymer matrix. Moisture related degradation is associated with chemisorptions and reactivity characteristics of the permeating environment and matrix material.

Typically, moisture transport in polymer resins can be described by classical Fickian diffusion. The diffusion process is similar for both thermoset and thermoplastic polymers and polymer composites.

The Fick's law for diffusion of moisture in resin materials is expressed as

$$\frac{\partial M}{\partial t} = D \frac{\partial^2 M}{\partial x^2}, \quad (2.4)$$

where, M represents the concentration of diffusing medium, x is a dimensional coordinate, and D is the diffusion coefficient that is temperature dependent. Applying appropriate boundary conditions and integrating, we derive an expression predicting moisture absorption with time,

$$\frac{M_t}{M_m} = \left(\frac{4}{h} \right) \left[\frac{Dt}{\pi} \right]^{\frac{1}{2}}. \quad (2.5)$$

Equation 2.5 represents the initial linear segment of the moisture diffusion profile, where M_t is proportional to \sqrt{t} .

Further manipulation of equation 2.5 shows that diffusion coefficient can be expressed as

$$D = \frac{\pi}{16} \left(\frac{h}{M_m} \right)^2 \left(\frac{M_2 - M_1}{\sqrt{t_2} - \sqrt{t_1}} \right)^2 \quad (2.6)$$

where,

D = the diffusion coefficient,

h = the laminate thickness,

M_m = the maximum moisture content, a constant independent of temperature,

M_t = moisture content at time t .

Moreover, the entire moisture-time diffusion profile is determined theoretically by the following expression.

$$M_t = M_m \left\{ 1 - \exp \left[-7.3 \left(\frac{Dt}{h^2} \right)^{0.75} \right] \right\}. \quad (2.7)$$

D often exhibits a dependence on temperature that follows an Arrhenius relationship given by

$$D(T) = D_0 \exp \left(\frac{-A_0}{RT} \right). \quad (2.8)$$

where,

D_0 = pre-exponential factor,

A_0 = the activation energy for diffusion,

R = the universal gas constant, and

T = the temperature measured on the absolute scale. ($^{\circ}\text{K}$)

The kinetics of water absorption in polymers is usually assumed to be a concentration-independent on Fickian diffusion process [38-41]. This model, which is usually applicable to the initial stages of moisture absorption process, fails to describe the whole phenomenon [42]. This complete phenomenon is explained by means of a Langmuir type diffusion process [43], in which the absorbed material can be divided into mobile and strongly bound types. Langmuir's model can be used to fit the experimental data. The two equations, 2.9 and 2.10, express the model.

$$D \frac{\partial^2 n}{\partial x^2} = \frac{\partial n}{\partial t} + \frac{\partial N}{\partial t}, \quad (2.9)$$

$$\frac{\partial N}{\partial t} = \gamma n - \beta n. \quad (2.10)$$

Here, n = number density of mobile molecules,

N = number density of bound molecules,

γ = probability per unit time, during which a bound molecule of water becomes mobile, and

β = probability per unit time that a mobile molecule of water became bound.

2.3.2 Effect of Moisture Absorption on Mechanical Properties

Water absorption results in the depression of morphological characteristics of plastic materials and loss of useful mechanical properties. Mechanical degradation of amine cured epoxy resin matrix by water is due to the formation of microcavities, and long-term exposure of the epoxy resin to high humidity [43]. Maggana and Pissis [42] concluded that in neat epoxy resin, degradation begins with water uptake, swelling and leaching of non-bound substances. The hydrolytic degradation of epoxy results from the scission of the polymer chain, which leads to a progressive reduction in molecular weight. Although relatively short-term exposure can lead to more or less reversible plasticization, more prolonged exposure to moisture can lead to crack growth and loss of material. Loss in tensile properties occurs rapidly after aging at higher temperatures and relative humidities. Elongation shows similar trends, although the loss of elongation is even more rapid. Lucas *et al.* [14,15] studied the variation in mechanical property of water

saturated epoxies with different exposure temperatures. They found that water absorption affected the tensile and flexural modulus of the polymer. Their results showed a decrease in the modulus after immersion in water for more than 1500 hours.

One primary advantage of thermoplastic resin over thermosetting composites is its negligible moisture absorption and reprocessing capabilities. Further, comparing the effect of moisture on the compressive properties of thermosetting and thermoplastic composites, it was found that the compressive strength and modulus of graphite reinforced thermoplastic APC-2 composites are comparatively higher than those of T-300 epoxy composite [16]. The physical impact of the absorbed moisture is to degrade the mechanical properties of the polymer [45-48] mainly in compressive strength where, failure is in the form of delamination, global specimen buckling, shear failure, and end brooming. Moisture also modifies the damping properties of the material.

CHAPTER 3

THERMO-OXIDATION OF CYANATE BASED POLYMER MATERIALS

3.1 Experimental Procedures

3.1.1 Materials Description

The materials used for this study were Hexcel 954-3, cyanate ester, (dark brownish-green colored) and Hexcel 996, siloxane modified cyanate ester, (light orange-brown colored). Hexcel 954-3 is a 350⁰F (177⁰C) curing cyanate ester resin with glass transition temperature (190⁰C) and excellent resistance to moisture absorption, outgassing and microcracking. Hexcel 954-3, cyanate ester chemically comprises of one or more formula of the general formula $\text{NCOAr}(\text{Y}_x\text{Ar}_m)_q\text{OCN}$, where $m = 0$ to 5, $q = 0$ to 5 and $x = 0$ up to 2. Ar is a single or fused aromatic or substituted aromatic linked onto the ortho, meta or para positions and Y is the linkage unit selected from the group consisting of oxygen, carbonyl, sulphur, sulphur oxides etc. Hexcel 954-3 also contains inorganic species that are advantageously combined with and bonded to the cyanate ester resin. The inorganic species may be amine, hydroxyl, epoxy, silicon, zirconium, aluminum, etc. Hexcel 954-3 cyanate ester having this composition show enhanced oxidation resistance, enhanced toughness and high glass transition temperature [22]. The schematic diagram of Hexcel 954-3 CE is shown in Figure 3.1

Hexcel 996, SMCE contains inorganic species such as siloxanes, which combines and bonds to the cyanate ester system. The siloxane molecular weight was about 4500. The inorganic species may be present in the resin body (cyanate ester functional monomers or oligomers) from 0.1 to 80 weight percent, preferably 1 to 50 weight percent and most preferably 1 to 30 weight percent. The siloxane inorganic species contain about 50-70

mole percent of methyl and 30-50 mole percent of phenyl groups present as substitutional groups. The schematic diagram of Hexcel 996, SMCE, is shown in Figure 3.2

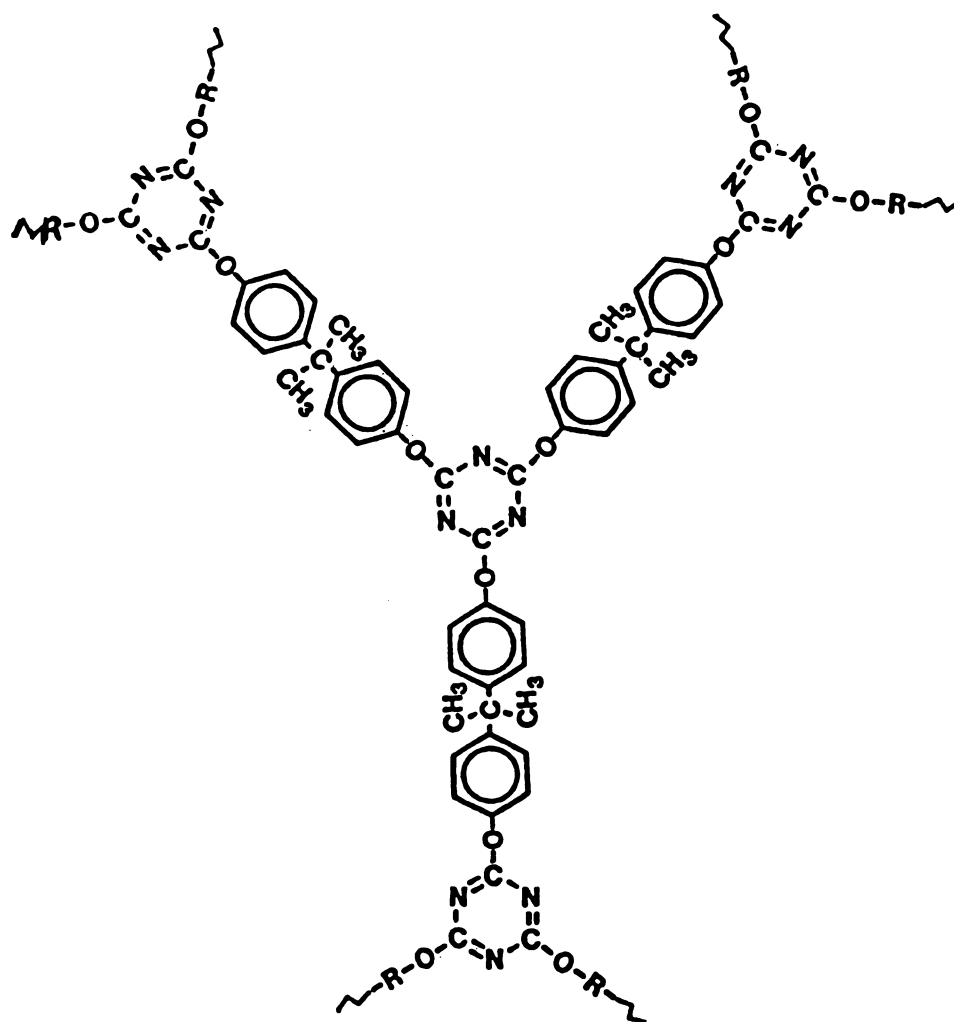
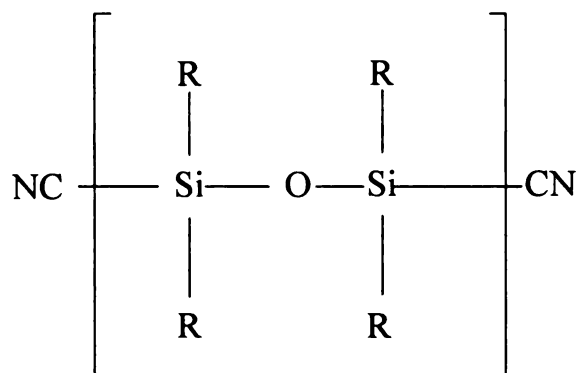


Figure 3.1 Schematic Structure of Cyanate Ester Network [1].



R = Pendant group
n = 4500

Figure 3.2 Schematic structure of siloxane modified cyanate ester [1].

Typical properties of Hexcel 954-3 cyanate ester resin and Hexcel 996 siloxane modified cyanate ester obtained from Hexcel's data sheet, are listed in Table 3.1 and Table 3.2 below.

Table 3.1 Typical physical properties of 954-3 CE resin at room temperature *.

PROPERTIES	RT
Tensile Strength	57 MPa
Tensile Modulus	2.8 GPa
Tensile Ultimate Strain, %	2.4
Flexural Strength	119 MPa
Flexural Modulus	3.0 GPa
Density	1.19 g/cc

Table 3.2 Typical physical properties of 996 SMCE resin at room temperature *.

PROPERTIES	RT
Tensile Strength	51 MPa
Tensile Modulus	3.0 GPa
Strain (%)	1.7
Flexural Strength	132 MPa
Flexural Modulus	3.2 GPa
Density	1.146 g/cc

* Hexcel's Manufacturer Data Sheet dated 3/23/99 and 3/20/98 respectively.

3.1.2 Preparation of the samples

Cyanate ester and siloxane modified cyanate ester were obtained in the form of neat resin panels from Hexcel Inc. The panels were polished on a lapping wheel to remove contaminants such as grease, mold release agents from the surfaces of the laminates. The laminates were further cut into samples of sizes 25.4 mm × 25.4 mm × 2.2 mm dimensions and 12.5 mm × 12.5 mm × 2.2 mm dimensions respectively using a diamond saw. The samples of size 12.5 mm × 12.5 mm × 2.2 mm dimensions were used for the thermo-oxidation experiments. The edges of the samples were subsequently ground using 600 grit abrasive papers to achieve consistently smooth edge surfaces. The sample surfaces were polished on polishing wheel containing silicon carbide and alumina as the polishing medium. All samples were marked with a vibrating pen and further cleaned in methanol using ultrasonic cleaner. The initial weight of the samples ranged from 2 to 2.5 gm. The samples were handled very carefully during the experiments to avoid any surface contaminations.

3.1.3 Gravimetric Experiments

Samples were tested in environmental test chambers, consisting of gaseous aging environment of ambient air maintained at 60⁰C, 80⁰C and 100⁰C with a fluctuation range of ±1⁰C. Gravimetric experiments were used to monitor weight change of specimens during thermal aging. Polymer samples were exposed to the aging environment for ~ 1200 h.

Samples were taken out of the environmental test chamber periodically during the aging experiment. Samples were weighed using the analytical electronic balance with 0.01 mg resolution. The experimental error of the measurement is $\pm 0.02\%$.

The percentage weight change is calculated as follows:

$$\Delta w \% = \left(\frac{w_t - w_0}{w_0} \right) \times 100 \quad (3.1)$$

3.1.4 Glass Transition Temperature Measurement Using DSC

The glass transition temperature of CE and SMCE for different stages of thermal aging was determined using a TA Instruments™ 930 differential scanning calorimeter (DSC) system [49]. DSC is used to determine the temperatures of thermal events such as glass transition, melting, phase transformations, Curie point transitions, reactions (including decomposition, devolatilization, crosslinking, etc). The heat liberated or consumed during these events, such as heat of fusion and heats of reaction, can also be accurately determined along with the specific heat capacity. The measurements from DSC provide quantitative as well as qualitative information about the physical and chemical changes that the sample undergoes. They include both endothermic (heat absorbed) and exothermic (heat released) processes. The DSC uses a two pan system, where the sample is placed in one pan and the other pan is left empty as a reference. Sample size is usually between 5-15 grams of the material. In the power compensated DSC the two pans are heated separately in a way that they achieve the same temperature simultaneously. In heat flux DSC the two pans are exposed to the same heat source and

the temperature difference between the two is measured. In either case, the objective is to measure the amount of energy absorbed or released from the polymer sample. The resulting exothermic or endothermic energy requirements for the sample are plotted against the temperature [50]. Modulated DSC method was utilized to obtain the T_g of CE and SMCE samples. Modulated DSC produces three signals consisting of heat flow, reversible heat flow and non-reversible heat flow. The T_g is obtained from the transition observed in reversible heat flow. The advantage of temperature modulated DSC is improved resolution and sensitivity, and the ability to separate overlapping phenomena.

The sample size used in this glass transition temperature (T_g) experiment varied from 3-15 mg. The samples were sealed in small aluminum pans to prevent any weight loss during the experiment, and the weight of each sample pan was measured before and after each test. The samples were put into testing chamber protected by pure nitrogen gas. The temperature range for heating was maintained between 25⁰C to 250⁰, and the temperature increase rate was 5⁰C/min. The T_g values were obtained by the intersection of two tangential lines of the DSC curves, which was automatically determined by the instrument's software. These measurements were obtained before and after the glass transition temperature regime [49].

3.1.5 Glass Transition Temperature Measurement Using TMA

Thermomechanical analysis (TMA) measures variations in the vertical displacements of a probe resting on top of a sample and is used to obtain physical property changes as a function of temperature and time. Some of the properties obtained by using TMA are thermal expansion, phase changes, glass transition temperature, melting temperatures, dimensional stability, modulus, compliance and deflection temperature under load and vicat temperature. TMA used for thermoset materials show typically two linear region, the first one associated with the glassy state and is followed by a change to a second linear region of higher slope associated with the rubbery state because of T_g [50]. The coefficient of thermal expansion and T_g of a thermoset are closely related to the degree of cure of the resin. Size of the samples used in this glass transition temperature experiment had the dimensions of 12 mm \times 8 mm \times 2 mm. The samples was held by the TMA probe in the vertical position. Precautions were taken to see that the sample did not touch the thermocouple during each test. They were enclosed in a furnace having an oxygen environment. The temperature range for heating was maintained between 25⁰C to 250⁰, and the temperature increase rate was 4⁰C/min. TMA profile of the material exhibits stress relief. Thermal cycling or annealing above T_g will smooth the curve but will not elevate T_g . Ideally, T_g is observed as an abrupt change in the slope of the linear expansion versus temperature curve. However, as often, relaxation occurs near T_g , the transition can be broad, depending upon such factors as cure state, internal stresses and test conditions.

3.1.6 FTIR Testing

Fourier transform infrared spectroscopy was used to determine the change of chemical structure of cyanate ester and siloxane modified cyanate ester materials associated with bonding characteristics at various stages [51]. A Bio-Rad, Excalibur Series FTIR was used for this study. The samples of dimensions 12.5 mm × 12.5 mm × 2.2 mm were polished to 0.25 mm film thickness. These thin films were aged in environmental thermal aging chambers in ambient air at 100°C for different periods of time up to 500 h. The sample was periodically removed from the chambers and allowed to cool to room temperature before transferring to a holder designed for FTIR testing. The FTIR scans for each sample in the thermal aging experiment were obtained. The peaks for (-C=C-H-) at 966 cm⁻¹ and at 911 cm⁻¹ were studied. Skeletal stretching at 1017 cm⁻¹ peak and between 2220-2250 cm⁻¹ for (-RNCO-), and changes in the aromatic ring at 810-820 cm⁻¹ were also studied. Thermal aging also showed changes in the carbonyl group (-O-C=O-) at 1726 cm⁻¹ peak.

3.1.7 X-ray Photoelectron Spectroscopy (XPS) Testing

X-ray photoelectron spectroscopy is a surface sensitive technique, which allows the determination of the elemental composition and binding energies of the elements in a depth of a few nanometers. XPS is based on photoelectric effect. When the polymer material is exposed to electromagnetic radiations of sufficient photon energy, photoelectrons are emitted. The XPS technique is highly surface specific due to the short range of the photoelectrons that are excited from the solid. The ejected electrons are then separated in an electrostatic spectrometer according to their energies ranging from 0-1100 eV. The energy of the photoelectrons leaving the sample was determined using a

concentric hemispherical analyzer giving rise to arbitrary count intensity versus binding energy spectrum. The binding energy of the peaks was characteristic of each element. The peak areas can be used (with appropriate sensitivity factors) to determine the composition of the materials surface. The shape of each peak and the binding energy can be slightly altered by the chemical state of the emitting atom [52]. Surface analysis was performed using a Perkin-Elmer Physical Electronics PHI5400 ESCA Spectrometer equipped with a standard magnesium X-ray source operated at 300 W (15 kV and 20 mA). Data was collected in the fixed analyzer transmission mode utilizing a position sensitive detector and hemispherical analyzer. The elemental composition of the surface was determined from survey spectra collected using pass energy of 89.45 eV. High-resolution spectra of the elements were obtained using pass energy of 22.5 eV and a step size of 0.1 eV. Binding energies were referenced to adventitious carbon and were measured with a precision of ± 0.1 eV.

3.1.8 Three-point Bend Test

The three point bend flexure testing was performed to study the effects of thermo-oxidation on mechanical properties of both CE and SMCE. The standard procedure (ASTM D790-90) was used as a guide for specimen preparation and testing. A representative sample size of six specimens was tested for each aging conditions consisting of as-received samples that were aged for 200, 500 and 900 hours respectively. Bend tests were conducted using Instron[®] screw driven mechanical test machine, with a 2000-lb load cell. The nominal specimen dimensions used in this study were 25.4 mm long and 7-8 mm wide and 2 mm thick. A crosshead speed of 10 mm/min was used in the test. The flexural strength was calculated by formula

$$S = \frac{3PL}{2bd^2} \quad (3.2)$$

Where, S= flexure strength (MPa)

P= breakload (KN)

L= outer (support) span (mm)

b = specimen width (mm)

d = specimen thickness (mm)

3.1.9 Microhardness testing

Hardness is the resistance of a material to local plastic deformation. Microhardness testing is an indentation method for measuring the hardness of a material on a microscopic scale. Microhardness has been successfully used to characterize metals and ceramics, where it has been shown to be sensitive to the chemical and microscopic structure of materials studied. A precision diamond indenter is impressed into the material at loads from 1 to 1000 gm. The indenter was forced into the specimen until a predetermined load of 10 gm was achieved. The impression length, measured microscopically, and the test load are used to calculate a hardness value. The indentations are made using a square-based pyramid indenter, on Vickers hardness scale. The indent can be precisely located with the microscope and its dimensions can be determined. Typically, the samples used for this study had the dimensions of 6.5 mm × 6.5 mm × 2.2 mm. The sample size of six specimens was tested for each aging condition. The Vickers hardness number was then computed using

$$HV = 1.854 \frac{P}{S^2} \quad (3.3)$$

where, P = applied indentation load (grams)

S= diagonal of indentation (μm)

3.2 Results and Discussions

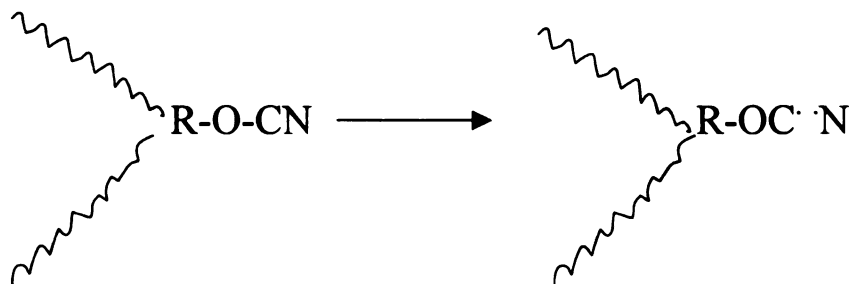
3.2.1 Assessment of Thermal Aging Effects of CE and SMCE Resins

3.2.1.1 Gravimetric Analysis

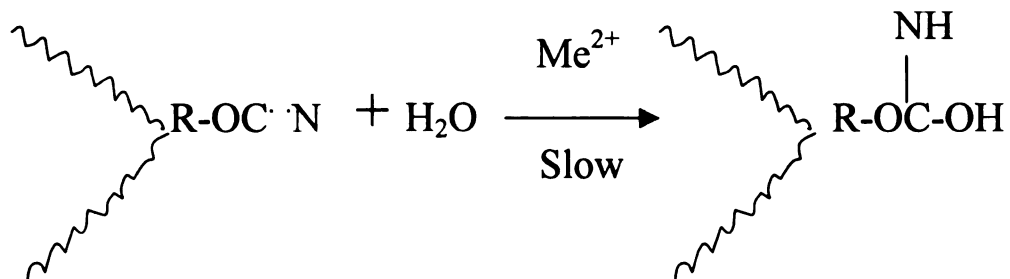
Gravimetric experiments were used to monitor the weight change of the specimens during thermal aging. The weight change of CE and SMCE are shown in Figure 3.3-3.7. CE specimens showed a weight reduction in the initial stages of thermo-oxidation and followed with weight gain after 9 hours of exposure. The initial weight loss is due to desorption of the moisture absorbed mostly on the specimen surface, while the gain in weight is due to the absorption of oxygen across the ester linkage. Shimp *et al.* [11] studied the thermo-oxidative degradation mechanism in CE polymer materials.

The following schematic diagram explains the thermal aging mechanism in CE

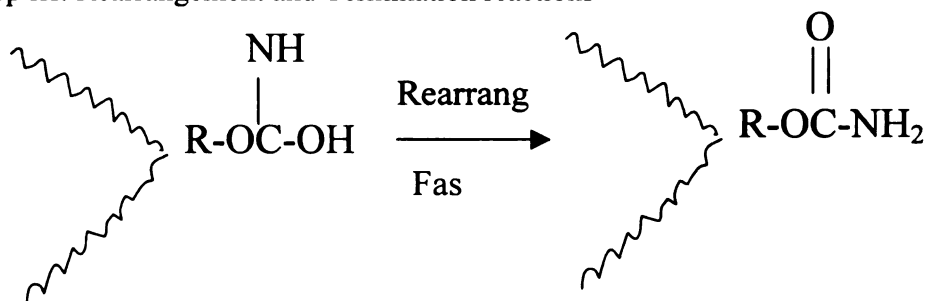
Step I: Thermal initiation of CE



Step II: Radical conversion



Step III: Rearrangement and Termination reactions



They proposed that the degradation mechanism began with the hydrolytic cleavage of the ester linkage, as shown in step I, and the subsequent attachment of oxygen across this ester linkage, as shown in step II, which resulted in gain of weight due to the absorption of oxygen by the polymer matrix. The radicals generated in steps I and II rearrange quickly generating a stable form of carbamate group. Here, the decomposition of hydroperoxides and the rearrangement step is a very important step in the polymer oxidation because the formation of oxidation products is caused by the degradation of these radicals. The thermal degradation and rearrangement of the hydroperoxides can

break down the polymer chain, forming new chemical groups such as carbonyl as shown in step III.

On the other hand, SMCE did not gain a significant amount of weight during thermal aging but the initial loss in weight seen in the Figure 3.4 for SMCE, is due to the desorption of moisture absorbed on the specimen surface. Figure 3.3 and Figure 3.4 show the thermo-oxidation curves for CE and SMCE respectively. These curves also compare the thermo-oxidation process in CE and SMCE at different temperatures. Figure 3.5-3.7 compare the thermo-oxidation process for CE and SMCE at each aging temperature.

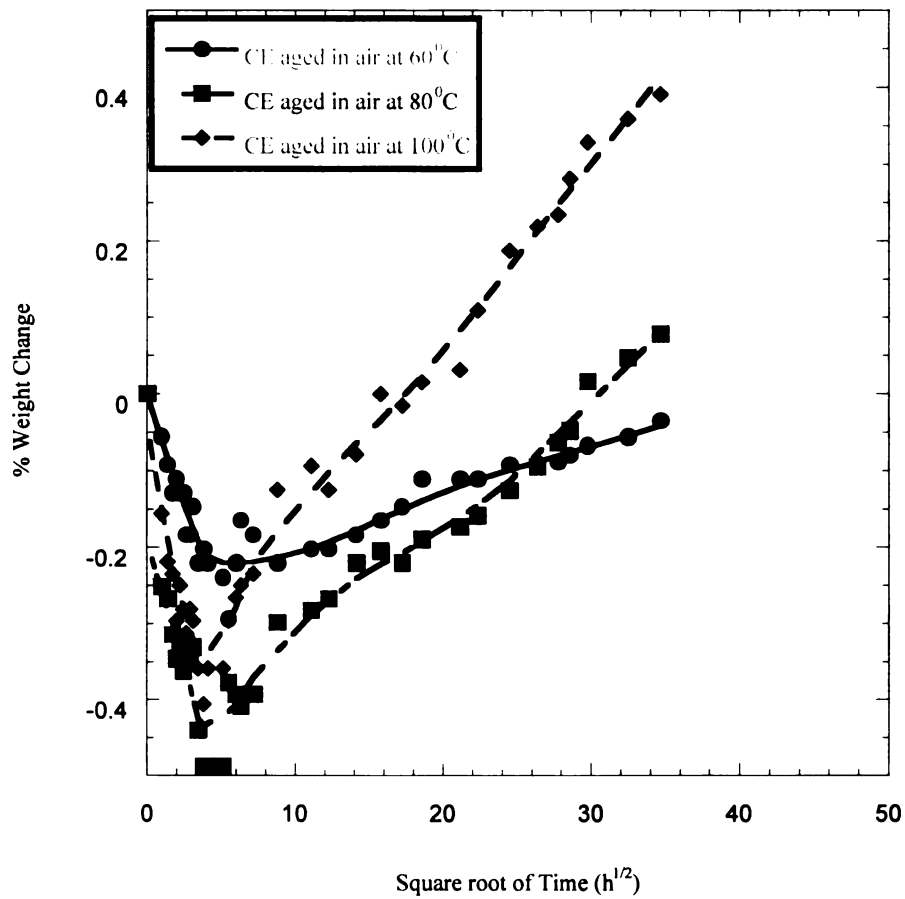


Figure 3.3 Comparison of % weight change for CE polymer when aged in air at 60°C, 80°C and 100°C, respectively for 1200 hours with square root of time.

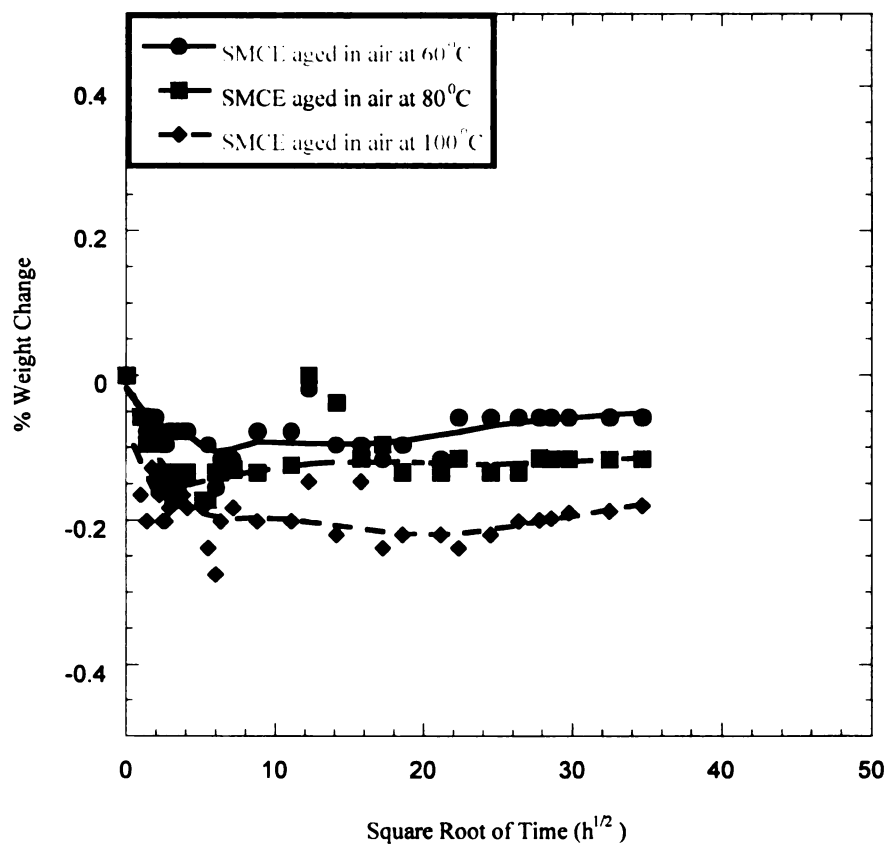


Figure 3.4 Comparison of % weight change for SMCE polymer when aged in air at 60°C, 80°C and 100°C, respectively for 1200 hours with square root of time.

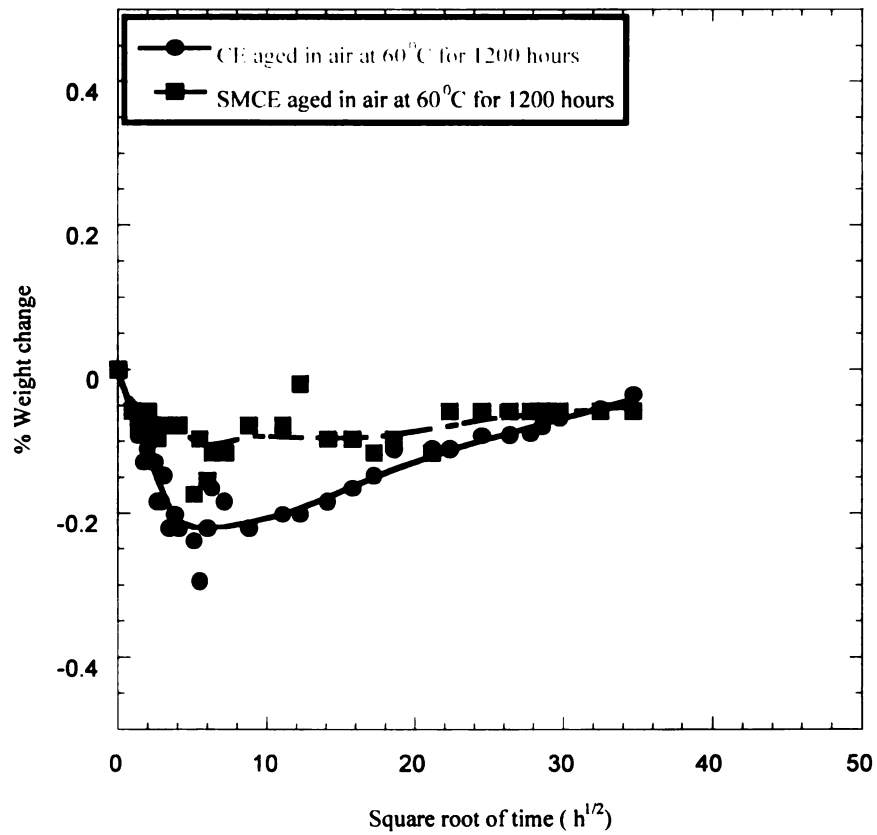


Figure 3.5 Comparison of weight change in CE and SMCE aged in ambient air at 60°C for 1200 hours with square root of time.

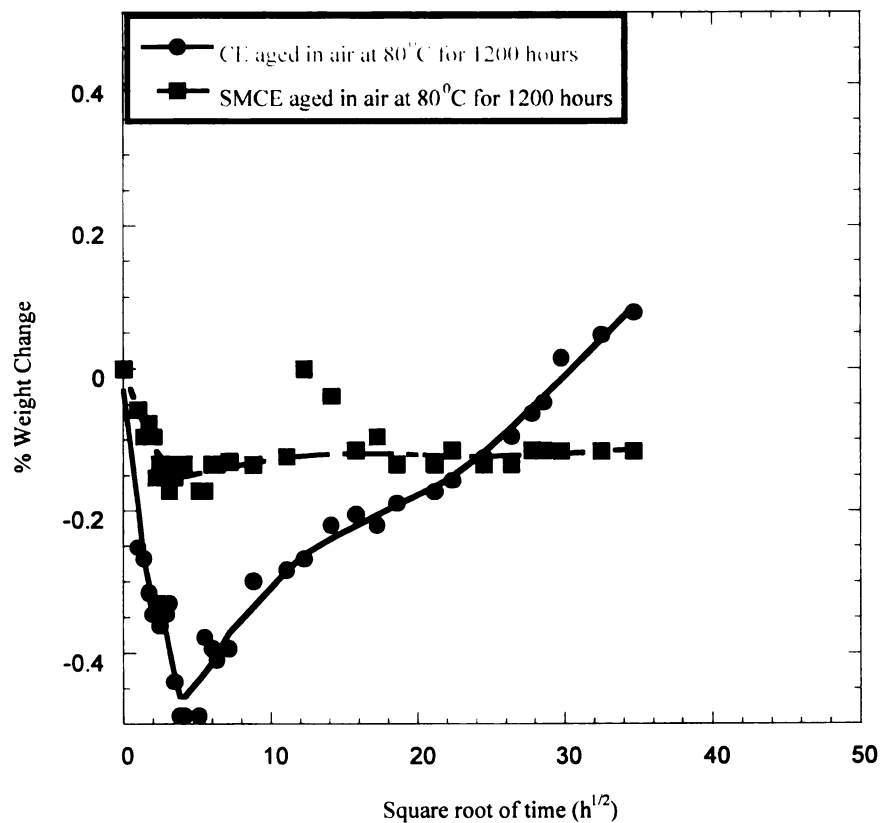


Figure 3.6 Comparison of weight changes in CE and SMCE aged in ambient air at 80°C for 1200 hours with square root of time.

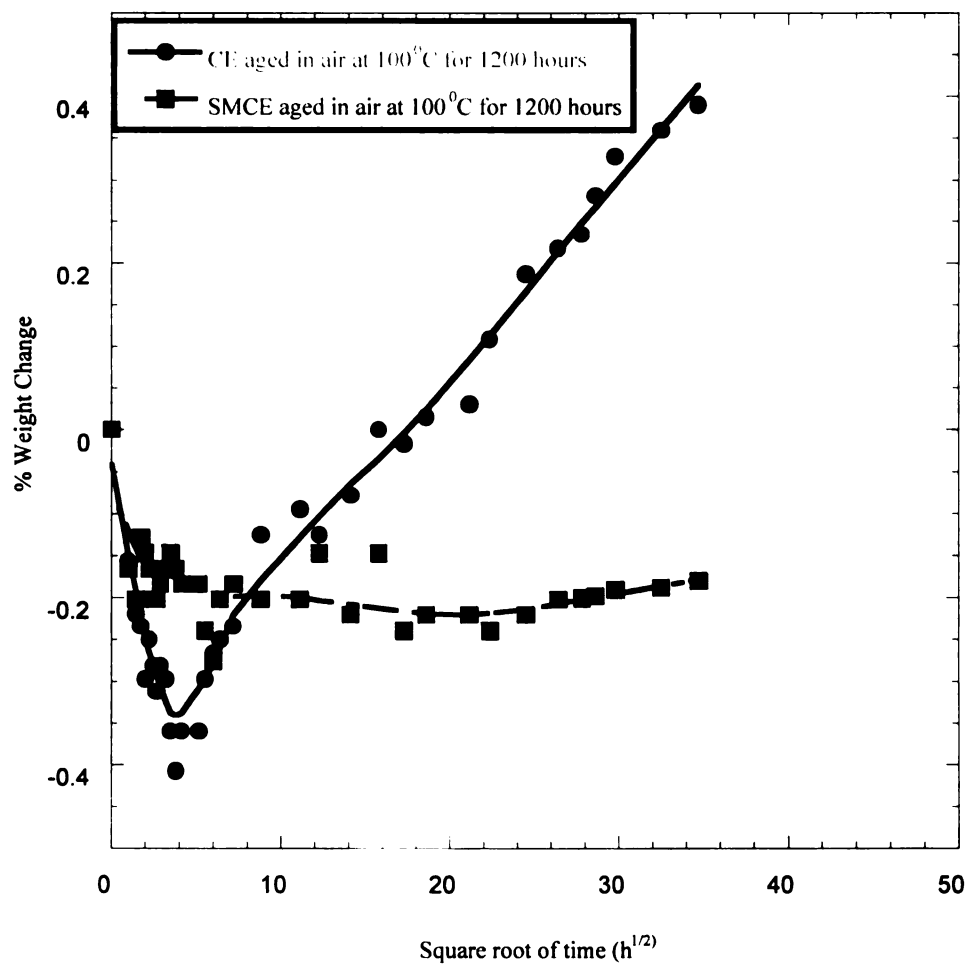


Figure 3.7 Comparison of weight change in CE and SMCE aged in ambient air at 60°C for 1200 hours with square root of time.

Figure 3.3, shows the thermal aging curves for cyanate ester (CE) polymer aged at different temperatures of 60⁰C, 80⁰C, and 100⁰C respectively. Gravimetric results show a greater increase in weight for CE aged in air at 100⁰C as compared to the CE samples aged in air at 80⁰C and 60⁰C. McKellop *et al.* [53] studied the oxidation in irradiated polyethylene. They observed that oxidation in polyethylene was confined only to the amorphous regions as crystalline cores were inaccessible to molecular oxygen. As a result amorphous regions continued to undergo oxidative chain scission accompanied by increase in oxidation. The high temperature also results in chain scissions of the polymer chains, which encourage the diffusion of oxygen at a faster rate. Thus, thermal aging of cyanate ester involves two basic mechanisms: (a) the diffusion of oxygen into the cyanate ester matrix and, (b) the chemical reaction associated with the free radicals. The thermal stability of polycyanurates varied depending on the nature of the bridging group. Polycyanurates of higher molecular weight showed excellent thermal stability and thermal degradation or crosslinking of the molecular chain, in polycyanurates containing alkoxy, piperidyl, chloro or phenoxy substituents in the s-triazine nucleus [56]. The resin was found to lose weight completely only at higher temperatures of 360-375⁰C. Here the loss in weight indicates the total degradation of the resin above the glass transition temperatures. This degradation process proceeds in several stages and is accompanied by weight loss amounting gradually to 95% of the initial value. At very high temperatures, almost or above glass transition temperature, degradation products of cyanate ester consist mainly of volatile products like carbon dioxide, carbon monoxide, hydrogen, phenols and bisphenols. In our experiment, thermo-oxidation takes place at a temperature of 100⁰C, which is much lower than the glass transition temperature. At this

temperature, the molecules generated by the thermo-oxidation reaction are likely to stay in the polymer, increasing the weight of the samples. In this case the weight gain is due to the consumption and retention of absorbed oxygen molecules. Similarly, we observed the thermal aging in siloxane modified cyanate ester polymer in Figure 3.4. SMCE also tends to lose weight at the initial stages of thermo-oxidation process, which indicates that there is desorption of moisture during the early stages of the aging. Later, as the thermo-oxidation process proceeds for 1200 hours we observe that there is no change in the weight of the sample with aging time. SMCE also remained unaffected by changes in aging temperatures. The thermal properties of SMCE depend on the nature of the pendant groups on the silicon atom [53]. Substitutional groups like phenyl group and methyl group present on the backbone of SMCE polymer chains raises the oxidative stability of the polymers. Pendant groups on the SMCE backbone increase the intermolecular forces because of its weak polarity in addition to steric hindrance. The intermolecular forces between the chains facilitate rigid crosslinking between the chains, thereby increasing the stability of SMCE to thermal aging. Figures 3.5-3.7 compare the thermal aging for CE and SMCE for each of the aging temperatures. These plots indicate that the weight of the CE samples progressively increased with aging time for all the aging temperatures. This showed that oxygen consumption increased with increase in aging temperature. On the other hand, SMCE showed no gain in weight as compared to CE pure resin. Furthermore, surface color of both the samples changed with aging. Further optical examination of the specimen showed that the discoloration started on the surface and moved gradually to the specimen's interior indicating that thermal aging is a surface phenomenon. As the aging time increase more and more chain decomposed

causing scission and thus increasing the diffusion of oxygen. Only initial weight loss was observed in SMCE, which indicated that the loss in weight was due to the evaporation of moisture absorbed on the specimen's surface.

Results of thermal aging of CE and SMCE materials are presented in Figures 3.8-3.10.

These figures represent the change in weight for CE and SMCE materials due to thermal aging with square root of time. Figure 3.8 shows the change in weight due to thermo-

oxidation in case of CE polymers. The weight change depends on diffusion rates of oxygen into the polymer, which is dependent on the temperature and aging time. The

slope for CE at 100⁰C is higher as compared to the slopes for CE aged at 80⁰C and 60⁰C respectively. This also indicates that the diffusion rate is higher in CE at higher

temperatures. Uzomah *et al.* [55] studied the effects of time and temperature on the

tensile yield properties of polypropylene. They found that, higher aging temperature

needed a smaller time interval to cause significant reduction in the properties. At longer

time intervals and higher temperature, faster rates of chain scission and volatilization of products occurred decreasing the crosslinking density leading to deterioration of the

polymer. Figure 3.9 shows the changes in weight due to thermal aging of SMCE

polymer materials. No change in the slopes of the plots, indicating that the diffusion

rates of oxygen in SMCE polymers maintained between 60⁰C and 100⁰C remained

relatively flat throughout the thermal aging process. Figure 3.10 shows the comparison in

weight change for CE samples aged in air at 60⁰C, 80⁰C and 100⁰C respectively, and for

SMCE polymer samples aged in air at 60⁰C for 1200 hours. CE showed change in

weight with aging time and temperature during thermal aging indicating that diffusion

rates of oxygen into the CE polymer depended on aging temperature, while SMCE showed no change in weight for all aging times and temperatures used in this study.

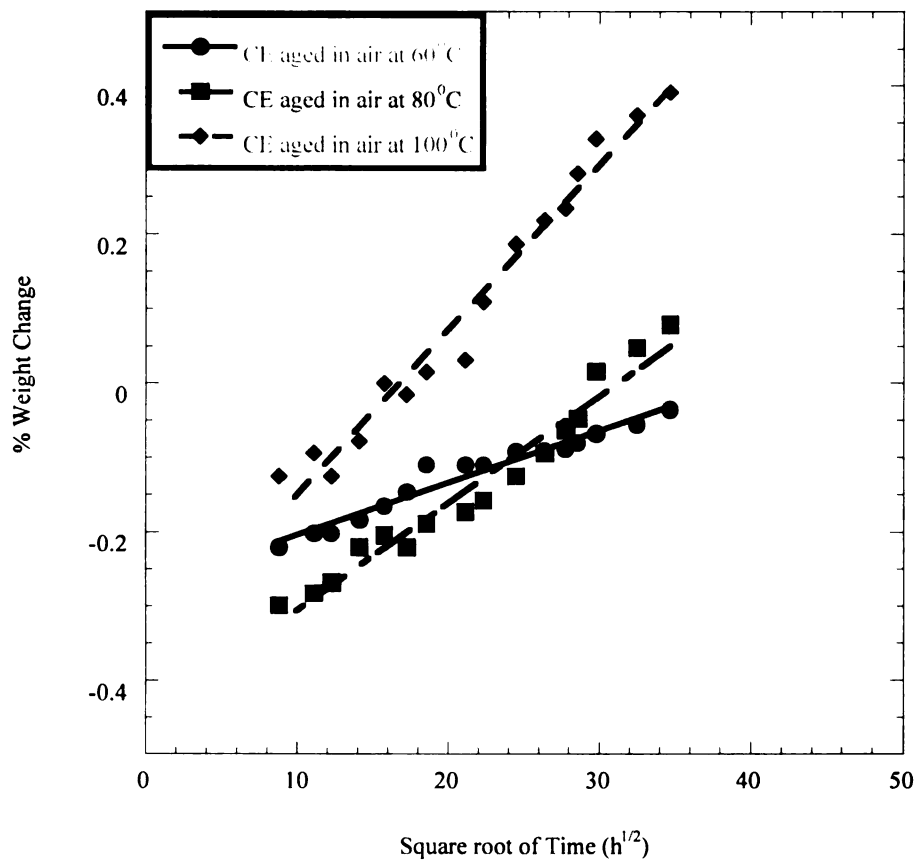


Figure 3.8 Comparison of diffusion rates of oxygen in CE polymer when aged in air at 60⁰C, 80⁰C, and 100⁰C respectively for 1200 hours with square root of time.

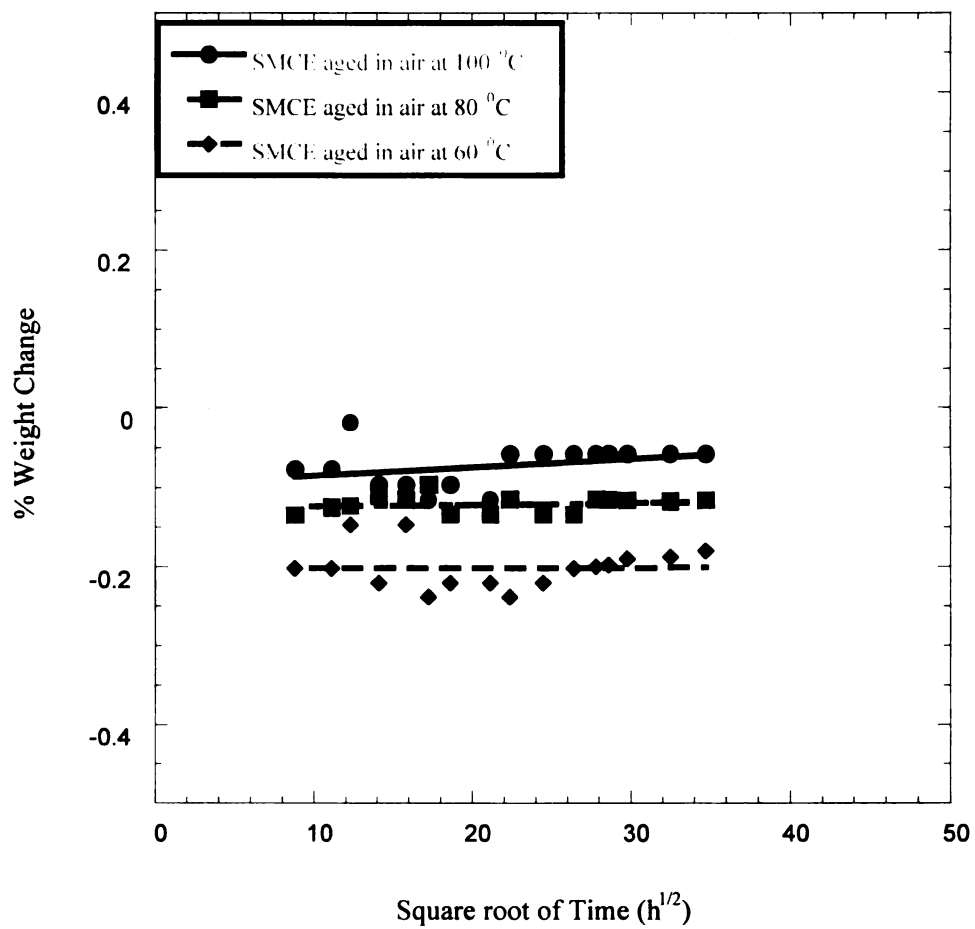


Figure 3.9 Comparison of diffusion rates of oxygen in SMCE polymer when aged in air at 60⁰C, 80⁰C, and 100⁰C respectively for 1200 hours with square root of time.

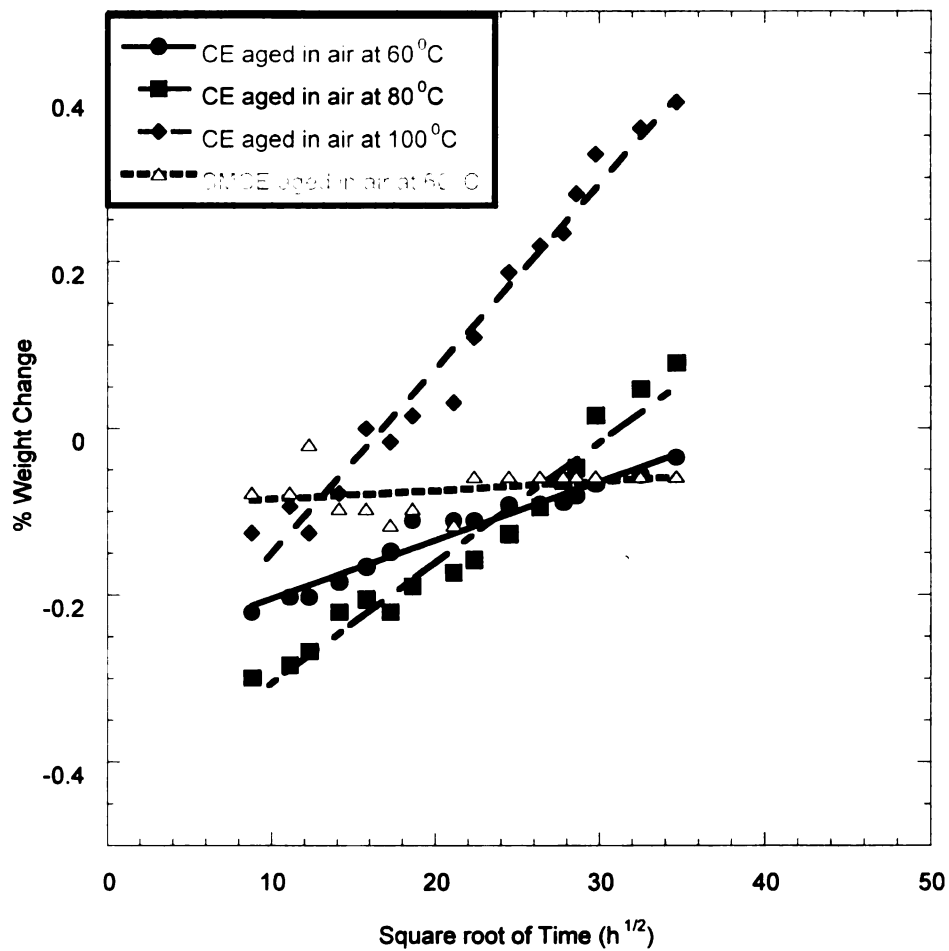


Figure 3.10 Comparison of diffusion rates in CE when aged in air at 60°C, 80°C and 100°C respectively for 1200 hours and SMCE aged in air at 60°C for 1200 hours with square root of time.

Basically, thermo-oxidation of polymers involves two steps

- (i) The diffusion of oxygen into the polymer material and
- (ii) The reaction of oxygen with the polymer network groups.

Thus, the rate of thermo-oxidation is usually controlled by one of these two steps. For the aging process the weight change is found to be proportional to the square root of time, $t^{0.5}$ [56]. Nam *et al.* [56] showed in their investigations that the thermo-oxidation is controlled by the rate of diffusion of oxygen into the polymer network. Their study was based on the weight change observed in bismaleimide/carbon fiber composite during the thermo-oxidation process, which was controlled by oxygen diffusion, and the reaction rate was found to be proportional to $t^{0.5}$. Similarly, results of the current study indicate that the thermo-oxidation was definitely controlled by the rate of oxygen diffusion into the resin matrix.

3.2.1.2 Glass Transition Temperature Using DSC

To evaluate the thermal aging of SMCE and CE samples in this investigation, we aged the samples at 100°C over a period of 900 hours and measured the glass transition temperature over this period of time. For this purpose differential scanning calorimeter (DSC) was utilized. The results are shown in Table 3.3 and 3.4. Table 3.3 illustrate that the glass transition temperature of CE remained the same when aged in air at 100°C for 900 hours. Table 3.4 shows that the glass transition temperature of SMCE also remained virtually unchanged when aged in ambient air at 100°C for 900 hours. SMCE shows no

degradation when aged in air. Paravatareddy *et al.* [2,5] also conducted numerous experiments on the physical aging of cyanate ester polymers. Their results showed a decrease in glass transition temperature of CE by 10-30% when aged in air for 3 months at 150⁰C. There is a decrease in glass transition temperature for CE polymers on the surfaces of the samples but as we proceed towards the interior of the samples from the surface the T_g remained unchanged. This difference can be well explained by the changes in the chemical structure of CE polymers on the surface of the sample. The CE molecules on the surface undergo a chemical change, which is attributed to the chain scission occurring in the amorphous regions of the polymer matrix due to diffusion and consumption of oxygen across the surface. Another possible reaction could occur here. These polymers would have long chains with free end groups, which have highly reactive polar groups that are susceptible to oxidation. On chain scission the polymer molecules obtained higher mobility, which resulted in the decrease in the T_g of the polymer on the surface of the polymer sample.

Shanahan *et al.* [59] studied the influence of gaseous environments on the thermal degradation of structural epoxy adhesive. Their experiments showed that the initial glass transition temperature of the adhesive decreased very rapidly in the initial stages of aging in air strongly suggesting that rapid molecular chain scission occurred in the polymer adhesive. Gravimetric experimental results showed that CE gained weight. The gain in weight was attributed to the absorption of oxygen by the amorphous region entrapped in the rigid crosslinked chains in the polymer matrix, which means, that chain scission of the polymer molecules present on the surface of the sample had to occur in order to allow oxygen to enter the chains and chemically react with the chains [54]. Chain scission of

the long polymer chains results in the decrease of cross-linking density in the initial stages of thermal aging, and subsequent increase in segmental mobility, which results in the decrease of glass transition temperature for the polymer molecules on the surface of the polymer. The chain scission of CE polymer chains produces more flexible chains that are able to move, thus lowering T_g . As the thermal aging proceed for a longer duration of time, more and more polymer backbone chains attain mobility, resulting in decrease in glass transition temperature of the polymer resin on the surface. Eriksson *et al.* [60] studied the effects of thermo-oxidation aging on mechanical, chemical and thermal properties of recycled polyamide 66. They showed that the surface area of aged polyamide samples underwent more severe degradation than the interior. To confirm this, they studied the elongation at break for aged and unaged samples. They found a decrease in elongation properties as compared with unaged samples. Oxidation in thermosets was generally known to occur in the amorphous regions, but oxidations also occurred in the crosslinked regions, on their surfaces and boundary regions.

Table 3.3 Glass transition temperature of CE aged in ambient air at 100⁰C **

Materials (CE)	Time for aging (hours)	T _g (°C)
As Received	0	196.29 ⁰ C
Heated in air at 100 ⁰ C	100	194.76 ⁰ C
Heated in air at 100 ⁰ C	300	190.47 ⁰ C
Heated in air at 100 ⁰ C	900	196.21 ⁰ C

Table 3.4 Glass transition temperature of SMCE aged in air at 100⁰C **

Material (SMCE)	Time for aging (hours)	T _g (°C)
As Received	0	158.60 ⁰ C
Heated in air at 100 ⁰ C	100	161.52 ⁰ C
Heated in air at 100 ⁰ C	300	158.77 ⁰ C
Heated in air at 100 ⁰ C	900	160.84 ⁰ C

** The glass transition temperature (T_g) of the samples CE and SMCE were obtained for only one set of samples.

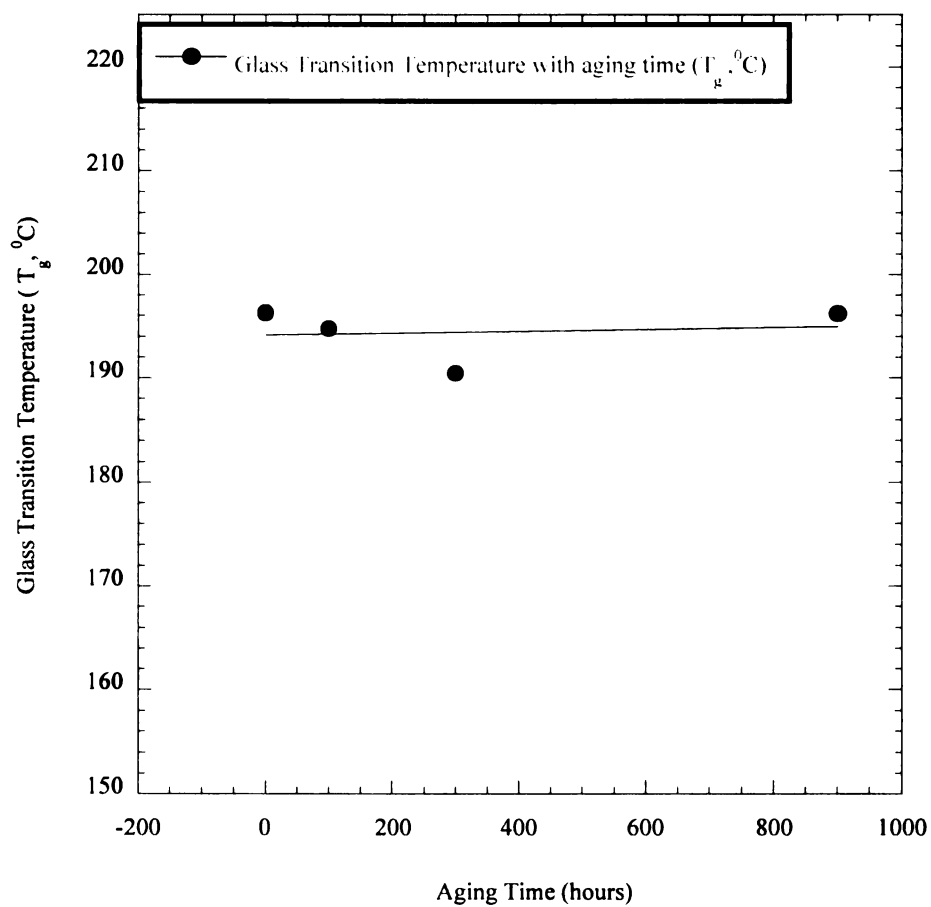


Figure 3.11 Changes in the Glass Transition Temperature of CE polymer with aging time

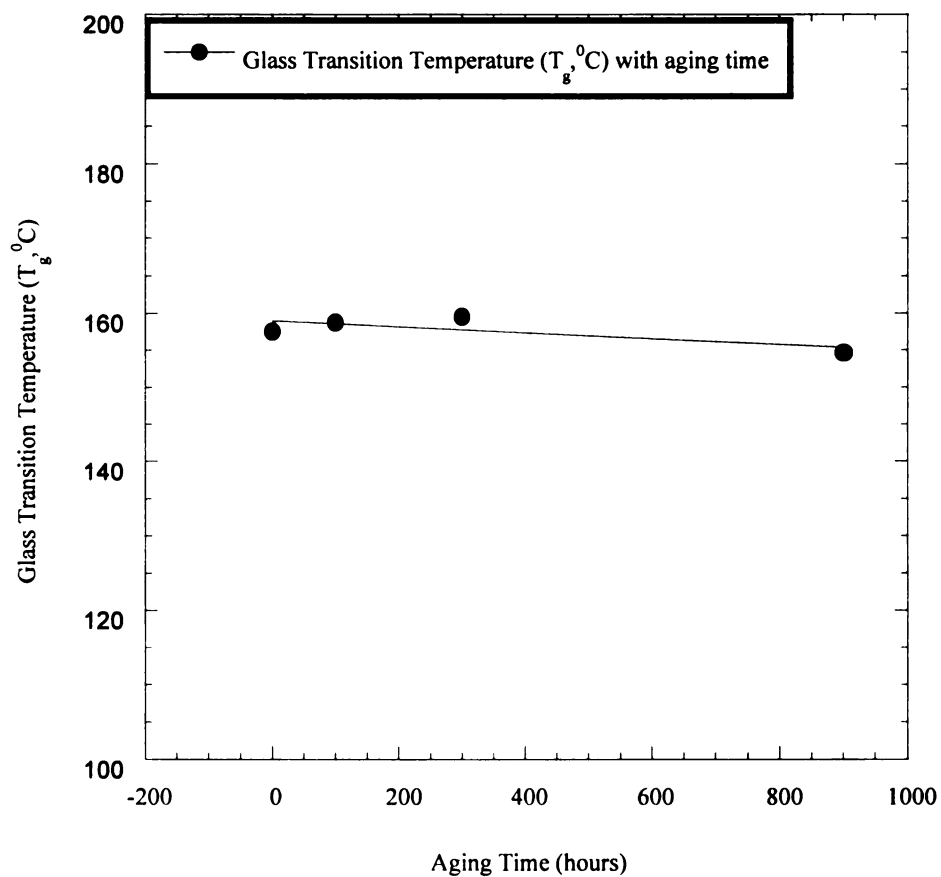


Figure 3.12 Changes in the glass transition temperature of SMCE with Aging time.

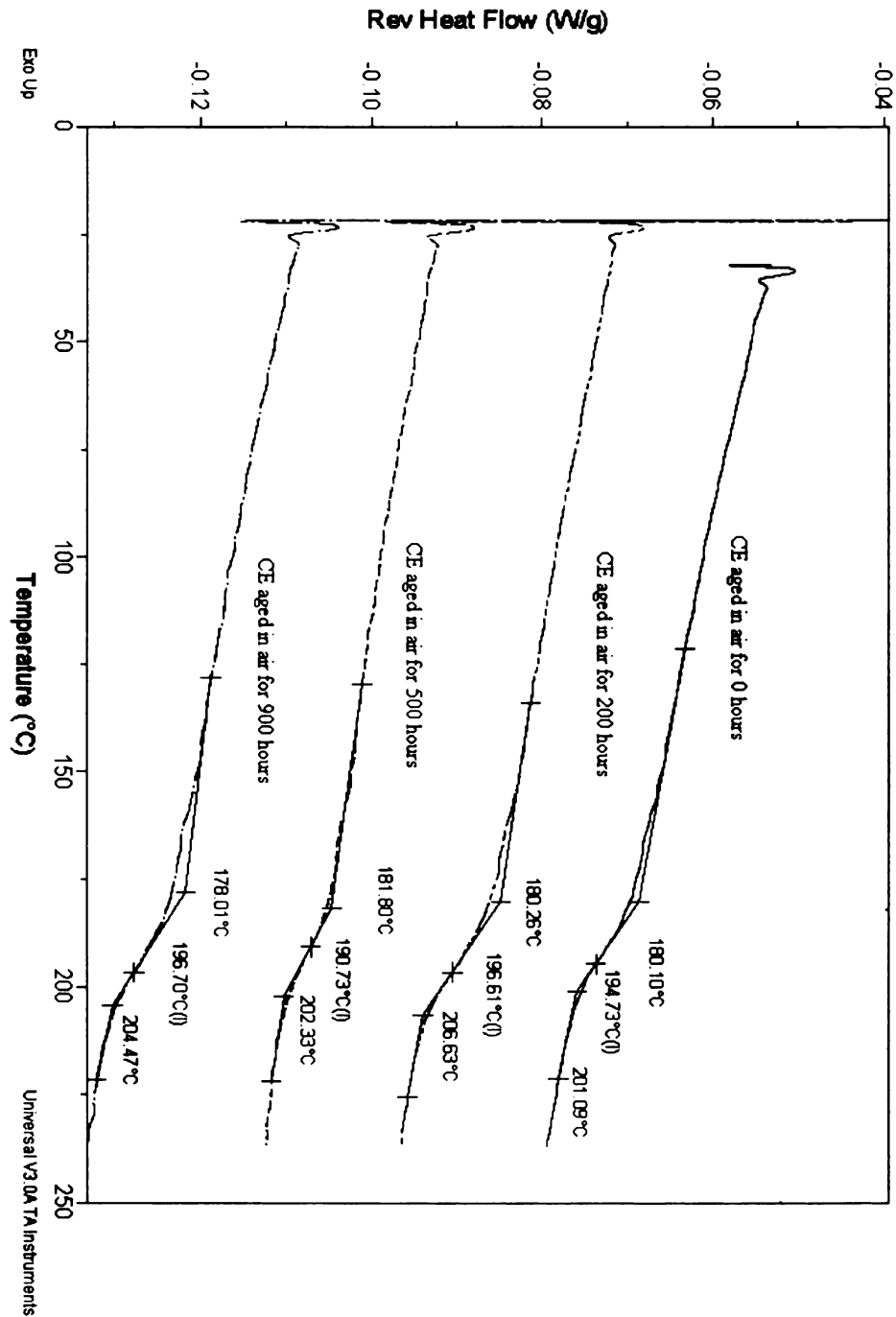


Figure 3.13 DSC scans showing the glass transition temperature for CE aged in air at 100°C for a period of 0 hours, 200 hours, 500 hours and 900 hours respectively

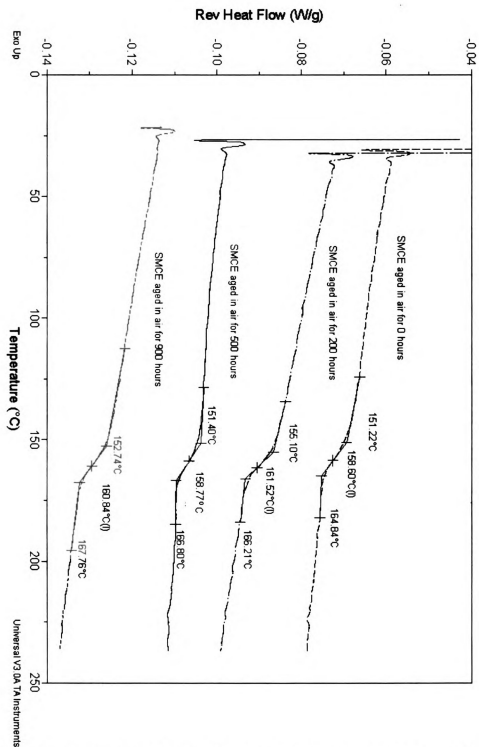


Figure 3.14 DSC scans showing the glass transition temperature for SMCE aged in air at 100°C for a period of 0 hours, 200 hours, 500 hours and 900 hours respectively

Figures 3.11 and 3.12 show the changes in glass transition temperature of CE and SMCE polymer materials during the thermo-oxidation process. Figure 3.11 indicates that the glass transition temperature of CE polymer is not affected by the thermo-oxidation occurring on the surface of the polymer sample. Higher diffusion of oxygen with increasing aging time, into the resin matrix causes chain scission on the surface of the sample, thus increasing the mobility of the backbone chain of the matrix and further resulting in decrease of glass transition temperatures in the surface regions of the polymer [59]. Figure 3.12 shows no change in glass transition temperature for SMCE with aging time. This indicates that SMCE does not undergo oxidation. The difference in thermo-oxidation degradation in SMCE and CE is related to their chemical structure. The chemical structure difference of SMCE and CE suggests that the thermal degradation of CE is due to the oxidation occurring across the (-OCN-) group in the triazine structure, which involves the chain scission of the molecules, while in case of SMCE the polymer forms a rigid structure thus impeding the diffusion of oxygen into the matrix. The DSC scans on Figures 3.13 and Figure 3.14 show the glass transition temperatures for CE and SMCE determined by the DSC software.

3.2.1.3 Glass Transition Temperature Measurement Using TMA

To study the thermal aging of SMCE and CE samples in this investigation, we aged the samples at 100⁰C over a period of 900 hours and measured the glass transition temperature over this period of time. For this purpose thermomechanical analysis was utilized. The results of glass transition temperature studies are shown in Figure 3.15 and Figure 3.16. Figure 3.15 shows that the glass temperature of CE remained virtually unchanged when aged in air at 100⁰C for up to 900 hours. In order to study the effects of thermal aging on glass transition temperature for CE aged in air at 100⁰C with thermal aging time, the experiments were further modified. The CE sample of size 12 mm × 8 mm × 2 mm was heated up to a temperature of 200⁰C with a ramp rate of 4⁰C / min and later cooled within the furnace to 100⁰C. The sample was once again heated to 250⁰C with a ramp rate of 4⁰C / min. The results for glass transition temperature obtained by the first run indicate that the T_g for CE remained virtually unchanged with aging time. Figure 3.15 shows the glass transition temperature for CE obtained by the first run in TMA instrument. The results for glass transition temperature obtained by the second run indicate that the T_g for CE decreased with aging time. Figure 3.16 shows the glass transition temperature of CE polymer obtained by the second run of the experiment. CE samples showed a decrease in T_g with aging time. The T_g decreased because the samples may be undergoing further thermal degradation in the unprotected oxygen environment present in the TMA instrument. This oxygen may have caused further degradation of the already aged and degraded samples. In this case oxygen further reacts with the degraded polymer chains. Figure 3.17 compares the T_g for aged CE polymer obtained from DSC

and TMA scans. TMA studies show that CE polymer undergoes further thermal aging in the TMA environment during the experiment resulting in T_g .

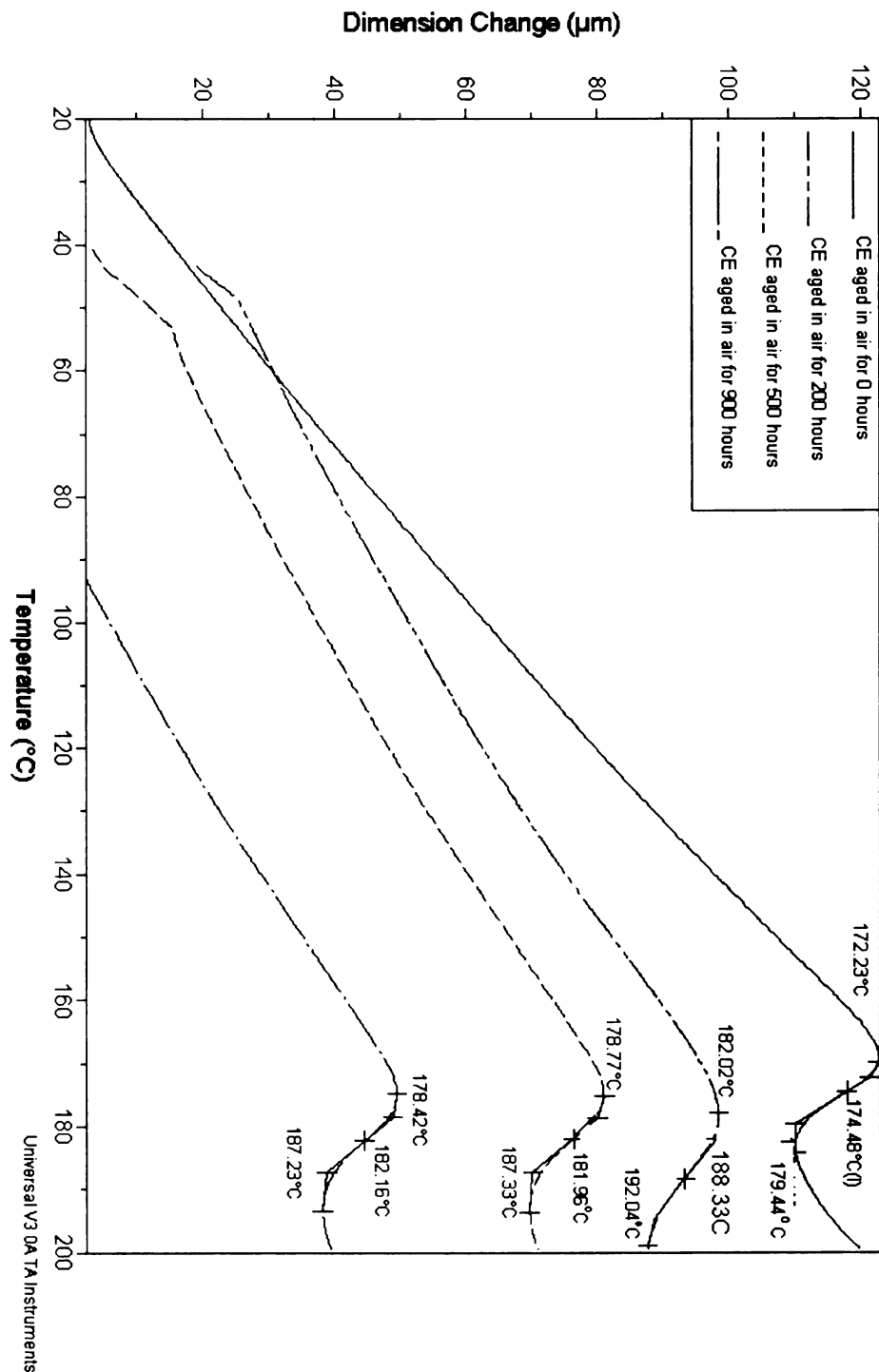


Figure 3.15 TMA scans showing the glass transition temperature range and the relaxation occurring in CE aged in air at 100°C for a period of 0 hours, 200 hours, 500 hours and 900 hours respectively and obtained by first run.

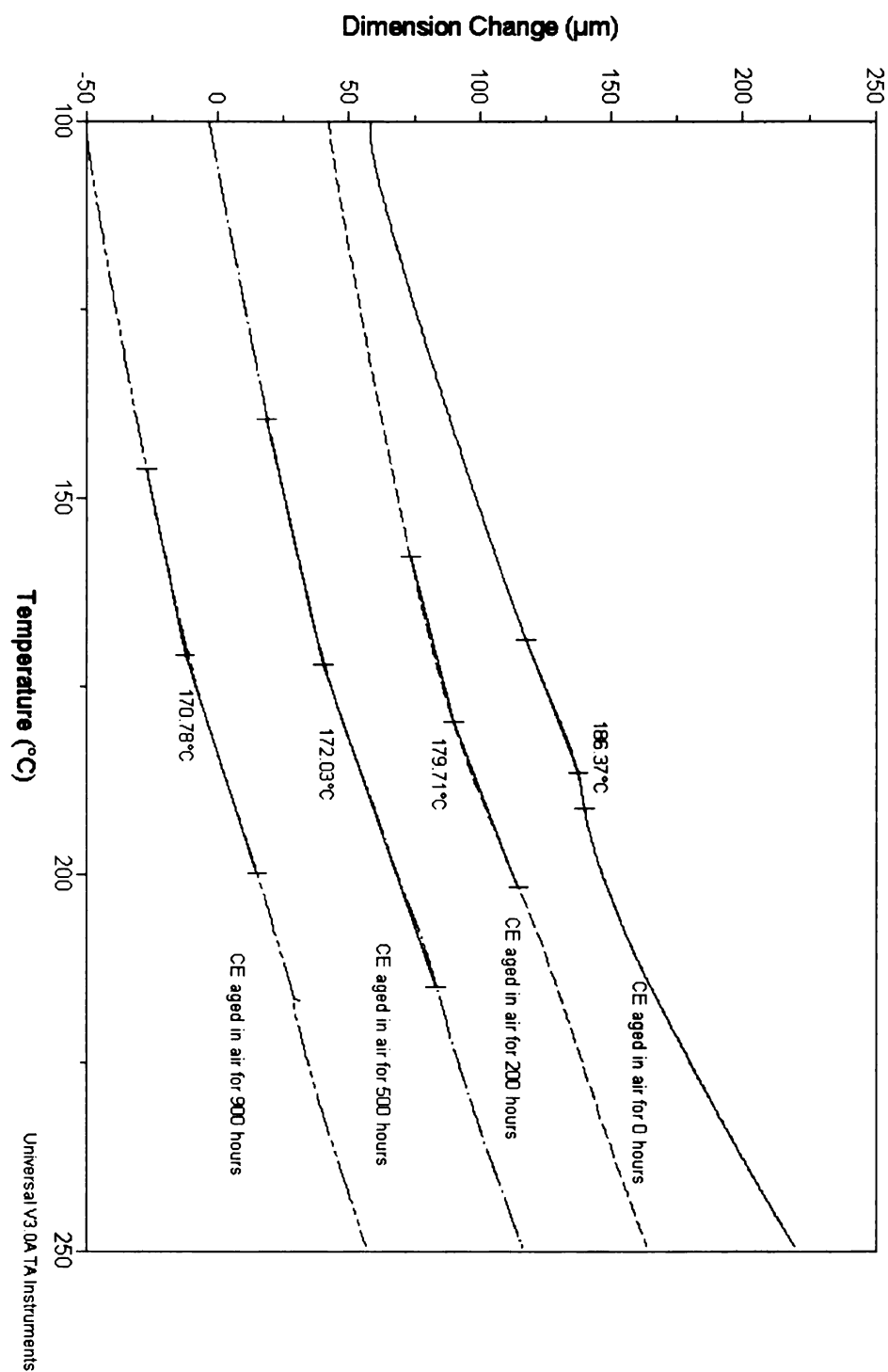


Figure 3.16 TMA scans showing the glass transition temperature for CE obtained by rerun of the same CE sample for the second time. The scans show a decrease in T_g for CE in the second run of TMA.

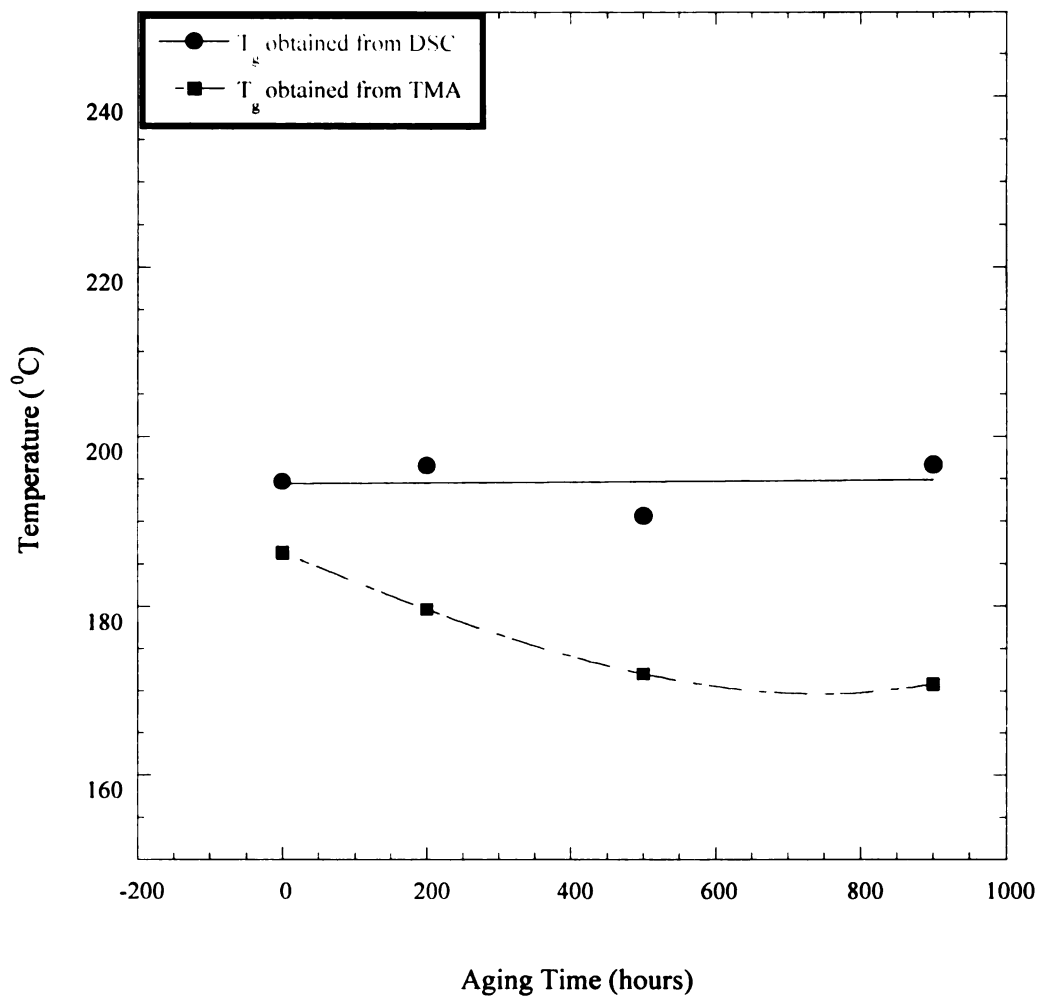


Figure 3.17 Comparison of glass transition temperatures of CE aged in air at 100°C for a period of 0 hours, 200 hours, 500 hours and 900 hours respectively, and obtained from DSC and TMA

3.2.1.4 Thermo-oxidation Mechanism in CE Using FTIR

Infrared spectroscopy, Bio-Rad, Excalibur Series, was used to determine the mechanism of thermo-oxidation and changes in the chemical structure of the specimens. The samples were aged in air at 100°C for up to 500 hours. From the experimental results, shown in Figure 3.18 and Figure 3.19, it is evident that the intensity of the peak at wavelength 1720-1730 cm^{-1} increases with thermal aging time. This peak represents the presence of carbonyl group ($-\text{OC}=\text{O}-$) [51]. The growth of the 1720-1730 cm^{-1} band is interpreted as resulting from the formation of carbonyl groups such as aldehydes, carboxylic acid and ketones, different degrees of hydrogen bonding, conformations of the carbonyl groups and their temperature dependence. In case of CE material, thermal aging in air results in the cleavage of the ester linkage, which is accompanied by the subsequent decomposition of the triazine ring via both heterolytic and hemolytic decompositions reactions [1]. These reactions are followed by trapping of cyanate molecules, which combine or react with diffusing oxygen to form carbonyl groups in the polymer. During the thermal aging process, number of change in the characteristic bonds occur, resulting in smaller products like carbon dioxide, and volatile products. One such change is observed in ($-\text{C}=\text{C}-\text{H}$) bond, which is indicated by the decrease in the intensity of the peaks at 911 cm^{-1} and 966 cm^{-1} with increase in aging time. The peaks of wavelength 911 cm^{-1} and 966 cm^{-1} , is the characteristic absorption of the ($-\text{C}=\text{C}-\text{H}-$) bonds of the isocyanate group. Other changes in the CE polymer include the changes in the peaks between 2220-2250 cm^{-1} which represent the stretching of ($-\text{RNCO}-$) groups in the matrix and between 810-820 cm^{-1} which represents changes in the aromatic ring structure within the polymer. From Figure

3.20, it is evident that SMCE does not change weight or undergoes oxidation, as there is no change found in the FTIR spectra for the sample aged in air.

Sepulveda *et al.* [62] studied the structural changes such as the oxidation level of LDPE due to thermo-oxidation and biological treatment. They used FTIR to estimate the presence of similar groups like carbonyl. They also determined that increasing the thermal duration treatment led to a significant increase in carbonyl group concentration due to higher oxidation of the molecule. Singh *et al.* [64], also studied the photo degradation and thermo-oxidation of SBS rubber using FTIR spectroscopic methods. They found that the initial oxidation process took place by the decrease in the intensity of absorption band of C-H groups and consequent increase in the carbonyl concentration.

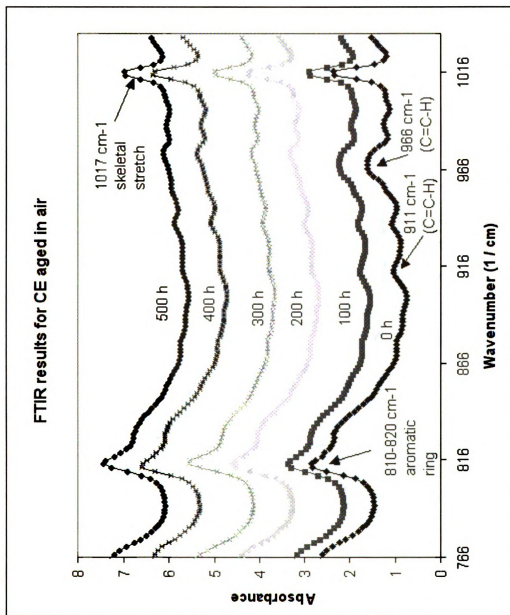


Figure 3.18 FTIR spectra ($766\text{--}1036\text{ cm}^{-1}$) of CE aged in ambient air at 100°C . Change in the spectra with aging time shows the decrease in the 911 cm^{-1} and 966 cm^{-1} peaks.

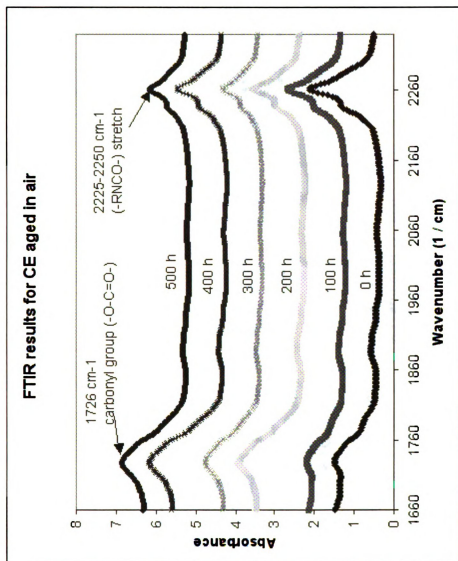


Figure 3.19 FTIR spectra ($1661\text{--}2340 \text{ cm}^{-1}$) of CE aged in ambient air. Change in the spectra with aging time shows the increase of the $(1650\text{--}1950) \text{ cm}^{-1}$ peak.

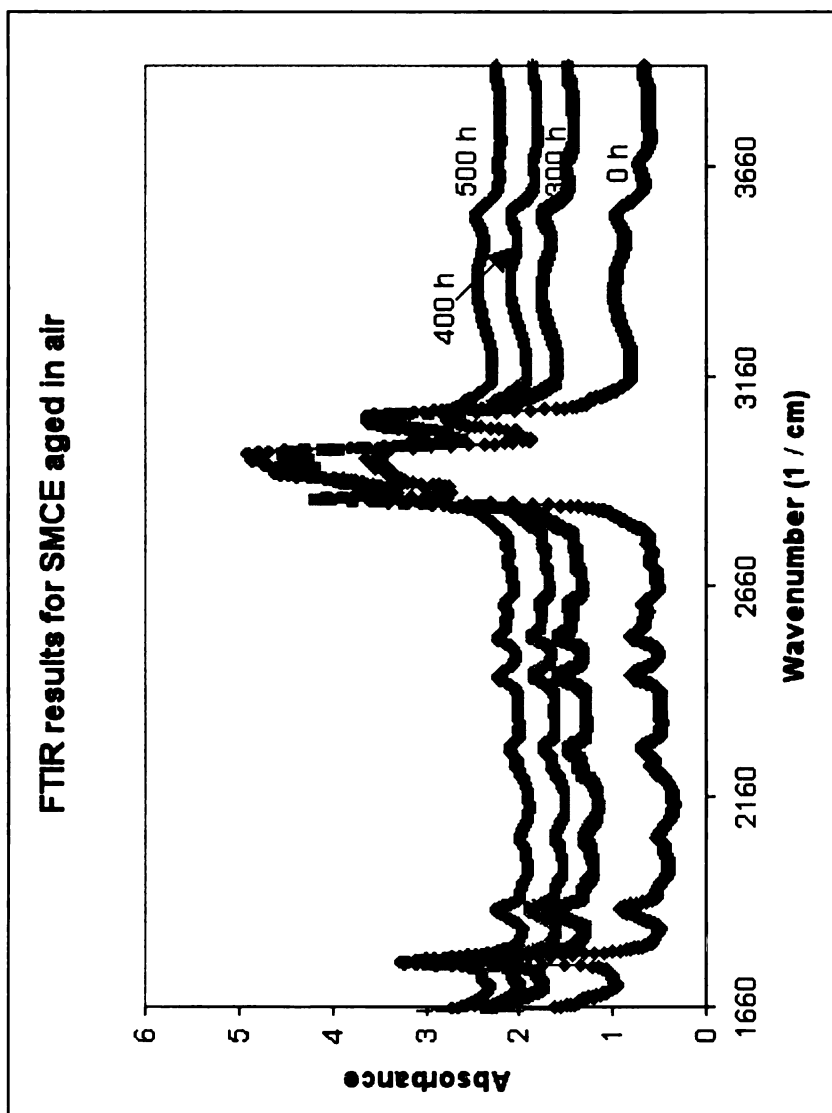


Figure 3.20 FTIR spectra ($1651\text{--}3977\text{ cm}^{-1}$) of SMCE aged in ambient air at 100°C . There is no change in the spectra with aging time.

3.2.1.5 Thermo-oxidative Mechanism in CE using X-ray Photoelectron Spectroscopy.

XPS techniques help to determine the composition of the materials surface. CE and SMCE polymer materials that were as-received and the samples that were aged for up to 900 hours in ambient air at 100⁰C, were studied using XPS. XPS results revealed the changes in the % atomic concentration of each element in the samples under study. It was observed that % atomic concentration of oxygen increased in aged samples than in as received samples for CE, and remained the same in SMCE. CE showed an increase in % atomic concentration of oxygen, indicating that chain scission occurred on the surface of the polymer sample. Chain scission was accompanied by diffusion of oxygen during the thermal aging process resulting in the absorption and consumption of oxygen by the polymer molecules in the resin matrix. SMCE showed no change in the atomic concentration of oxygen on thermal aging, confirming that SMCE was remained unaffected by thermal aging process. Figure 3.22 shows the XPS results for CE and SMCE polymer aged in air at 100⁰C for a period of 0 hours, 500 hours and 900 hours respectively. The figure clearly shows that the atomic concentration for CE increased with aging time. Oxygen has diffused into the polymer matrix and hence we observe the increase in atomic concentration of oxygen across the surface of the polymer sample. SMCE showed no increase in the atomic concentration of oxygen, which indicates that SMCE remained unaffected by thermal aging. XPS spectra for CE in Figures 3.23-3.25 show the consumption and diffusion of oxygen into the CE polymer materials. The atomic concentration of oxygen on the surface of the CE polymer material increased. On comparing the results for CE samples aged in air at 100⁰C for 500 hours and 900 hours, the atomic concentration of oxygen for CE aged for 500 hours was found to be more than

the atomic concentration of oxygen for CE aged for 900 hours. The decrease in oxygen content for CE aged for 900 hours may be due to the loss of some material from the oxide layer during handling. On the other hand, the XPS spectra for SMCE in Figures 3.26-3.28 show that the surface atomic concentration of oxygen in SMCE remained unchanged throughout the thermal aging process. We observed a peculiar outlier in case of CE aged for 500 hours. We observed an increase in % atomic concentration for oxygen and silicon as compared to the % atomic concentration of oxygen and silicon for CE aged for 900 hours

Table 3.5 and Table 3.6, show the results in atomic concentration of oxygen and silicon for as received and aged CE and SMCE, obtained from XPS.

Table 3.5: XPS results showing the atomic concentration for oxygen and silicon elements in CE material.

Cyanate Ester (CE)	Atomic Concentration (%)	
	Oxygen (O)	Silicon (Si)
1) As received	11.3	0.5
2) Aged for 500 hours	30.6	5.0
3) Aged for 900 hours	21.8	0.8

Table 3.6: XPS results showing the atomic concentration for oxygen and silicon elements in SMCE material.

Siloxane Modified Cyanate Ester	Atomic Concentration (%)	
	Oxygen (O)	Silicon (Si)
1) As received	13.5	8.2
2) Aged for 500 hours	14.5	9.6
3) Aged for 900 hours	14.6	9.3

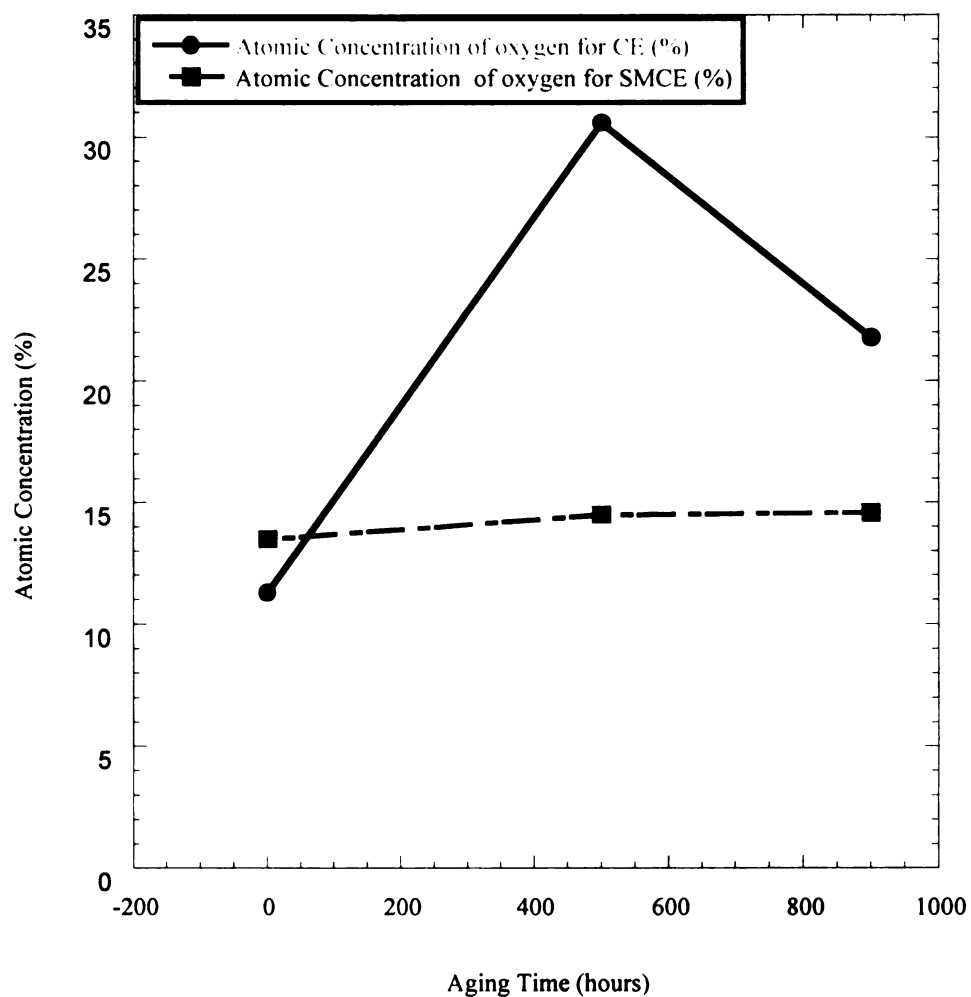


Figure 3.21 XPS results showing the atomic concentration for CE and SMCE aged in air at 100⁰C for a period of 0 hours, 500 hours and 900 hours respectively.

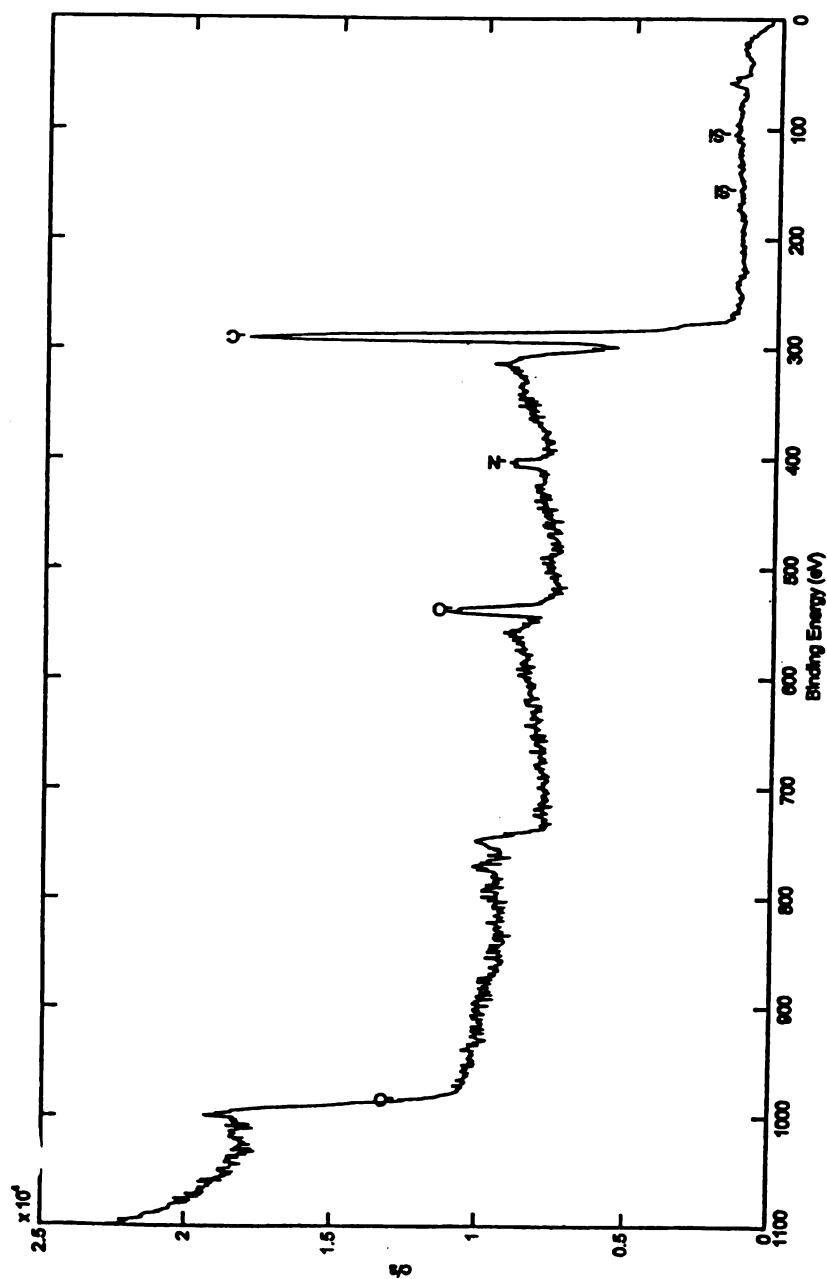


Figure 3.22 XPS spectrum showing the atomic concentration and binding energies for CE sample aged in air for 0 hours.

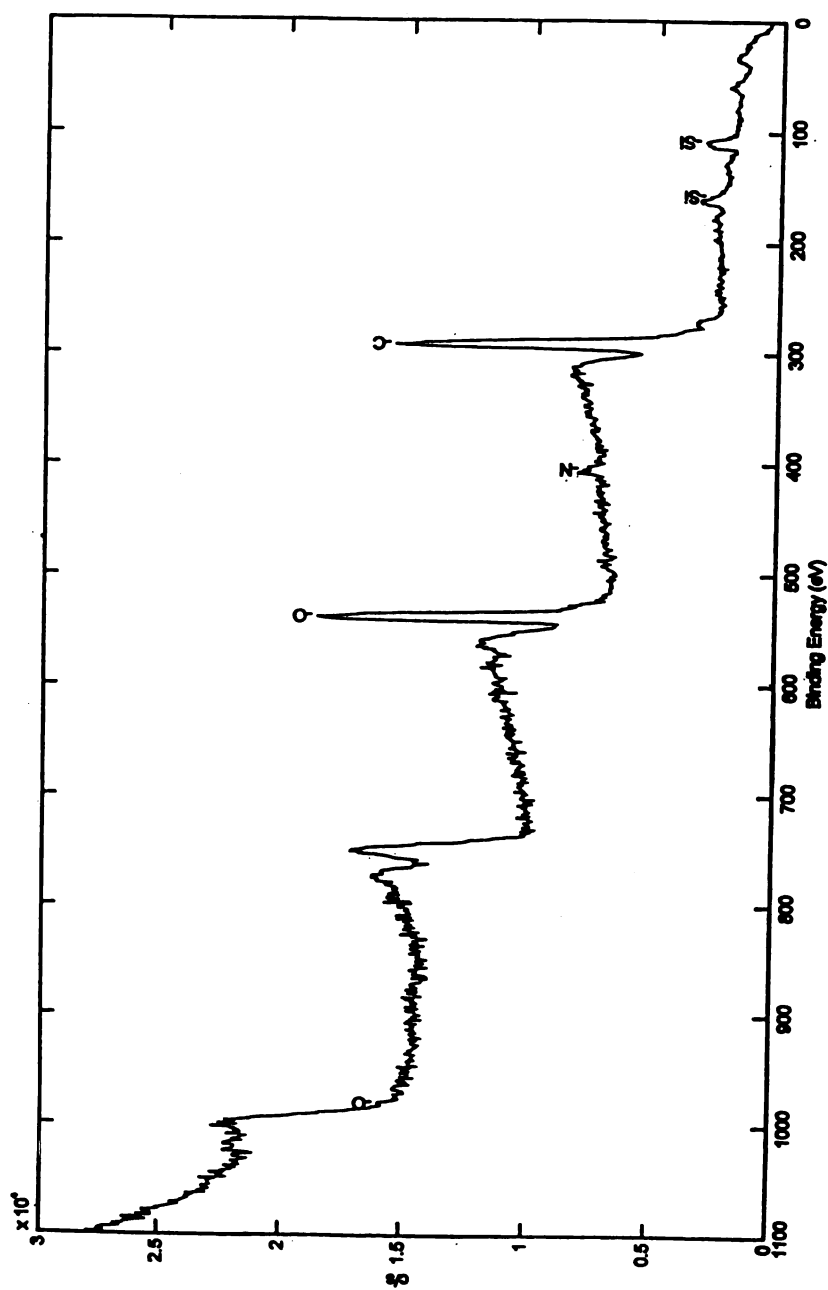


Figure 3.23 XPS spectrum showing the atomic concentration and binding energies for CE aged in air at 100°C for 500 hours.

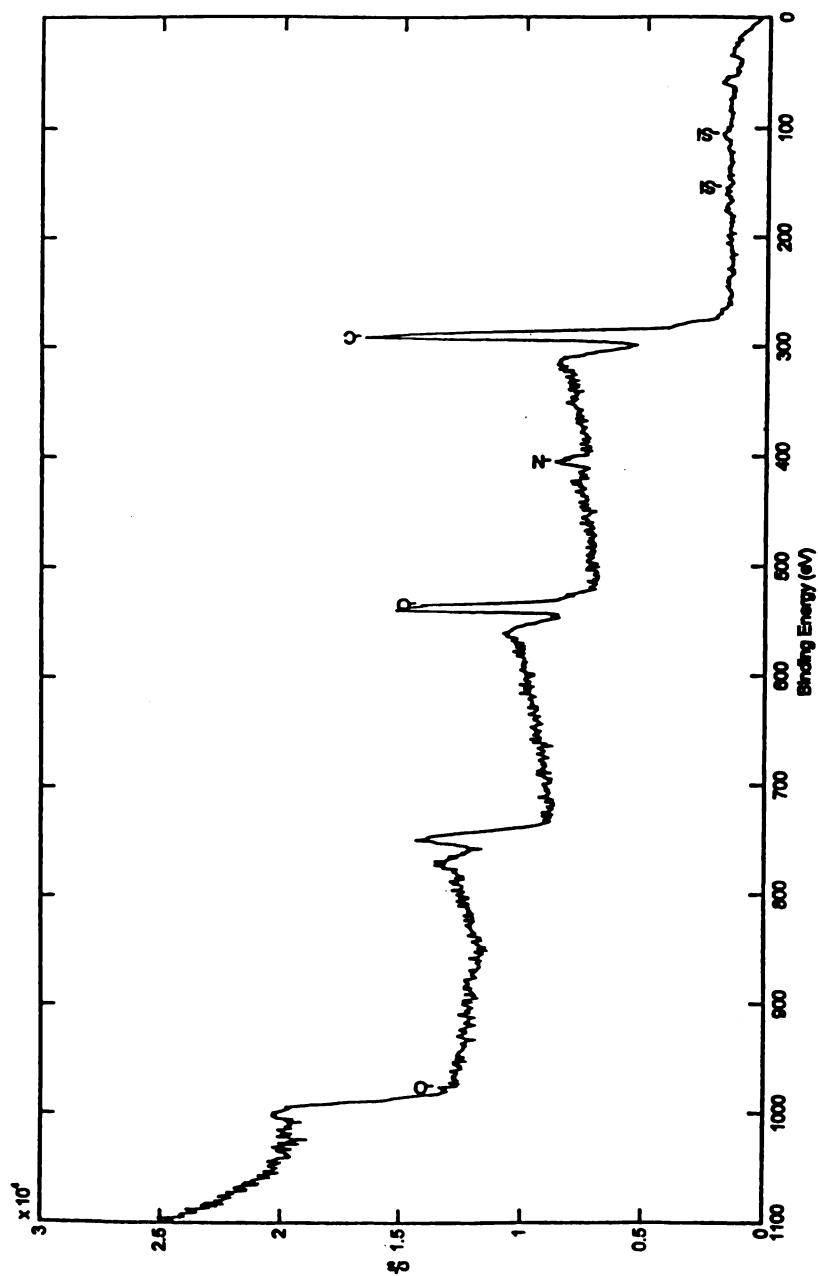


Figure 3.24 XPS spectrum showing the atomic concentration and binding energies for CE aged in air at 100°C for 900 hours.

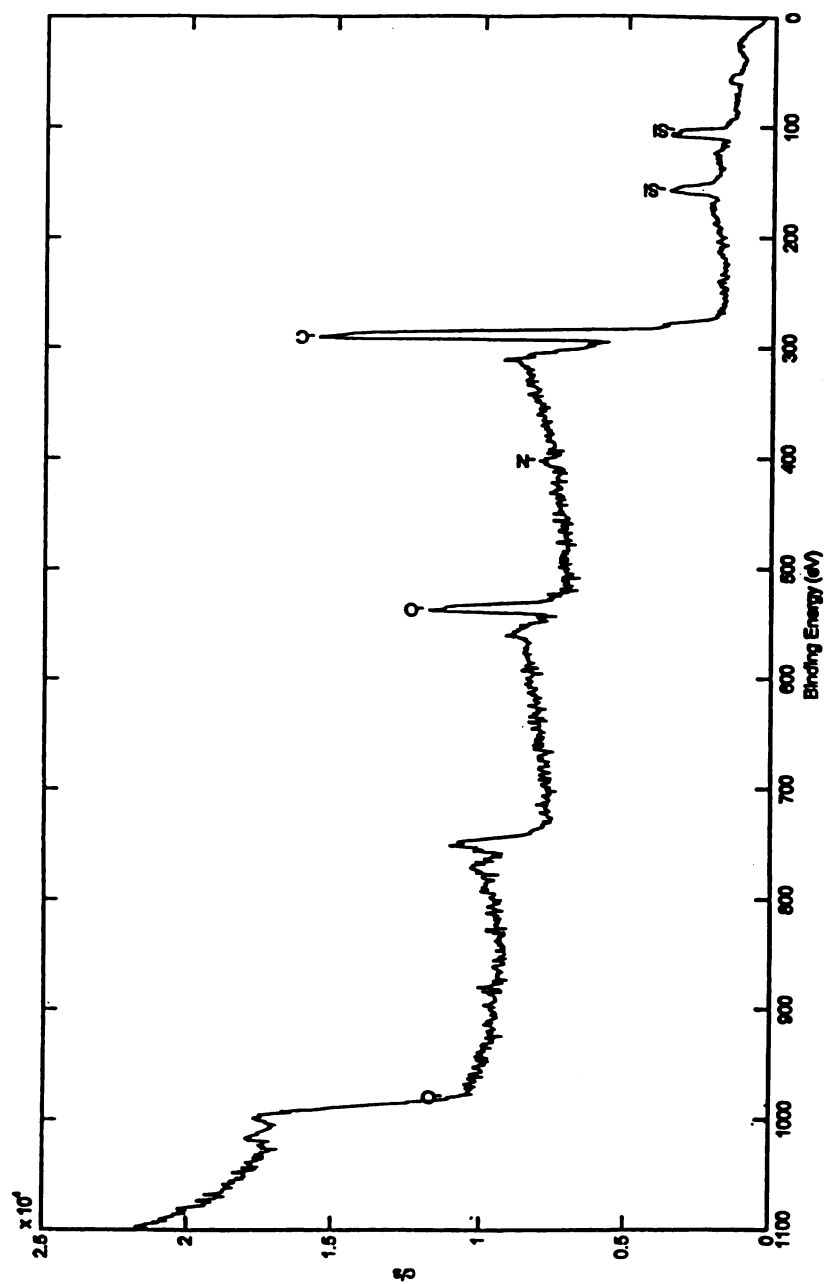


Figure 3.25 XPS spectrum showing the atomic concentration and binding energies for SMCE aged in air for 0 hours.

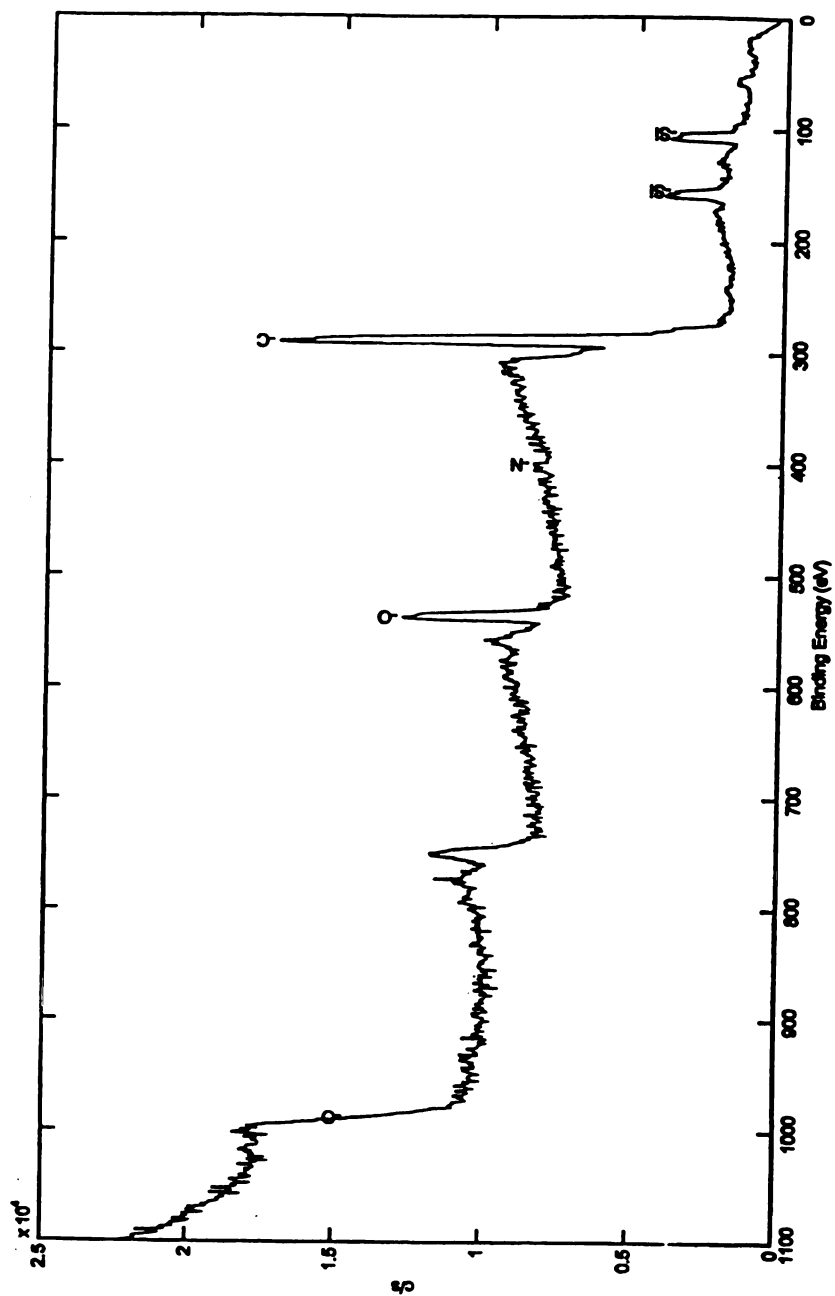


Figure 3.26 XPS spectrum showing the atomic concentration and binding energies for SMCE aged in air at 100°C for 500 hours.

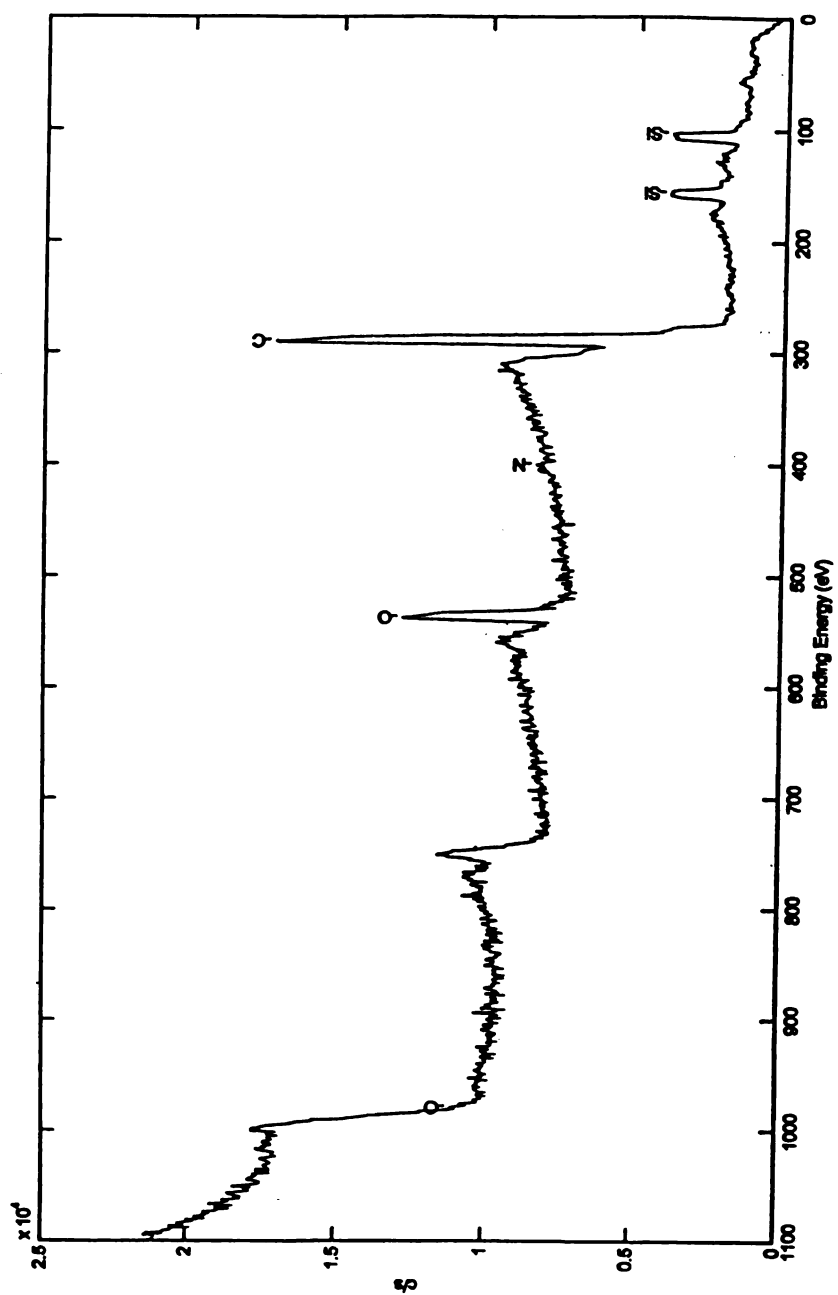


Figure 3.27 XPS spectrum showing the atomic concentration and binding energies for SMCE aged in air at 100⁰C for 900 hours.

3.2.1.6 Three-point Bend Test

To further study the effects of thermo-oxidation of cyanate ester and siloxane modified cyanate ester polymeric materials, three-point bend test were used to characterize the flexural strength of these polymeric resin materials before and after aging. The results from three-point bend tests are shown in Figure 3.30. Flexural strengths were determined for SMCE and CE samples aged in ambient air at 100⁰C for a period of 0 hours, 200 hours, 500 hours and 900 hours respectively. Three point bend test results show a decrease in flexural strength of CE by about 20%. Figure 3.29 further explains the decrease in flexural strength observed in CE.

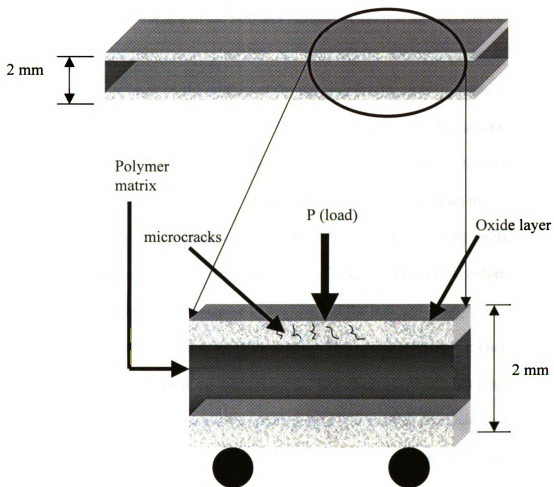


Figure 3.28 Illustration of the oxide layer formed due to the thermo-oxidation for a 3-point bend specimen. During 3-point bend testing, microcracks readily nucleate and grow in the oxide layer at low applied loads. Such microcracking at low loads leads to lower flexural strength in this material.

Figure 3.28 shows the surface of polymer sample after exposure to thermal aging. An oxide layer is formed on the surface of the polymer sample on thermal aging. The oxide increases in thickness with increase in aging time and temperature. On application of fairly low loads this oxide layer on the surface of the polymer cracks, as it is unable to withstand the load due to its brittle structure [63]. In case of CE polymer, the flexural strength trend shows a decrease in strength with aging time and temperature. Obviously, as the aging temperature and time increased, the thickness of the oxide layer on the surface of the sample increased with consequent decrease in the thickness of the interior bulk polymer that has not undergone thermal aging. The flexural strength test performed on this bulk polymer decreases with decrease in thickness of the bulk polymer. The decrease in flexural strength is also attributed to the chain scission of the CE chains on the surface of the polymer sample on thermal aging. The chain scission takes place along the -OCN- bonds of the polycyanurate, which breaks into smaller molecules, and recombines or crosslink later to form a brittle oxide layer. Larger decreases in flexural strength with increase in aging time, indicates that diffusion of oxygen and chain scission increased with increase in aging time [53]. In comparison, the flexural strength of SMCE remained the same after it was aged in ambient air at 100⁰C for 900 hours. SMCE polymer does not form any oxide layer on thermal aging.

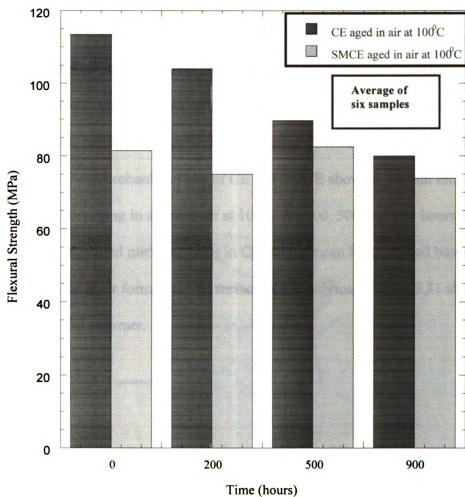


Figure 3.29 Three-point bend results showing the changes in flexural strength for CE and SMCE aged in ambient air at 100°C for a period of 0 hours, 200hours, 500hours and 900 hour respectively.

3.2.1.7 Microhardness Testing

Microindentation is a common and simple technique used to measure the micromechanical behavior of polymers and its correlation with microstructure.

Microhardness test was used to characterize the effect of oxidation on the hardness of CE and SMCE materials before and after the thermal aging. The results were plotted on Fig 3.31. Result from the microhardness test of CE and SMCE shows a gradual increase in the hardness of CE on aging in ambient air at 100⁰C for 200, 500 and 900 hours respectively. The increased microhardness in CE polymer can be explained based on the structure of the oxide layer formed on the surface of CE polymer. Figure 3.31 shows the microhardness for CE polymer.

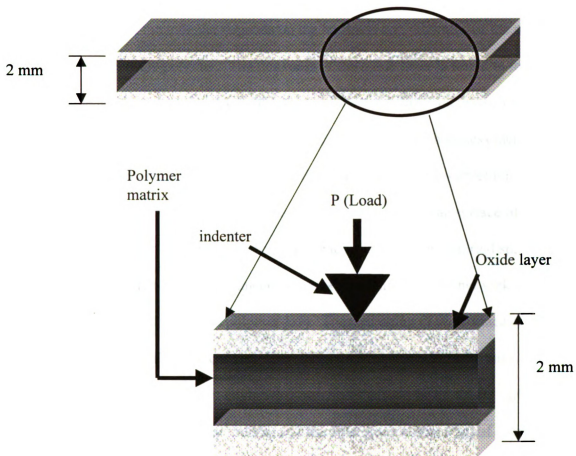


Figure 3.30 Illustration showing the oxide layer which forms on the surface of CE specimens during thermal aging in air. Microhardness was determined on such specimens.

Figure 3.30 shows the formation of oxide layer on the surface of thermal aging. The depth of penetration of the indenter depends on the hardness and thickness of the oxide layer on the surface of the polymer. The thickness of the oxide layer is found to increase with aging time and temperature. As the thickness of the oxide layer increase, it becomes more difficult for the indenter to penetrate the oxide layer and hence hardness increases. Increased microhardness can be further explained on the basis of micro-structural changes occurring on thermal aging on the surface of CE polymer. The surface of CE polymer may be modified to form a carbon-rich surface consisting of distorted sp , sp^2 , and sp^3 carbon atoms that may interconnect to form a three-dimensional network and thereby increase the hardness of CE polymer [65]. Thermal aging of the surface of CE polymer results in absorption and consumption of oxygen into the polymer chains. The oxide surface consists of two layers comprising outermost carbon layer, where carbon atoms are combined with sp^2 and sp^3 bonds, and the other layer comprising of chemical links with oxygen atoms, such as O-H and C=O as well as ester groups. The three-dimensional crosslinking provided by these two layers account for the increased hardness observed on the surface of CE polymer.

SMCE polymer does not undergo any change during thermal aging, no oxide layer is formed on the surface and therefore, the microhardness remained unchanged for all aging time and temperatures.

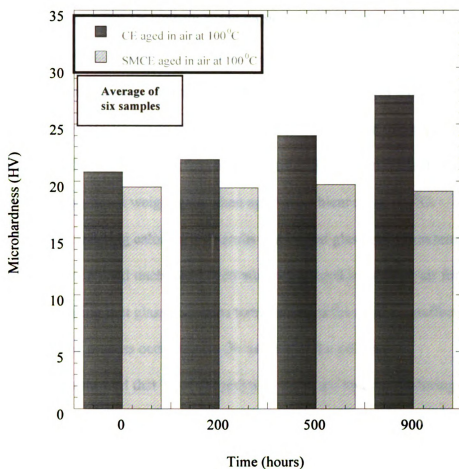


Figure 3.31 Microhardness test results showing the changes in microhardness for CE and SMCE aged in ambient air at 100°C for a period of 0, 200, 500 and 900 hours respectively.

3.2 Summary and Conclusions

The thermo-oxidation effect on cyanate based polymer materials can be summarized as follows:

- (i) Gravimetric experiments show that cyanate ester gains weight when aged in ambient air at 100⁰C due to the absorption and consumption of oxygen by the polymer molecules on the surface of the sample. Siloxane modified cyanate ester shows no significant weight gain when aged in ambient air at 100⁰C.
- (ii) Differential scanning calorimetric results shows that glass transition temperature of aged CE remained unchanged even after being aged in ambient air for 900 hours, indicating that glass transition temperature of the resin is unaffected by the thermal aging process occurring on the surface of the polymer.
- (iii) TMA results showed that T_g of CE polymer remained unaffected during the first run of the experiment but in the rerun experiment showed a decrease in the T_g, indicating that aged CE polymers was undergoing further degradation within the TMA environment.
- (iv) FTIR shows that thermo-oxidation process in CE results in formation of carbonyl groups and subsequent rearrangement of other molecules within the matrix. There is an increase in peak height for carbonyl group with aging.
- (v) XPS results show that surface concentration of oxygen in cyanate ester increases with aging time indicating the consumption and absorption of oxygen on the surface of the polymer sample.
- (vi) Three-point bend test results show a decrease in flexural strength in the CE material indicating that chain scission and consumption of oxygen during the

thermo-oxidation process deteriorating the mechanical properties of the CE polymers. The decrease in flexural strength could be related to the low-stress induced microcracks in the oxide layer formed on the surface of the CE polymer. There is no change found in the flexural strength of SMCE polymers.

- (vii) Microhardness results show an increase in microhardness of CE with decrease in depth of penetration of the indent, which indicating that diffusion of oxygen on the surface of the polymer results in a surface layer containing carbon-rich bonds and high contents of O-H and C=O groups, form a three-dimensional structure on crosslinking. This structure leads to the increase in microhardness observed on thermal aging.

CHAPTER 4

HYGROTHERMAL EFFECTS ON CYANATE BASED POLYMER MATERIALS

4.1 Experimental Procedure

4.1.1 Moisture Absorption Methods

All hygrothermal exposed samples were cut into the dimensions of 25 mm × 25 mm × 2 mm from the polymer panel with a diamond saw. The surface of the samples was ground to a finish of 0.05 μm using the polishing wheel containing silicon carbide and alumina as the polishing medium. The edges were subsequently ground using 600 grit abrasive paper to maintain consistently smooth edge surfaces. The specimens were further cleaned in methanol in ultrasonic cleaner and labeled with a vibrating pen. A set of samples containing 24 specimens was aged in ambient air at 100°C for a period of 1000 hours before exposing them to moisture. Another set of samples containing 24 specimens were baked out in argon for 5 days, to remove absorbed moisture on the surfaces and to eliminate residual stress caused by sample fabrication. These two sets of samples were removed from their ovens and their initial weights were obtained by using an analytical balance with 0.01 mg resolution. Specimens were then placed in chambers containing distilled water maintained at constant temperatures of 45°C, 60°C, 75°C and 90°C respectively. The temperature variation is $\pm 2^\circ\text{C}$. Specimens were removed from the water chambers periodically and weighed. Once the specimens were taken out of their environmental chambers, the surface water was absorbed using clean dry filter paper. Then, the specimens were left for 2-3 minutes at the ambient temperature and humidity conditions before weighing. These specimens were again weighed using an analytical

balance with 0.01 mg resolution. The experimental error of the test is $\pm 0.02\%$. The percentage moisture absorbed in the resin material is calculated using equation 3.1

Gravimetric experiments, three-point bend test and microhardness were used to investigate surface modifications and weight gain.

4.1.2 Gravimetric Experiments

Specimens were tested in environmental test chambers containing distilled water maintained at 45°C , 60°C , 75°C and 90°C respectively. Gravimetric experiments as mentioned earlier in section 3.1.3 were used to monitor weight of specimens during moisture absorption. Specimens were exposed to distilled water for a period of 2000 hours. Specimens were taken out of the water chambers periodically during the moisture absorption experiment. Specimens were weighed using the analytical electronic balance with 0.01 mg resolution. The experimental error of the measurement is $\pm 0.02\%$. The percentage weight change is calculated by using equation 3.1 given in section 3.1.3.

4.1.3 Glass Transition Temperature (T_g) Experiments

Differential scanning calorimeter was used to study the T_g of moisture absorbed samples. Samples of size of 25.4 mm \times 25.4 mm \times 2 mm were exposed to environmental chambers containing distilled water maintained at temperatures of 90⁰C, 75⁰C, 60⁰C and 45⁰C respectively. The T_g of the as-received samples was determined using a TA Instruments™ 930 differential scanning calorimeter (DSC) system. The sample size used in DSC instrument varied from 3-15 mg. Specimens of this dimension were cut from material exposed to moisture at different temperatures for the same 2000 hours. The samples were sealed in small aluminum pans to prevent any weight loss during the experiment, and the weight of each sample pan was measured before and after each test. The samples were put into testing chamber maintained with pure nitrogen atmosphere. The temperature range for heating was maintained between 25⁰C to 250⁰C, and the temperature increase rate was 10⁰C/min. The T_g values were obtained by the intersection of two tangential lines of the DSC curves, automatically provided by the instrument's software.

4.1.4 Microhardness Testing

The specimens that were used for this test had a dimension of 25 mm \times 25 mm \times 2 mm. A precision diamond indenter is impressed into the material at loads from 1 to 1000 gm. The indenter was forced into the specimen until a predetermined load of 10 gm was achieved. The impression length, measured microscopically and the test load are used to calculate a hardness value. The indentations are made using a square-based pyramid indenter, Vickers hardness scale. The hardness impressions can be precisely located with the microscope to perform tests on microscopic features. A representative sample of six

specimens was tested for each moisture absorption conditions, aged in air for 1000 hours and later then exposed to moisture and baked out in argon for a period of 5 days and later exposed to moisture at different temperatures. For every experiment, the hardness of the specimens was tested and the average data was plotted. The Vickers hardness number was then computed using the equation 3.3

4.2 Results and Discussion

4.2.1 Assessment of Moisture Absorption Effects of CE and SMCE resins

4.2.1.1 Gravimetric Analysis

Figures 4.1-4.6 show the weight change profiles for cyanate ester and siloxane modified cyanate ester polymer materials. Two sets of samples were prepared for this experiment. One set of samples were aged in ambient air at 100⁰C for 1000 hours and later exposed water, and another set of samples were baked out in argon at 100⁰C for a period of 5 days and later exposed to water absorption for 2000 hours. These materials were exposed to environmental chambers containing distilled water, and maintained at different temperatures of 90⁰C, 75⁰C, 60⁰C and 45⁰C respectively. The symbols in the plots represent the experimental data points of water absorption under different conditions. Each data point plotted was based on the average values from three samples. The moisture absorption experiments of CE and SMCE polymer materials show that the water-absorption curves follow Fick's law in the early stage, and at later stages deviate from the Fickian behavior, and become non-Fickian .

Some researchers [1,55] have observed the non-Fickian moisture absorption of cyanate ester materials. They suggested that non-Fickian water-absorption is caused by chemical interaction or reaction of water molecules with the cyanate ester polymer network. The chemical interaction caused the sample to keep gaining weight even after the pseudo-saturation moisture level in the resin matrix network. The chemically absorbed water in the polymer network can be attributed to the non-Fickian behavior observed in cyanate ester.

Hydrolysis was also observed in cyanate ester due to the presence of the chemical interactions. Leo *et al.* [19] showed that cyanate ester laminates stored in humid condition at high temperature exhibited hydrolysis and blistering phenomena. They found that cyanate ester blisters much faster than epoxies, although cyanate ester networks absorb less water than do epoxies. Figure 4.3 shows the curves for moisture absorption in cyanate ester polymer that was exposed to moisture in environmental chambers containing distilled water. The profiles compare the water absorption for CE at different temperatures. As seen from Figure 4.3, CE absorbs moisture to a greater extent at higher temperatures. These profiles also compare the diffusion of moisture for two sets of CE samples, one aged in ambient air at 100⁰C and exposed to moisture, and the other baked out in argon for 5 days before immersing the samples in 100% humidity. Water uptake in CE samples aged in air at 100⁰C and subsequently exposed to water is much higher as compared to the CE samples baked out in argon and then exposed to water. The difference within the same material is seen because CE aged in ambient air at 100⁰C undergoes chain scission during thermal aging forming products of low molecular weight, and high mobility within the resin. During the moisture absorption process,

water molecules diffuse at a faster rate in these aged samples and behave as a plasticizer within the polymer matrix thus increasing the segmental mobility. The diffusion of moisture in CE samples aged in air at 100⁰C and maintained in chambers containing water at 90⁰C was also found to be higher than the diffusion of moisture into samples aged in air at 100⁰C but maintained in water at lower temperatures. The rate of diffusion of moisture molecules into the polymer matrix depends on temperature. At higher temperatures of water, the diffusion of water molecules is faster, as the water molecules attain the required activation energy for diffusion, much earlier as compared to the molecules maintained at lower temperatures. On the other hand, Figure 4.4 shows the moisture absorption curves for SMCE samples maintained in chambers containing distilled water at temperatures of 90⁰C, 75⁰C, 60⁰C and 45⁰C respectively. In case of SMCE samples, one can conclude that SMCE absorbs less moisture as compared to CE polymer materials. SMCE samples aged in air at 100⁰C and later exposed to water showed an increase in moisture absorption as compared to SMCE samples baked out in argon for 5 days and later exposed to water. SMCE polymer is a rigid structure, which impedes the diffusion of moisture molecules into the matrix.

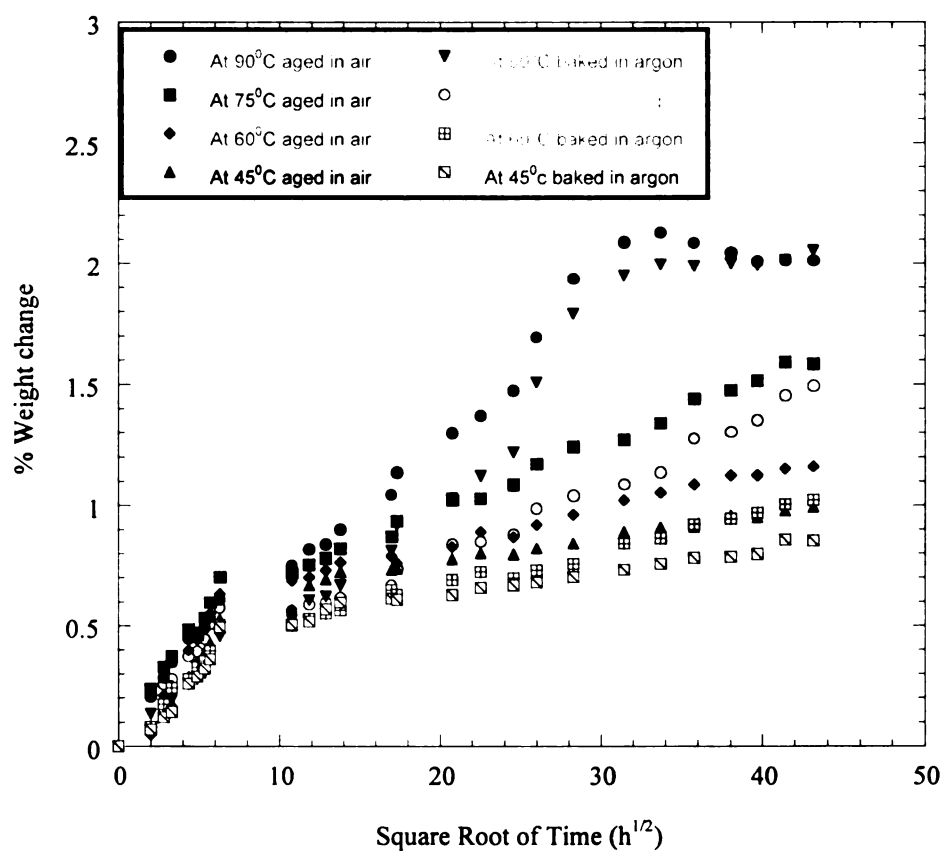


Figure 4.1 Water absorption curves of cyanate ester at different environmental temperatures with square root of time. The plots compare the moisture absorption for CE aged in air and at 100°C for 1000 hours and baked out in argon for 5 days.

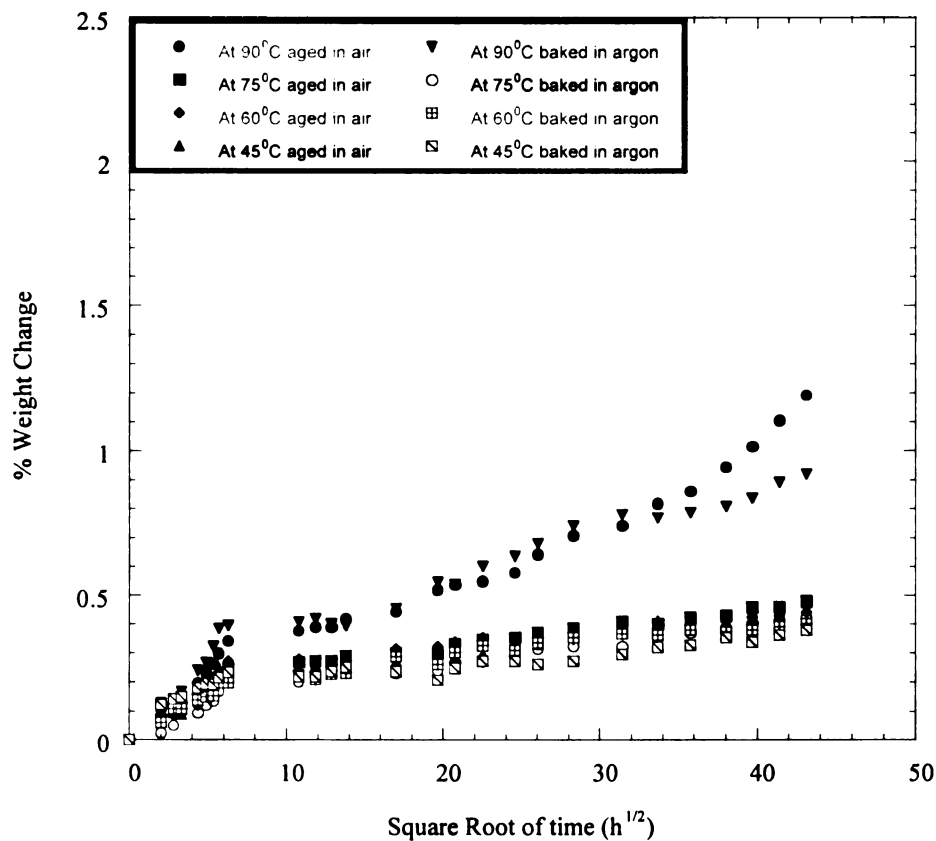


Figure 4.2 Water absorption curves of SMCE at different environmental temperatures with square root of time. The plots compare the moisture absorption for SMCE aged in air and at 100⁰C for 1000 hours and baked out in argon for 5 days.

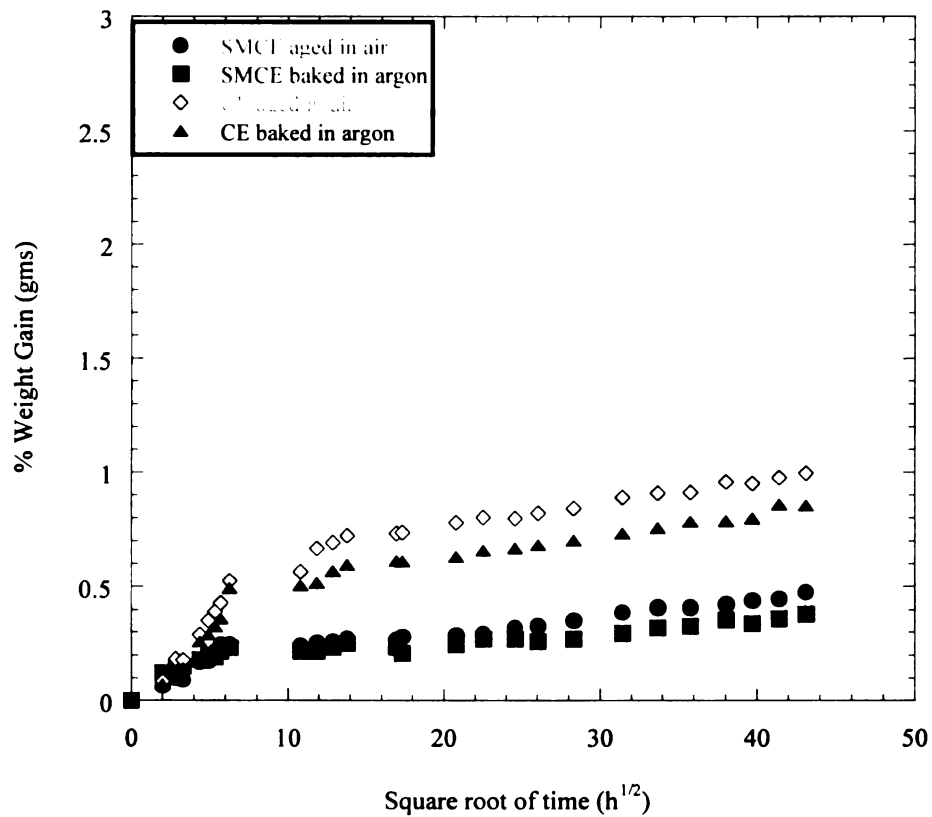


Figure 4.3 Water Absorption curves comparing the weight change of CE and SMCE exposed to environmental chambers containing distilled water maintained at 45°C with square root of time.

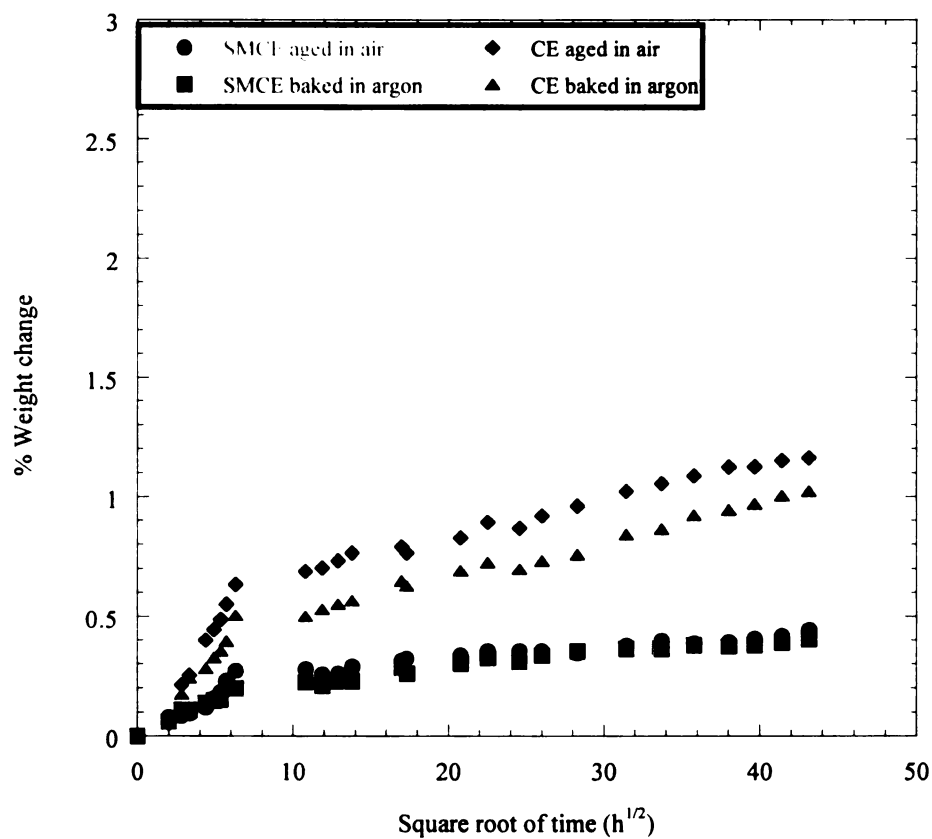


Figure 4.4 Water Absorption curves comparing the weight change for CE and SMCE exposed to environmental chambers containing distilled water maintained at 60°C with square root of time.

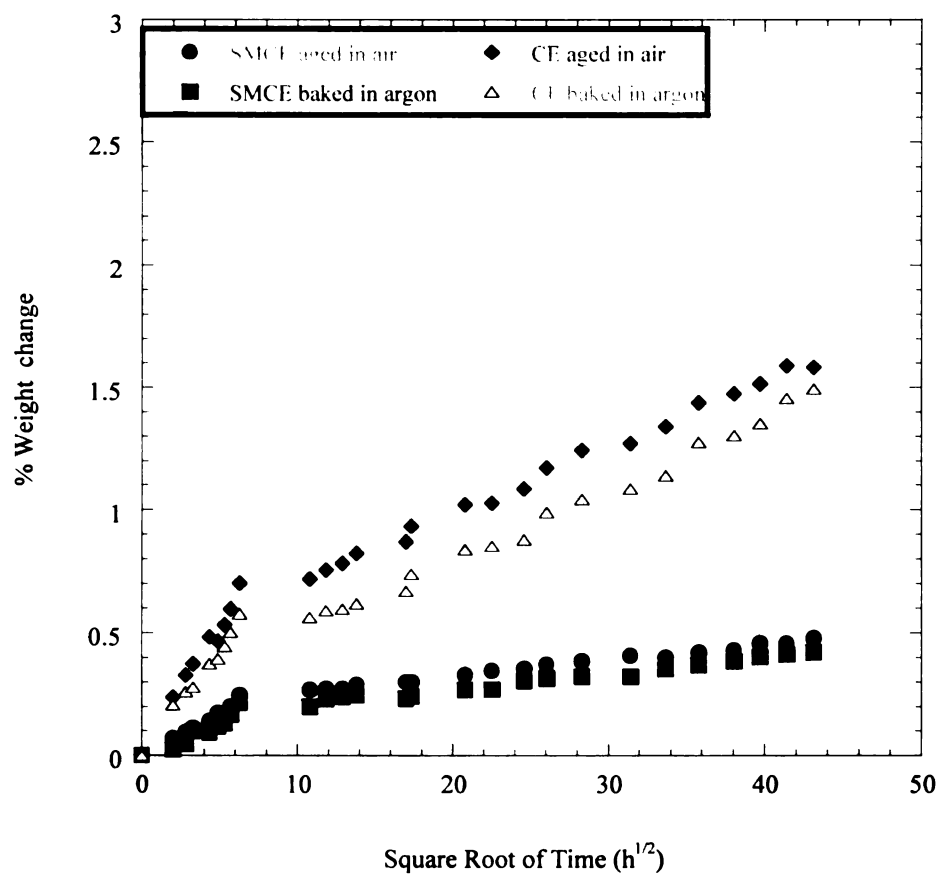


Figure 4.5 Water Absorption curves comparing the weight change for CE and SMCE exposed to environmental chambers containing distilled water maintained at 75°C with square root of time.

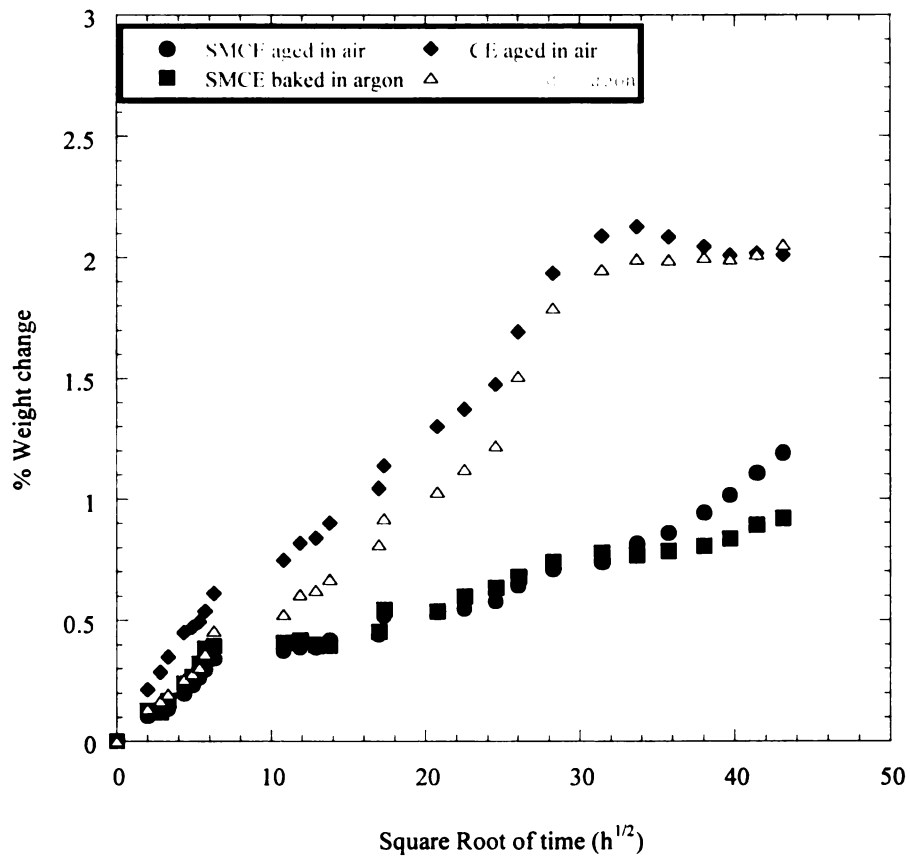


Figure 4.6 Water Absorption curves comparing the weight change for CE and SMCE exposed to environmental chambers containing distilled water maintained at 90°C with square root of time.

The comparison of water absorption profiles for CE and SMCE was further studied in Figure 4.3-4.6. Comparisons were made between samples aged in ambient air at 100⁰C for 1000 hours and then exposed to water and samples baked out in argon for a duration of 5 days and then exposed to water. It was found that the samples, which were aged in ambient air for 1000 hours showed higher water absorption rates as compared to the samples, baked out in argon. The temperature also played an important role here. At higher temperatures the rate of diffusion of water molecules is higher. The samples aged in air and exposed to water at 90⁰C, absorbed moisture at a faster rate as compared to the samples maintained at the other temperatures. Further comparing the water absorption in CE and SMCE materials, it was observed that CE absorbed more moisture than SMCE at all temperatures. A valid reason given here was that thermo-oxidation of CE involved chain scission of macromolecules and surface degradation, which made the material more susceptible to moisture absorption.

Figures 4.7- 4.10 show the comparison of weight change in CE and SMCE polymer aged in air at 100⁰C for 1000 hours and exposed to water maintained at 45⁰C, 60⁰C, 75⁰C and 90⁰C respectively and CE and SMCE samples baked out in argon for 5 days and later exposed to water maintained at 45⁰C, 60⁰C, 75⁰C and 90⁰C respectively. Each figure represents the diffusion rates of moisture absorption process for the initial 49 hours. CE and SMCE samples preaged in air at 100⁰C and later exposed to water showed higher diffusion rates as compared to CE and SMCE samples presaged in argon at 100⁰C for periods of 5 day. CE samples preaged in air at 100⁰C and exposed to water also shows higher diffusion rates as compared to CE samples preaged in argon at 100⁰C for periods of 5 days and exposed to water. CE samples undergoes thermal aging, which causes

chain scission. On exposure to moisture absorption, the water molecules easily diffuse into the degraded polymer samples.

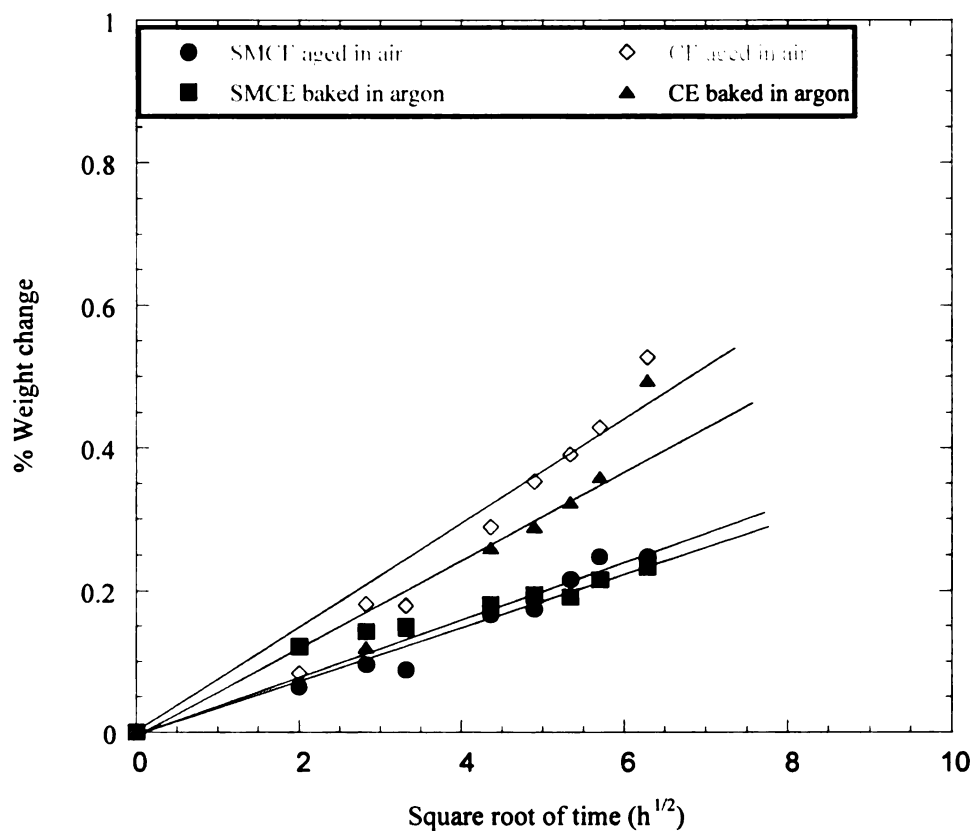


Figure 4.7 Comparison of diffusion rates in CE and SMCE polymer when exposed to moisture absorption at 45°C for 2000 hours with square root of time.

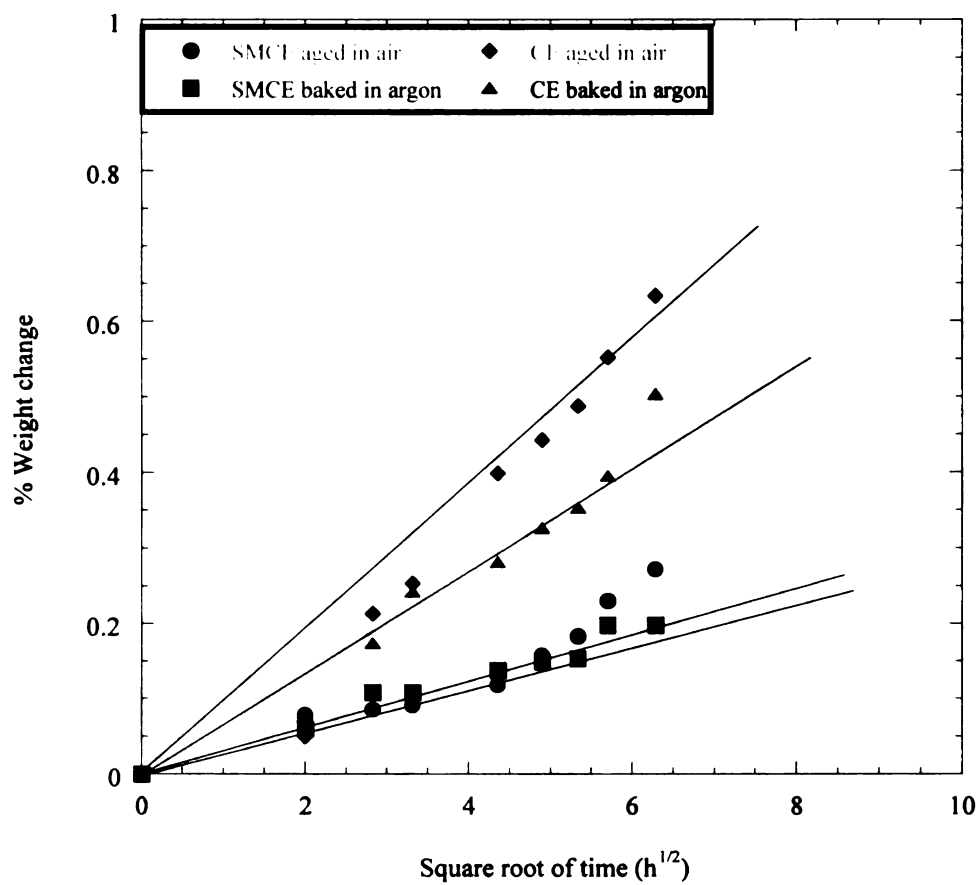


Figure 4.8 Comparison of diffusion rates in CE and SMCE polymer when exposed to moisture absorption at 60°C for 2000 hours with square root of time.

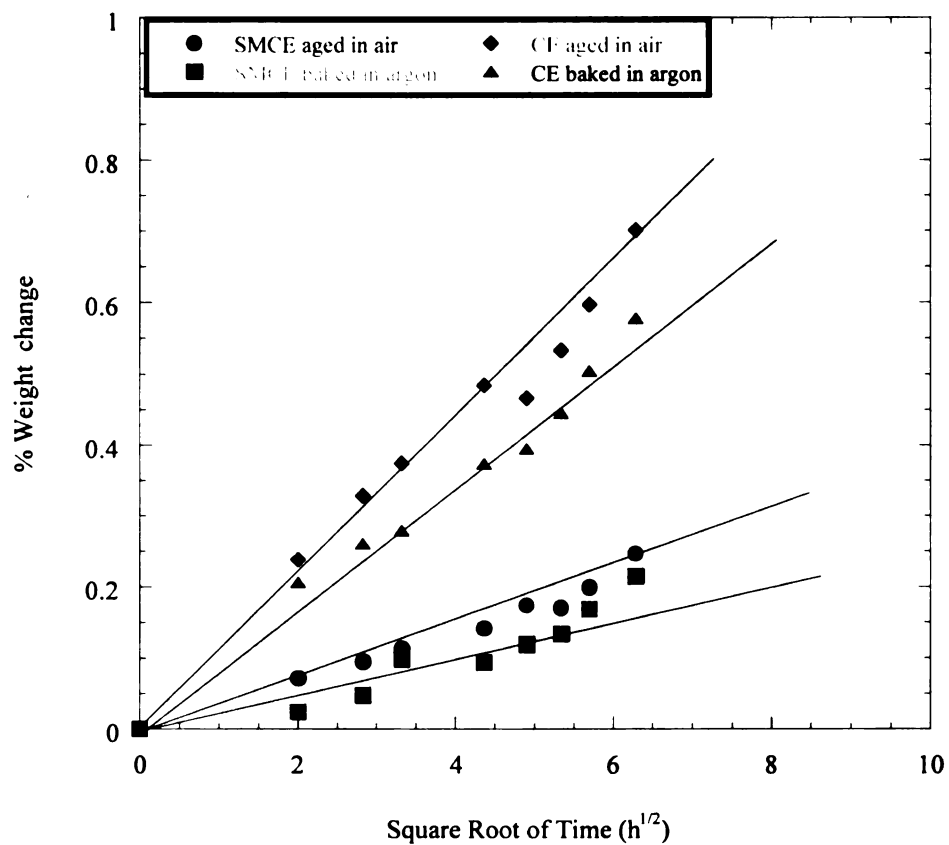


Figure 4.9 Comparison of diffusion rates in CE and SMCE polymer when exposed to moisture absorption at 75°C for 2000 hours with square root of time.

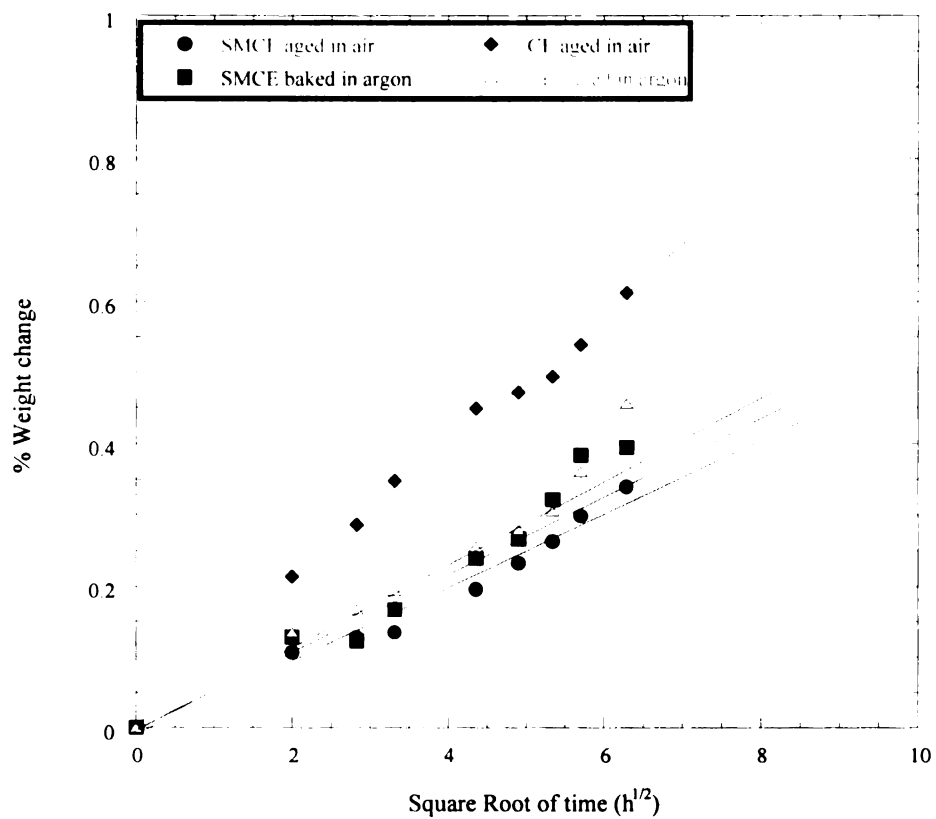


Figure 4.10 Comparison of diffusion rates in CE and SMCE polymer when exposed to moisture absorption at 75°C for 2000 hours with square root of time.

4.2.1.2 Glass Transition Temperature Using DSC

Glass transition temperature is an important parameter that determines the polymer materials usage to commercial and industrial applications. The glass transition temperature is lowered or decreases when the polymer absorbs moisture. This affects a number of useful mechanical properties.

To evaluate the thermal aging in our SMCE and CE samples, we aged the samples at 100⁰C over a period of 1000 hours and immersed these samples in chambers containing distilled water maintained at 45⁰C, 60⁰C, 75⁰C and 90⁰C respectively for a period of 2000 hours and finally measured the glass transition temperature. For this purpose differential scanning calorimeter (DSC) was utilized. The results are shown in Table 4.1. Table 4.1, shows that the glass transition temperature of SMCE remained unchanged for most of the temperatures. The T_g for SMCE sample exposed to water at 90⁰C showed a decrease in the glass transition temperature indicating that SMCE undergoes degradation when exposed to water at higher temperatures. Figures 4.8- 4.16 show the DSC scans for glass transition temperature for SMCE samples aged in ambient air at 100⁰C for a period of 1000 hours and baked out in argon at 100⁰C for a period of 5 days. Problems were encountered in obtaining the glass transition temperature of moisture absorbed CE samples. Glass transition temperature for moisture absorbed CE samples were not comparable to the results obtained by researchers [1]. Further tests would be required in future to determine the T_g for moisture absorbed samples by proper analytical techniques.

Table 4.1 Glass transition temperature for moisture absorbed SMCE polymer materials **

Siloxane Modified Cyanate Ester	Glass Transition Temperature For SMCE polymer
(1) As received	157.59 ⁰ C
(2) SMCE aged in air at 100 ⁰ C and exposed to water at 45 ⁰ C for 2000 hours	152.09 ⁰ C
(3) SMCE aged in air at 100 ⁰ C and exposed to water at 60 ⁰ C for 2000 hours	158.99 ⁰ C
(4) SMCE aged in air at 100 ⁰ C and exposed to water at 75 ⁰ C for 2000 hours	156.29 ⁰ C
(5) SMCE aged in air at 100 ⁰ C and exposed to water at 90 ⁰ C for 2000 hours	133.95 ⁰ C
(6) SMCE baked in argon for 5 days at 100 ⁰ C and exposed to water at 45 ⁰ C	156.42 ⁰ C
(7) SMCE baked in argon for 5 days at 100 ⁰ C and exposed to water at 60 ⁰ C	152.93 ⁰ C
(8) SMCE baked in argon for 5 days at 100 ⁰ C and exposed to water at 75 ⁰ C	156.51 ⁰ C
(9) SMCE baked in argon for 5 days at 100 ⁰ C and exposed to water at 90 ⁰ C	135.63 ⁰ C

** The glass transition temperatures are the T_g results taken for one sample at each temperature.

Table 4.1 shows the glass transition temperature (T_g) for SMCE samples aged in air at 100°C for 1000 hours and later exposed to chambers containing distilled water at different temperatures and the other set of samples containing SMCE again, only this time, they were baked out in argon for a period of 5 days. SMCE showed a decrease in the T_g for samples exposed to water at 90°C . Shanahan and his coworker [64] studied the irreversible hygrothermal effects on epoxy resin. Their experiment involved the exposure of epoxy polymer to water maintained at 50°C , 70°C and 90°C respectively. They found that diffusion of water into the polymer led to the introduction of carbonyl groups in the resin and chain scission of crosslinked structure. The water diffusion also led to the decrease in T_g . The decrease in T_g is swelling dependent. The temperature increase also facilitates water diffusion and swelling of the polymer.

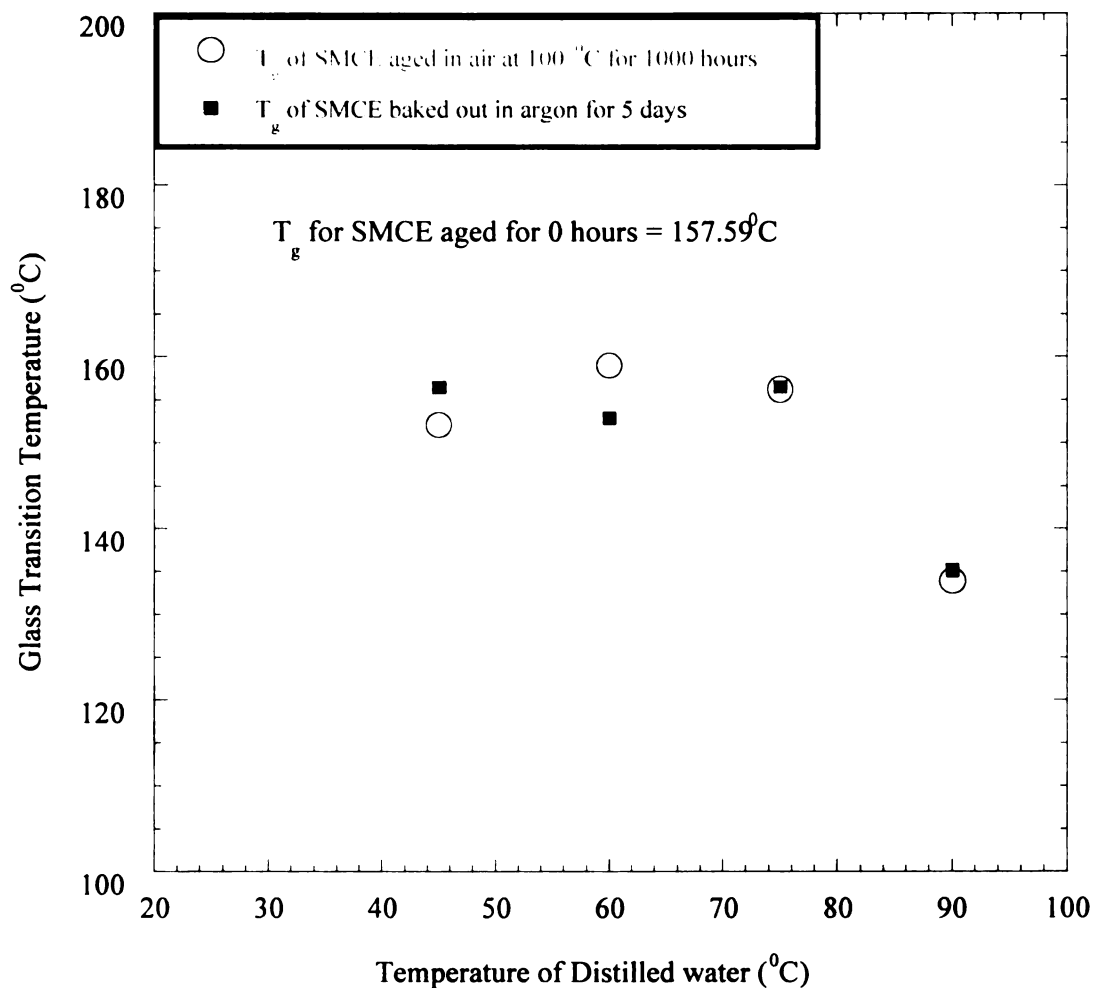


Figure 4.11 Comparison of glass transition temperature for SMCE samples Aged in air at 100°C for 1000 hours and baked out in argon for 5 days and Exposed to water maintained at 45°C, 60°C, 75°C and 90°C respectively.

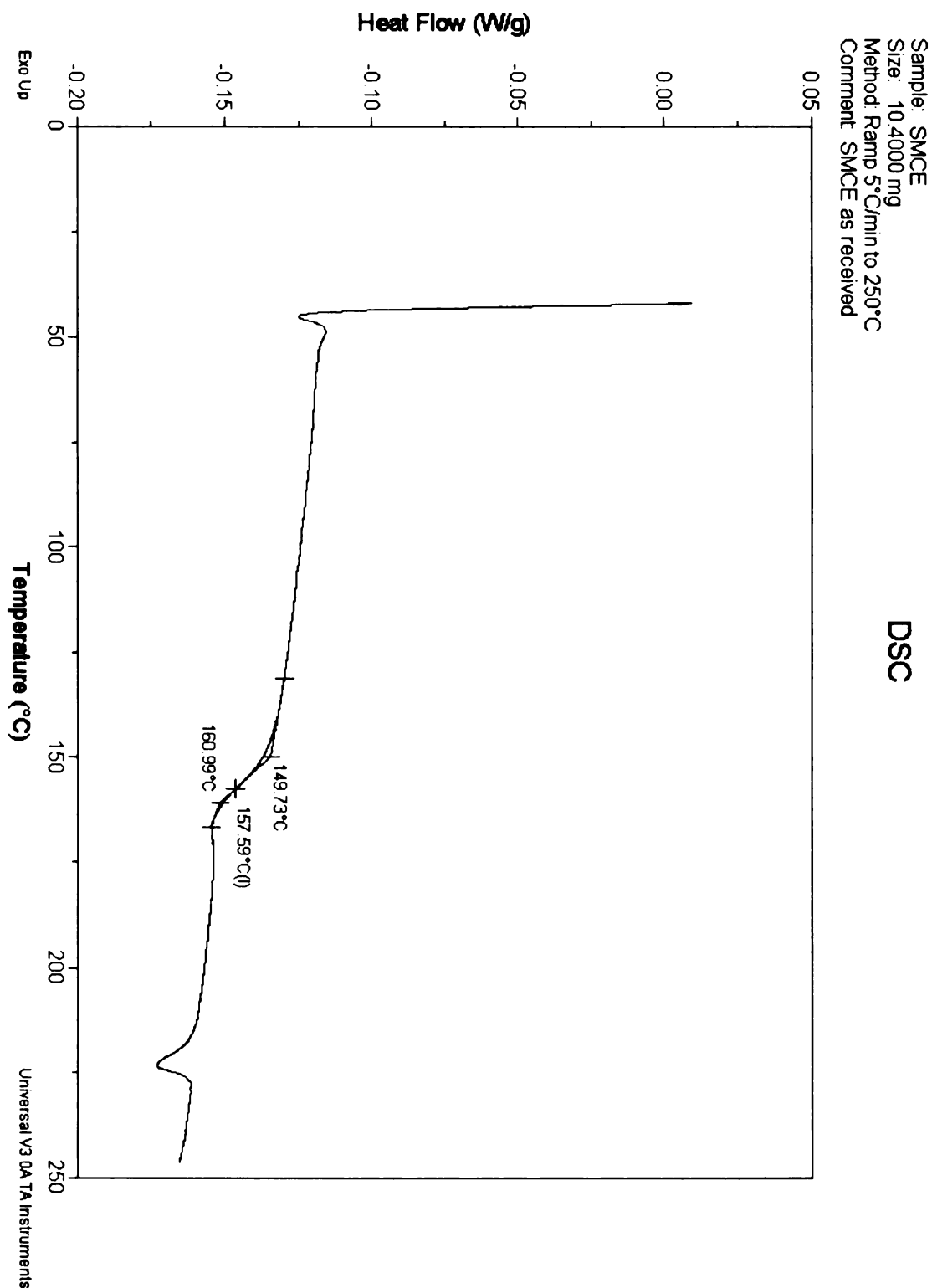


Figure 4.12 DSC scan showing the T_g for SMCE aged in air for 0 hours

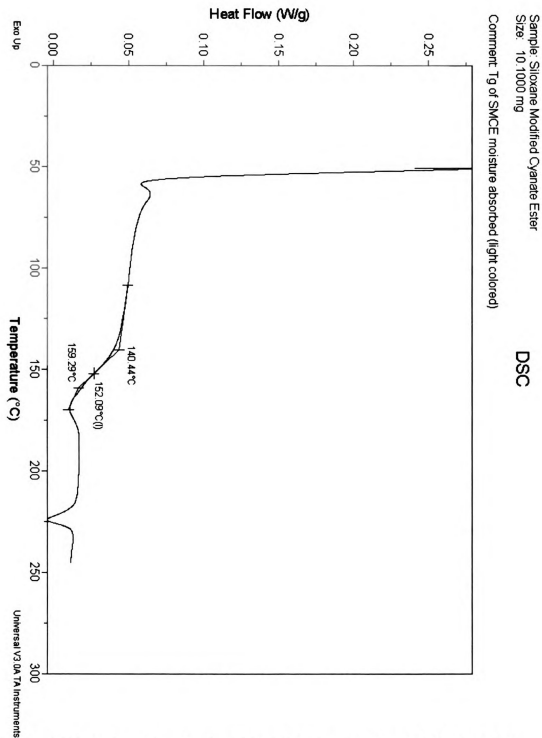


Figure 4.13 DSC scan showing the T_g for SMCE aged in air at 100°C for 1000 hours and exposed to water at 45°C for 2000 hours

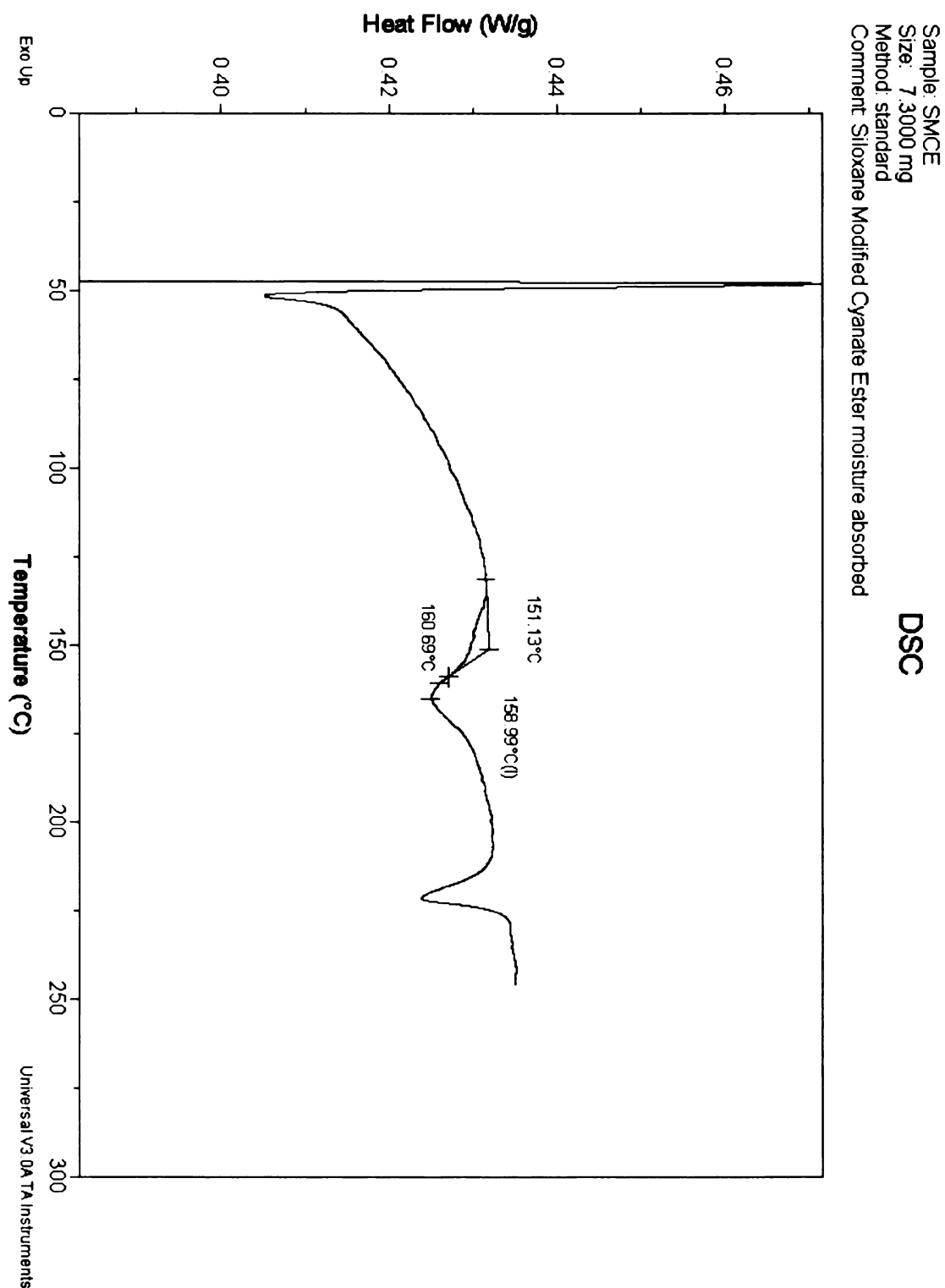


Figure 4.14 DSC scan showing the T_g for SMCE aged in air at 100°C for 1000 hours and exposed to water at 60°C for 2000 hours.

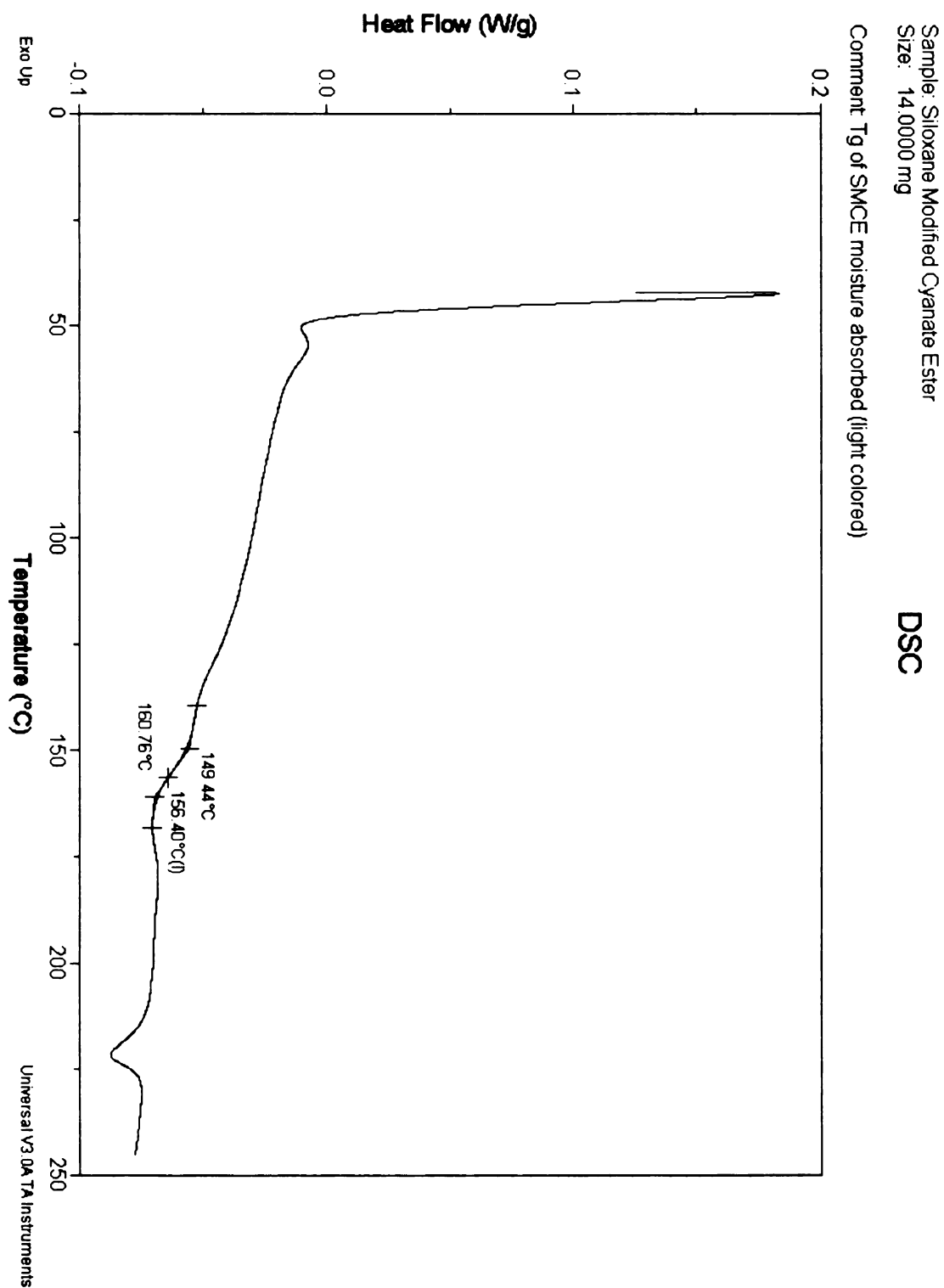


Figure 4.15 DSC scan showing the T_g for SMCE aged in air at 100°C for 1000 hours and exposed to water at 75°C for 2000 hours

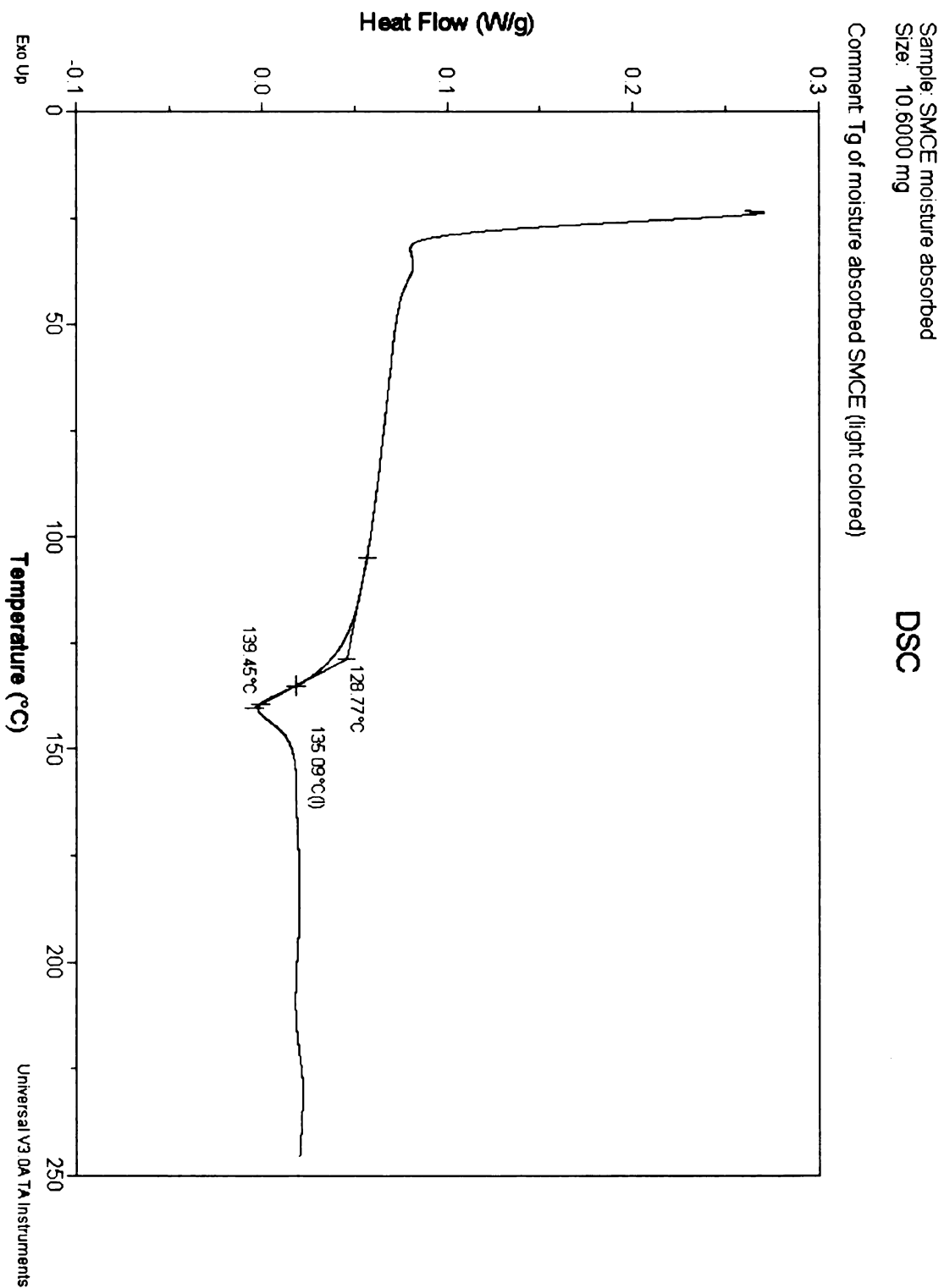


Figure 4.16 DSC scan showing the T_g for SMCE aged in air at 100°C for 1000 hours and exposed to water at 90°C for 2000 hours

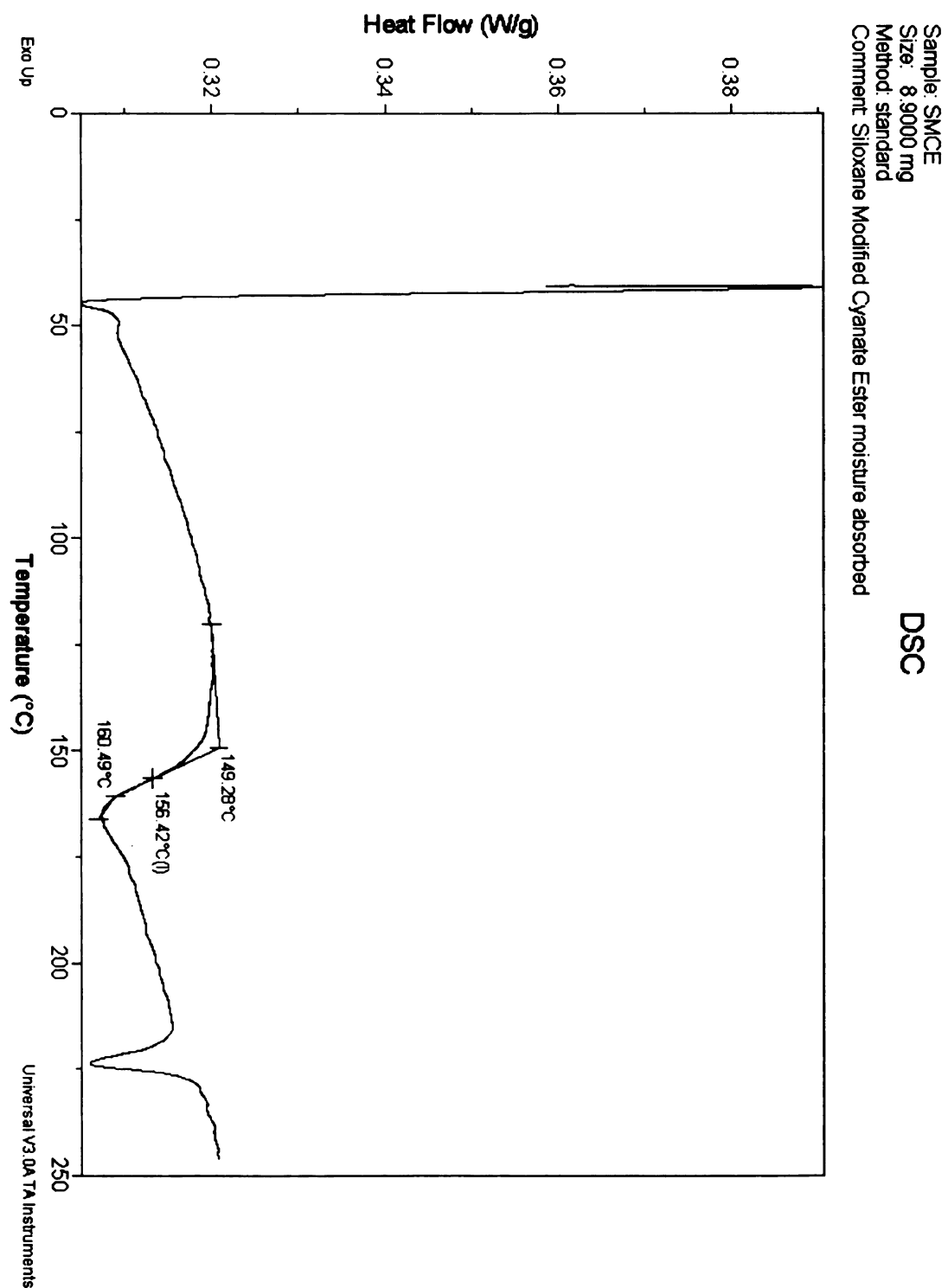


Figure 4.17 DSC scan showing the T_g for SMCE baked out in argon at 100°C for 5 days and exposed to water at 45°C for 2000 hours

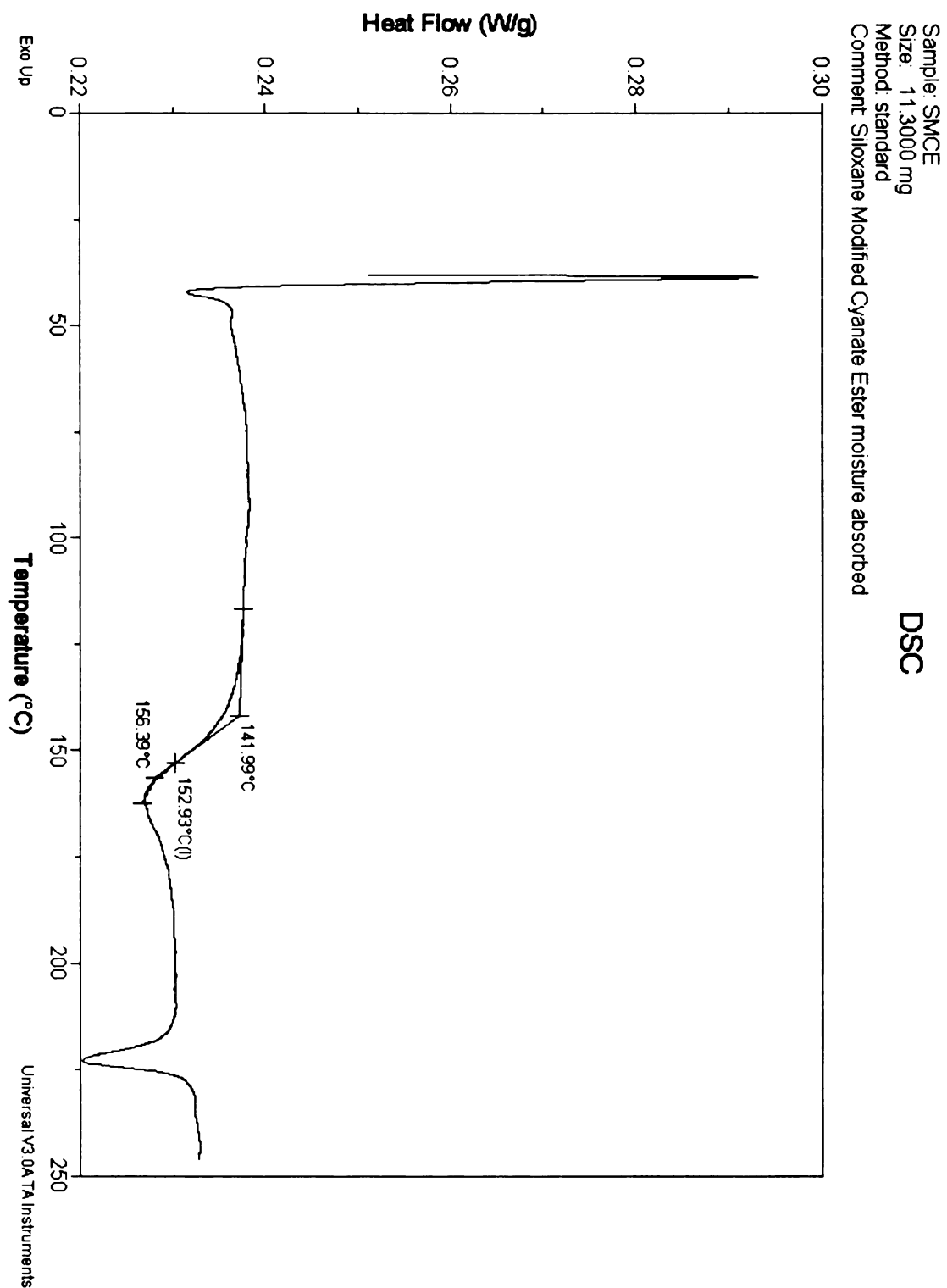


Figure 4.18 DSC scan showing the T_g for SMCE baked out in argon at 100°C for 5 days and exposed to water at 60°C for 2000 hours

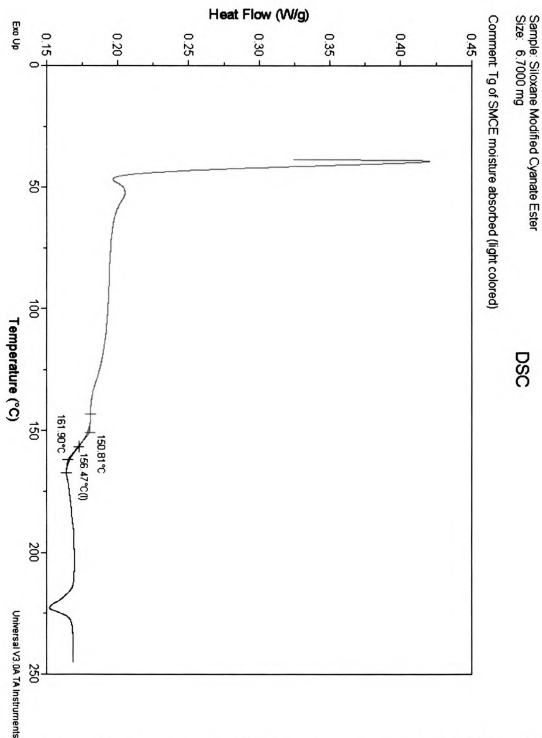


Figure 4.19 DSC scan showing the T_g for SMCE baked out in argon at 100°C for 5 days and exposed to water at 75°C for 2000 hours

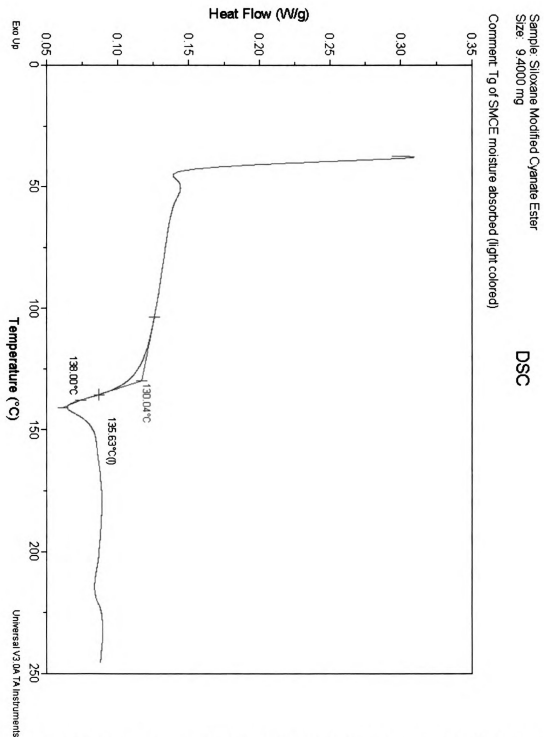


Figure 4.20 DSC scan showing the T_g for SMCE baked out in argon at 100°C for 5 days and exposed to water at 90°C for 2000 hours

4.2.1.3 Microhardness Test

The results obtained by microhardness testing for moisture absorbed samples are shown in Figure 4.16. From the figure we observed that CE shown an increase in microhardness as compared to SMCE materials. On further comparing within the CE materials we observed that CE aged in air at 100⁰C and later exposed to water at different temperatures showed higher microhardness results than the CE materials baked out in argon at 100⁰C for 5 days and later exposed to water at different temperatures. The difference in microhardness is explained by the changes occurring to the chemical structure of the CE polymer due to moisture absorption process. CE samples aged in air and later exposed to water absorb moisture, which acts as a plasticizer and lubricates the molecules on the surface of the polymer, reorienting them and allowing to crosslink. The crosslinked surface results in the increased hardness observed in CE polymer. In case of SMCE polymers, we observed a very significant change in microhardness with moisture absorption. SMCE polymer contains pendant groups in the backbone of the polymer chain. These pendant groups increase the intermolecular force of attraction between the polymer chains in the matrix in addition to its steric hindrance. This structure of SMCE impedes the diffusion of water into the polymer matrix and hence the microhardness of SMCE remained unchanged.

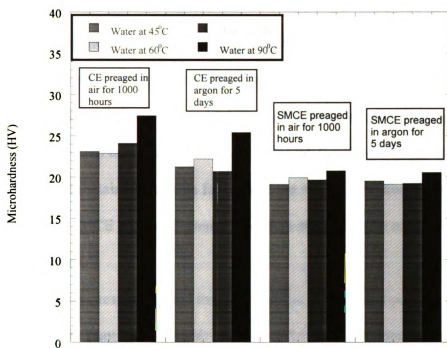


Figure 4.21 The results determining the microhardness for CE and SMCE exposed to preaging conditions and submerged in water for 2000 hours at 45°C, 60°C, 75°C and 90°C respectively.

4.3 Summary and Conclusions

- (i) Gravimetric experiment results show that the water diffusion in cyanate ester polymer materials was Fickian in the initial stages of moisture absorption process and becomes non-Fickian in the later stages. CE aged in air at 100⁰C and later exposed to water showed higher moisture absorption as compared to CE baked out in argon and later exposed to water. Diffusion of moisture molecules thus depends on temperature and concentration of diffusing species. SMCE showed a very significant increase in weight during moisture absorption process.
- (ii) Glass Transition temperature results showed that T_g of SMCE decreased by 20%, at 90⁰C and remained the same for most of the water absorption temperatures. Therefore, SMCE was unaffected by moisture absorption for most of the temperatures.
- (iii) Microhardness results showed that the hardness of CE based polymer materials increased for samples aged in air at 100⁰C and exposed to water as compared to samples baked out in argon for 5 days and exposed to water. The microhardness results for SMCE showed significant changes in microhardness due to moisture absorption process.

CHAPTER 5

CONCLUSIONS AND RECOMMENDATIONS

5.1 Conclusions

The major findings of this thesis are concluded as follows :

- (1) Cyanate ester gained weight when aged in ambient air indicating the diffusion and consumption of oxygen molecules, while siloxane modified cyanate ester showed no gain in weight when aged in ambient air for a long period of time.
- (2) Glass transition temperature of aged cyanate ester remained unchanged when aged in ambient air at 100⁰C as thermal aging was occurring on the surface of the polymer sample and the T_g for the entire sample was not dependent on the aging effects on the surface, while T_g of aged SMCE remained unchanged when aged in ambient air at 100⁰C for the same duration of time.
- (3) Changes in the chemical structure of CE polymer materials clearly indicate that CE underwent thermo-oxidation to form carbonyl groups. The presence of this carbonyl group indicated the consumption and diffusion of oxygen into the matrix.
- (4) The % atomic concentration of oxygen in CE polymers increased with thermal aging. The increase in % atomic concentration in oxygen indicates the consumption and diffusion of oxygen by the polymer resin. SMCE remained unaffected by thermal aging.
- (5) Mechanical properties include changes in flexural strength of CE with thermal aging. Flexural strength of CE decreased by 20% after being aged for 1000 hours, while the flexural strength of SMCE remained unchanged.

- (6) Microhardness of CE increased with thermal aging. SMCE showed very significant change in microhardness on thermal aging.

All the above results indicate that the polymer network degrades due to thermo-oxidation, a process that is governed by the oxygen diffusion in the polymer matrix.

- (7) Water diffusion in CE follows the Fickian mode in the initial stages of diffusion process but becomes non-Fickian in the later stages after a time period of square root of 6 hours. CE samples aged in air absorb water to a greater extent as compared to CE samples baked out in argon. CE samples also absorb more moisture when exposed to higher temperatures. SMCE absorbs moisture to a lesser extent as compared to CE materials.

- (8) T_g remained unchanged for SMCE exposed to water at lower temperatures but decreased when exposed to water absorption at higher temperatures.

- (9) Microhardness for CE based polymer materials increased for samples aged in air at 100°C and exposed to water as compared to samples baked out in argon for 5 days and exposed to water. The microhardness results for SMCE showed very significant change in microhardness during moisture absorption process.

5.2 Recommendations

Although the current study illustrates the effect of thermal degradation and moisture absorption in CE and SMCE polymers, the following investigations are recommended to develop a clear understanding of the operative mechanisms for the same.

- (1) A study of thermal aging and hygrothermal effects on the molecular weight and molecular weight distribution of polymers.
- (2) A deep understanding of the synthesis and/or cure of these polymers is often critical for their successful application in different environments. Studying the degradation of such polymers with different synthesis and curing rate in different environment
- (3) To utilize DSC to further monitor the changes in the polymer over aging time. Changes in the degree of curing and melting peak temperatures for samples cut from the superficial layers of thermally aged samples
- (4) Chromotagraphy techniques could be utilized for further elemental analysis for molecular structure identification

BIBLIOGRAPHY

1. Hamerton, I., "*Chemistry and Technology of Cyanate Ester Resins*," Blackie Academic and Professional, Glasgow, (1994)
2. Parvatareddy, H., Wang, J. Z., Dillard, D.A., Ward, T.C., "Environmental Aging of High Performance Polymeric Composites: Effects on Durability," *Composites Science and Technology*, VOL. 53, (1995) pp. 399-409.
3. Liu, Z., "*Thermo-Oxidation and Hygrothermal Effects on Cyanate Ester Polymer Materials*," Masters Thesis, Michigan State University, (1999).
4. Srinivasan, S. A., Mcgrath, J. E., "Amorphous Phenolphthalein-based Poly (arylene ether)-Modified Cyanate Ester Networks: Effect of Thermal Cure Cycle on Morphology and Toughenability," *Journal of Applied Polymer Science*, VOL. 64, No. 1, (1997) pp. 167-178.
5. Parvatareddy, H., Wang, J. Z., Lesko, J. J., Dillard, D. A., and Reifsnider, K. L., "An Evaluation of Chemical Aging/Oxidation in High Performance Composites Using the Vickers Micro-Indentation Technique," *Journal of Composite Materials*, VOL. 30, (1996) pp. 210-230.
6. Lee, S. S., Kim, S. C., "Physical Aging of Polydimethylsiloxane-Modified Epoxy resin," *Journal of Applied Polymer Science*, VOL. 69, (1998) pp. 1291-1300.
7. Nakamura, T. M., Takahashi, K., "Effects of Moisture Absorption on the Dynamic Interlaminar Fracture Toughness of Carbon/Epoxy Composites," *Journal of Composite Materials*, VOL. 34, (2000) pp. 630-648.
8. Soles, C. L., Lee, A. F., "A Discussion of the Molecular Mechanisms of Moisture Transport in Epoxy Resins," *Journal of Polymer Science: Part B: Polymer Physics*, VOL. 38, (2000) pp. 792-802.
9. Hamerton, I., and Hay, J. N., "Recent Technological Developments in Cyanate Ester Resins," *High Performance Polymers*, VOL. 10, (1998) pp. 163-174.
10. Shimp, D. A., and Ising, S. J., *35th Int. SAMPE Symp. And Exhibition*. 35, (1990) pp. 1045.

11. Shimp, D. A., Christenson, J. R., and Ising, S. J., *34th Int. SAMPE Symp.* Exhib. 34, (1989) pp. 222.
12. White, J. R., Turnbull, A., "Review: Weathering of Polymers: Mechanisms of Degradation and Stabilization, Testing Strategies and Modelling," *Journal of Materials Science*, VOL. 29, (1994) pp. 584-613.
13. Audouin, L., Langlois, V., Verdu, J., "Review: Role of Oxygen Diffusion in Polymer Ageing: Kinetic and Mechanical Aspects," *Journal of Materials Science*, VOL. 29, (1994) pp. 569-583.
14. Zhou, J., and Lucas, J. P., "Hygrothermal Effects of Epoxy Resins. Part II: Variations of Glass Transition Temperature," *Polymer*, VOL. 40, (1999) pp. 5513-5522.
15. Zhou, J., and Lucas, J. P., "The Effects of a Water Environment on Anomalous Absorption Behavior in Graphite / Epoxy Composites., *Composite Science and Technology*, VOL. 53. (1995) pp. 57-64.
16. Mahmood, S., Walker, L., Jeelani, S., "Effect of Moisture and Temperature Induced Degradation in Tensile Properties of Kevlar-Graphite/Epoxy Hybrid Composites", *Materials Research Laboratory., Tuskegee University*, (1987)
17. Vanlandingham, M. R., Eduljee, R. F., Gillespie, J. W., "Moisture Diffusion in Epoxy System," *Journal of Applied Polymer Science*, VOL. 71, (1999) pp. 787-798.
18. Zhou, J., "PhD Dissertation: Hygrothermal Effects of Epoxy Resins and Graphite/Epoxy Composites," *Michigan State University*, (1996).
19. Kasehagen, L. J., Haury, I., Macosko, C. W., Shimp, D. A., "Hydrolysis and Blistering of Cyanate Ester Networks" *Journal of Applied Polymer Science*, VOL. 64, (1997) pp. 107-113.
20. Cinquin, J., and Abjean, P., *Proceedings of 38th International SAMPE Symposium*, (1993) pp. 1539
21. Kasehagen, L. J., and Macosko, C. W., "Structure Development in Cyanate Ester Polymerization.", *Polymer International*, VOL. 44 (1997) pp. 237-247.
22. Arnold, C. A., Md, D., MacKenzie, P. D., Riz, C., *United States Patent*, Hexcel Inc, (1996).

23. Iijima, T., Maeda, T., Tomoi, M., "Toughening of Cyanate Ester Resin by N-Phenylmaleimide-Styrene Copolymers", *Journal of Applied Polymer Science*, VOL. 74, (1999) pp. 2931-2939.
24. Brydson, J. A., "*Plastics Materials*," Publisher Butterworth Scientific, Boston, (1982).
25. Madorsky, S. L., "*Thermal Degradation of Organic Polymers*," VOL.7, Interscience Publishers, A Division of John Wiley & Sons, Inc. New York.
26. Kelen, T., "*Polymer Degradation*," Published by Van Nostrand Reinhold Company Inc. New York.
27. Langlois, V., Meyer, M., Audouin, L., Verdu J., "Physical Aspects of the Thermal-Oxidation of Cross-Linked Polyethylene," *Polymer Degradation and Stability*, VOL. 36, (1992) pp. 207-216.
28. Rychly, J., Matisova-Rychia, L., Csmorova, K., Achimsky, L., Audouin, L., Tcharkhtchi, A., Verdu, J., "Kinetics of Mass Changes in Oxidation of Polypropylene," *Polymer Degradation and Stability*, VOL. 58, No.3, (1997) pp. 269-274.
29. Anton-Prinet, C., Mur, G., Gay, M., Audouin, L., Verdu, J., "Change of Mechanical Properties of Rigid Poly (vinylchloride) During Photochemical Aging," *Journal of Materials Science*, VOL. 34, No.2, (1999) pp. 379-384.
30. Langlois, V., Audouin, L., Courtois, P., Verdu, J., "Change of Mechanical Properties of Cross-linked Polyethylene During its Thermo-oxidative Aging," *Angewandte Makromolekulare Chemie*, VOL. 208, (1993) pp. 47-64.
31. Achimsky, L., Audouin, L., Verdu, J., Rychla, L., Rychly, J., "The Effect of Oxygen Pressure on the Rate of Polypropylene Oxidation Determined by Chemiluminescence. *European Polymer Journal*, VOL.35, No.4, (1999) pp. 557-563.
32. Dawkins, J. V., "*Developments in Polymer Characterisation-4*," Applied Science Publisher, London and New York. Chapter 3: Fourier Transform Infrared Spectroscopy of Synthetic Polymers, pp. 91-129.
33. Odian, G., "*Principles of Polymerization*," Wiley, New York, (1991).

34. Merdas, I., ThomINETTE, F., Verdu, J., "Humid Aging of Polyetherimide. II. Consequences of Water Absorption on Thermomechanical Properties," Journal of Applied Polymer Science, VOL. 77, (2000) pp.1445-1451.
35. Park, Y., Ko, J., Ahn, T.K., Choe, S., "Moisture Effects on the Glass Transition and the Low Temperature Relaxations in Semiaromatic Polyamides," Journal of Polymer Science and Polymer Physics, VOL. 35, (1996) pp. 807-815.
36. Smith, L. S. A., and Schmitz, V., "The Effect of Water on the Glass Transition Temperature of Poly (methyl methacrylate)," Polymer, VOL. 29, (1988) pp. 1871-1878.
37. Agarwal, N., and Farris, R. J., "Water Absorption by Arcylic-Based Latex Blend Films and its Effects on Their Properties," Journal of Applied Polymer Science, VOL. 72, pp. 1407-1419.
38. Theocaris, P. S., Kontou, E. A., Papanicolaou, G. C., Journal of Polymer Science, VOL. 28, (1983) pp. 3145.
39. DeNeve, B., Shanahan, M. E. R., "Water-Absorption by an Epoxy-Resin and Its Effect on the Mechanical Properties and Infrared Spectra," Polymer, VOL. 34, (1993) pp. 5099-5105.
40. Zheng, Q., Morgan, R. J., "Synergistic Thermal-Moisture Damage Mechanisms of Epoxies and Their Carbon-fiber Composites," Journal of Composite Materials, VOL. 27, (1993) pp. 1465-1478.
41. Shen, C. H., Springer, G. S., "Effects of Moisture and Temperature of Tensile-Strength of Composite-Materials," Journal of Composite Materials, Vol. 11, (1977) pp. 2-16.
42. Maggana, C., Pissis, P., "Water Sorption and Diffusion Studies in an Epoxy resin System," Journal of Polymer Science: Part B: Polymer Physics, VOL. 37, pp.1165-1182.
43. Bonniau, P., Bunsell, A. R., Journal of Materials Science, VOL. 23, (1989) pp. 2331.
44. Charles, A. R., and Bauer, R. S., "*Moisture-Related Failure*," Shell Development Company, (1984).
45. Mateen, A., and Siddiqi, S. A., "Effect of Moisture on Hammer-Milled Glass-Fiber-Reinforced Polyurethane," JMEPEG, VOL. 5, (1996) pp. 598-600.

46. Jabarin, S. A., and Lofgren, E. A., "Effect of Water Absorption on Physical Properties of High Nitrile Barrier Polymers," *Polymer Engineering and Science*, VOL. 26, No.6, (1986) pp. 405-409.
47. Lucas, J. P., and Odegard, B. C., "Moisture Effects on Mode 1 Interlaminar Fracture Toughness of a Graphite Fiber Thermoplastic Matrix Composite," *Advances in Thermoplastic Matrix Composite Materials*, ASTM STP 1044, (1989) pp. 231-238.
48. Haque, A., and Jeelani, S., "Environmental Effects on the Compressive Properties: Thermosetting versus Thermoplastic Composites," *Journal of Reinforced Plastics and Composites*, VOL. 2, (1992) pp. 146-157.
49. DSC 2920, "*Differential Scanning Calorimeter Operator's Manual*," TA Instruments, DE 19720, (1993).
50. *Engineering Materials Handbook*, Engineering Plastics, VOL.2 ASM International, (1988).
51. Snively, C. M., Koeing, J. L., "Fast FTIR Imaging: A New Tool for the Study of Semicrystalline Polymer Morphology," *Journal of Polymer Science Part B: Polymer Physics*, VOL. 37, No.17, (1999) pp. 2353-2359.
52. Briggs, D., and Seah, M. P., "*Practical Surface Analysis, Auger and X-ray Photoelectron Spectroscopy*, VOL. 1
53. Ycom, B., Yu, Y. J., Mckellop H. A., Salovey, R., "Profile of Oxidation in Irradiated Polyethylene," *Journal of Polymer Science Part A: Polymer Chemistry*, VOL. 36, (1998) pp. 329-339.
54. Seymour, R. B., and Carraher, C. E., "*Structure-Property Relationships in Polymers*," Plenum Press, New York, (1984).
55. Uzomah, T. C., and Ugbolue, S. C. O., "Time And Temperature Effects on the Tensile Yield Properties of Polypropylene," *Journal of Applied Polymer Science*, VOL. 65, (1997) pp. 625-633.
56. Nam, J. D., and Seferis, J. C., *Sample Quaterly*, VOL. 24, No.1, (1992), pp. 10-18.
57. Nakamura, Y., Mori, K., Tamura, K., and Saito, Y., *Journal of Polymer Science, Part A*, VOL. 17, (1969) pp. 3089-3097.

58. Crissman, J. M., Mckenna, G. B., "Physical and Chemical Aging in PMMA and Their Effects on Creep and Creep-Rupture Behavior," *Journal of Polymer Science and Polymer Physics*, VOL. 28, No. 9, (1990) pp. 1463-1473.
59. Buch, X., and Shanahan, M. E., "Influence of Gaseous Environment on the Thermal Degradation of a Structural Epoxy Adhesive," *Journal of Applied Polymer Science*, VOL. 76, (2000) pp. 987-992.
60. Eriksson, P. A., Boydell, P., Eriksson, K., Manson, J. A. E., Albertsson, A. C., "Effect of Thermal-Oxidative aging on Mechanical, Chemical, and Thermal Properties of Recycled Polyamide 66," *Journal of Applied Polymer Science*, VOL. 65, (1997) pp. 1619-1630.
61. Hillermeier, R. W., and Seferis, J. C., "Environmental Effects on Thermoplastics and Elastomer Toughened Cyanate Ester Composite System.," *Journal of Applied Polymer Science*, VOL. 77, No.3, (2000) pp. 556-567.
62. Volke-Sepulveda, T., Favela-Torres, E., Manzur-Guzman, A., Limon-Gonzalez, M., Trejo-Quintero, G., "Microbial Degradation of Thermo-Oxidized Low-Density Polyethylene," *Journal of Applied Polymer Science*, VOL. 73, (1999) pp. 1435-1440.
63. Tretinnikov, O. N., and Ikada, Y., " Surface Characterization of Ion-implanted Polyethylene," *Journal of Polymer Science: Part B: Polymer Physics*, VOL. 36, (1998) pp. 715-725.
64. Singh, R. P., Desai, S. M., Solanky, S. S., Thanki, P. N., "Photodegradation and Stabilization of Styrene-Butadiene-Styrene Rubber," *Journal of Applied polymer Science*, VOL. 75, (2000) pp. 1103-1114.
65. DeMeuse, M. T., Gillham, J. K., and Parodi, F., " Evolution of Properties of a Thermosetting Isocyanate/Epoxy/Glass Fiber Model Composite System with Increasing Cure," *Journal of Applied Polymer Science*, VOL. 64, No.1, (1997) pp. 27-38.
66. Shyichuk, A.V., White J. R., "Analysis of Chain Scission and Crosslinking Rates in the Photo-Oxidation of Polystyrene," *Journal of Applied Polymer Science*, VOL. 77, (2000) pp. 3015-3023.

67. Xioa, G.Z., and Shanahan, M. E. R., "Irreversible Effects on Hygrothermal Aging on DGEBA/DDA Epoxy Resin," *Journal of Applied Polymer Science*, VOL. 69, (1998) pp. 363-369.

MICHIGAN STATE UNIVERSITY LIBRARIES



3 1293 02112 3124